The Use of a Ring Shear Tester to Evaluate the Flowability

of Pharmaceutical Bulk Solids

INAUGURAL – DISSERTATION

zur

Erlangung des Doktorgrades der

Mathematisch-Naturwissenschaftlichen Fakultät der

Heinrich-Heine-Universität Düsseldorf

Vorgelegt von

Hind Jaeda

aus Libyen

Düsseldorf, 2009

Aus dem Institut für Pharmazeutische Technologie und Biopharmazie

der Heinrich-Heine-Universität Düsseldorf

Mathematisch-Naturwissenschaftliche Fakultät der

Heinrich-Heine-Universität Düsseldorf

Referent: Prof. Dr. Peter Kleinebudde

Korreferent: Prof. Dr. Jörg Breitkreuz

Table of content

List of abbreviations:

Abbreviation	Meaning
Ar.200	Aerosil® 200
Ar.200 V	Aerosil® 200 V
Ar.R972	Aerosil® R972
Ar.R972 V	Aerosil® R972 V
COM888	Compritol® 888 ATO
DYN114	Dynasan® 114
DYN116	Dynasan® 116
DYN118	Dynasan® 118
IMW900	Imwitor® 900 K
PRATO5	Precirol® ATO 5
WIT42/44	Witocan® 42/44
AOR	Angle of repose
RSD	Relative standard deviation
RST	Ring shear tester
SD	Standard deviation
SSA	Specific surface area

List of figures:

List of tables:

Table 1: Shear cells used in this work

Table 2: Slope, intercept and correlation coefficient r as represented with the linear regression equation for all binary mixtures.

Table 3: Active ingredients and excipients used in these experiments

Table 4: lipids used in this study

Table 5: Further information about active ingredients used in this work

Table 6: Further information about excipients used in this work

Table 7: Glidants used in this study

Table 8: Further information about lipids used in this study

1 Introduction

1.1 Flowability

The word "Flow" is a verb referring to the continuous motion or movement in a stream. However, the term flowability refers to the plastic deformation of a bulk solid due to the loads acting on it. A free flowing powder is the one flowing easily without obstructions for example through a silo or a hopper, while a poor flowing powder is the one experiencing obstructions during handling [1, 2, 3, 4]. Therefore the formulation of free flowing powders is a crucial and essential requirement for a successful production [5]. Flowability of pharmaceutical powders affects mixing, filling and dosing processes and determines whether a product fulfils the requirements of quality control, e.g. weight content and content uniformity. Since approximately 80% of pharmaceutical products or the ingredients required for their manufacture are in powder form [6] and the fact that most of these powders are not free flowing [2], the assessment of their flowability is a crucial and essential step in the development process. Flowability estimation is also important to design the suitable powder handling equipment, e.g. bins and silos. Briefly, the early assessment of the flowability saves financial costs and time as well [7].

1.1.1 Flow patterns and problems

Powders follow one of two flow patterns: mass flow or funnel flow. In mass flow (also referred to as first in first out), which is the desirable hopper flow pattern, all of the powder in the hopper is in motion [1, 2, 8, 9]. In funnel flow (also referred to as first in last out), the central core of powder exits the bin or hopper first, followed by the powder at the sides of the container [10, 11, 12].
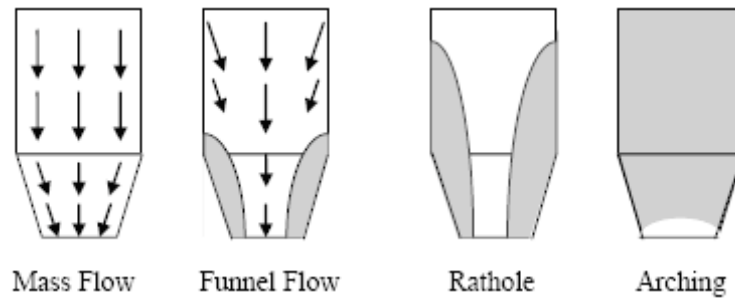
Fig 1: Powder flow patterns and common problems (from [12])

Typical problems which occur at the storage of bulk solids are: (1) **Arching** (doming) where a stable arch or dome is formed above the outlet preventing any discharge. This problem accompanies often mass flow pattern. In case of fine grained, cohesive bulk solid, the reason of arching is the strength (unconfined yield strength) of the bulk solid caused by the adhesion forces acting between the particles. (2) **Ratholing** (piping) occurs in case of funnel flow if only the bulk solid above the outlet is flowing out, while the material along the sides remains in its place forming a stagnant or also called a dead zone. If the bulk solid consolidates increasingly with increasing period of storage at rest, the risk of ratholing increases **(**see Fig 1). (3) **Flooding** occurs if arches and ratholes are formed and collapse alternately. Thereby fine bulk solids can flow out of the silo or hopper like a fluid. This behaviour causes a lot of dust. (4) **Segregation** or de-mixing is also possible according to particle size or particle density differences. However, at mass flow the segregation effect is reduced significantly **[**2, 8, 10, 12, 13].

1.1.2   Flow behaviour of powders (forces and stresses)

Unlike fluids, flow behaviour of powders can not be described only by knowing the name and the chemical structure of the material. This is due to the many parameters besides the chemical composition which influence their flow behaviour such as; particle size, shape, surface texture, electrostatic charge, moisture content and temperature. Besides the actual state of consolidation plays an important role. A powder behaves like a fluid in the fluidized

state, whereas it behaves like a solid if it has been compacted before. Therefore, during storage and transportation of powders, loose and slightly compressed bulk solids are dealt with [11].

In order to explain stresses acting in a powder, it is essential to mention the forces from which those stresses are calculated. When dealing with bulk solids or powders the state of load acting upon it does not consider individual particles, but the forces acting on the boundary areas of volume elements and the resulting deformations [2]. In a powder forces acting on an area (A) are:

*The normal force F_N; force acting perpendicular to area A.

*The shear force F_S; force acting parallel to area A.

To describe the load acting on a powder independently of the dimensions of the area, stresses are calculated from the forces to obtain:

*The normal stress $\sigma = F_N/A$; stress acting perpendicular to area A.

*The shear stress $\tau = F_S/A$; stress parallel to area A.

If a force in any direction is acting on a plane, the resolution of this force into a perpendicular and a parallel component yields the normal and shear stresses acting on the plane [2]. To simplify the understanding of powders behaviour some well known facts in bulk solids technology have to be mentioned. Different shear stresses emerge in different cutting planes due to friction and a bulk solid can transmit shear stresses even if it is at rest. Therefore powders can have sloped surfaces even at rest. Normal stresses are mainly compressive stresses also defined as positive normal stresses. Generally, stress conditions can be represented with Mohr stress circles (see figure 10). The unit used for stress is Pa (Pascal) according to the international system of units (SI) [2, 11, 14].

Fig.2 shows a bulk solid element in a container (assumptions: infinite filling height, frictionless internal walls). In the vertical direction, positive normal stress ($\sigma_v > 0$) is exerted on the bulk solid. To avoid misleading it has to be mentioned that the behaviour of a bulk

solid is quite different from that of a fluid. If the bulk solid was to behave like a Newtonian fluid, the stresses in the horizontal and vertical directions would be of equal magnitude. In reality within the bulk solid (Fig.2) the horizontal stress, σ_h, is a result of the vertical stress, σ_v, and is less than the vertical stress exerted on the bulk solid from the top. The ratio of horizontal stress to vertical stress is the stress ratio, K (also known as λ).

$$K = \frac{\sigma_h}{\sigma_V}$$
<div align="right">Equation 1</div>

Typical values of K are between 0.3 and 0.6 [1, 2, 11].
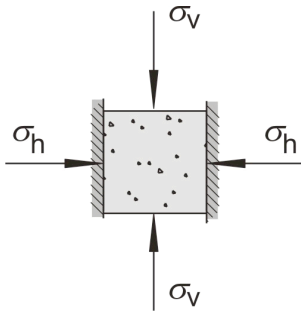
Fig.2: Element of bulk solid (from [1])

In a bulk solid different stresses can be found in different cutting planes. No shear stresses τ are exerted on the top or bottom surfaces of the bulk solid element in Fig.3; i.e. the shear stresses in these planes are equal to zero. Also no shear stresses are acting at the lateral walls (assumed as frictionless). Using a simple equilibrium of forces at a volume element with triangular cross-section cut from the bulk solid element shown in Fig.2, on the left of (Fig.3), the normal stress, σ_α, and the shear stress, τ_α, acting on a plane inclined by an arbitrary angle α, can be calculated. After some mathematical transformations (not considered here), it follows that:

$$\sigma_\alpha = \frac{\sigma_v + \sigma_h}{2} + \frac{\sigma_v - \sigma_h}{2}\cos(2\alpha)$$
<div align="right">Equation 2</div>

$$\tau_\alpha = \frac{\sigma_v - \sigma_h}{2}\sin(2\alpha)$$
<div align="right">Equation 3</div>

<div align="center">4</div>

The pair of values (σ_α, τ_α), calculated according to equations (2) and (3) for all possible angles can be plotted in a σ,τ-diagram. If one joins all plotted pairs of values, a circle emerges; i.e., all calculated pairs of values form a circle in the σ,τ-diagram. The circle is called "the Mohr stress circle". The Mohr circle is a graphical representation of any two dimensional stress state proposed in 1892 by Christian Otto Mohr. It was the leading tool used to visualize relationships between normal and shear stresses, where it represents the stresses in all possible cutting planes within a bulk solid element. The centre of the Mohr stress circle is always located on the σ-axis at $\sigma_m = (\sigma_v + \sigma_h)/2$ and $\tau_m = 0$. The radius of the circle is $\sigma_m = (\sigma_v - \sigma_h)/2$. Each Mohr stress circle has two points of intersection with the σ-axis. The normal stresses defined through these points of intersection are called the principal stresses, whereby the larger principal stress (the major principal stress) is designated as σ_1 and the smaller principal stress (the minor principal stress) is designated as σ_2. If both principal stresses are given, the Mohr stress circle is well defined.

In the example of Fig.2 the vertical stress, σ_v, which is greater than the horizontal stress, σ_h, is the major principal stress, σ_1, and the horizontal stress, σ_h, is the minor principal stress, σ_2. Therefore, a stress circle is defined clearly only if at least two numerical values are given, i.e., σ_1 and σ_2. [1, 2]
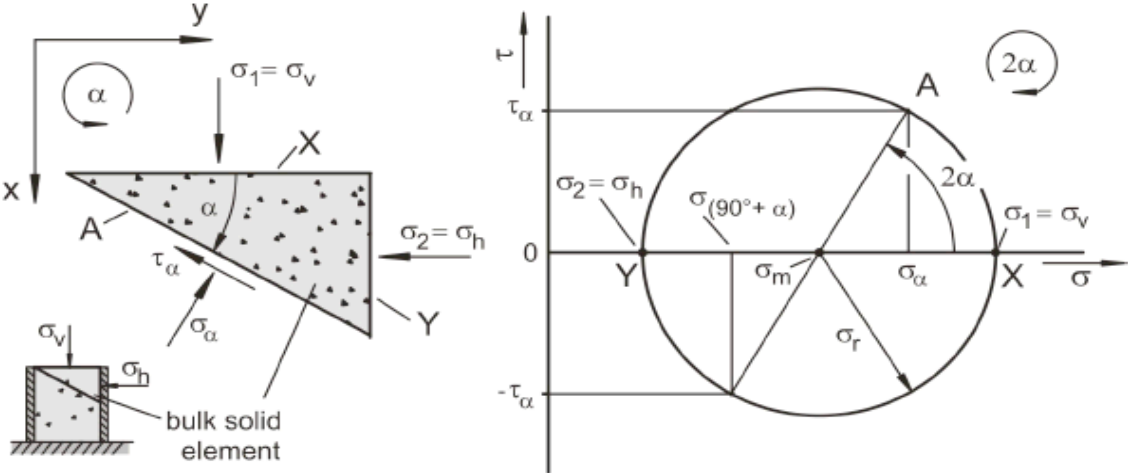
Fig.3: Force of equilibrium on an element of bulk solid, the Mohr stress circle (from [1])

1.1.3 Adhesive forces

Whether a bulk solid is freely or poorly flowing, depends on the ratio between the interparticle forces and the gravitational forces [5, 15, 16, 17]. The ratio of interparticle force to the gravitational force is inversely proportional to the square of the particle diameter [5, 17]. Particles are cohesive if the interparticle adhesive forces exceed the particles weight, for example most materials with diameters smaller than 30 μm. Therefore small particles stick more strongly together and flow poorly with decreasing particle size [5, 16, 17]. Different mechanisms create adhesive forces between individual particles. Major adhesive forces are due to liquid bridges, electrostatic, and van der Waals interactions [2]. Regarding fine, dry bulk solids at short interparticle distance (below 50 nm down to the contact distance of around 0.4 nm) [5, 15, 16], van der Waals forces are the prevailing interparticle forces. Van der Waal forces are based on electric dipoles of atoms and molecules. Electrostatic forces are due to different electric potentials of particle surfaces. In case of moist bulk solids, liquid bridges between the particles usually are most important, where the particles are attracted to each other due to surface tension [1, 2].

All types of adhesive forces described above are dependent on the distance between particles and on particle size. On one hand, van der Waals forces are large at small distances, and decrease strongly with increasing distance and are almost negligible at distances above 10^{-7} m. Also liquid bridges are large at small distance but decrease only slightly with increasing distance. On the other hand electrostatic forces are small at small distances and do not decrease that much with increasing distance. Thus for the flow of dry powders the influence of electrostatic forces at such small distances is negligible [2], see Fig. 4.
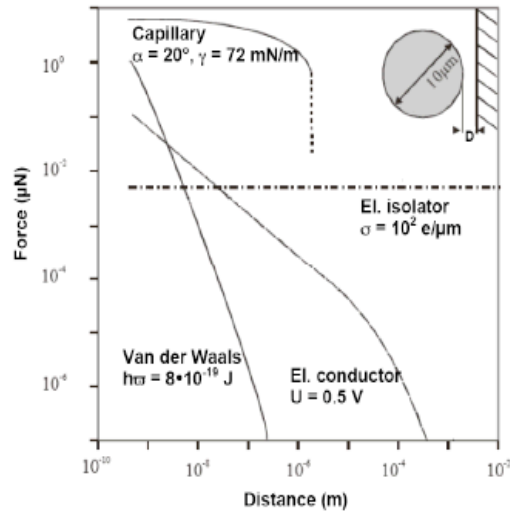
Fig. 4: Dependency of forces on the distance between a flat surface and a sphere, where d = 10µm (from [18])

The particle size has also a great influence on adhesive forces, as the forces are proportional to the particle diameter [16, 19]. The adhesive forces due to liquid bridges are the largest, followed by van der Waals forces, while the electrostatic force is the smallest. Since the particle weight is proportional to the third power of the diameter, the weight force becomes the dominant force above a particular size, see Fig. 5.
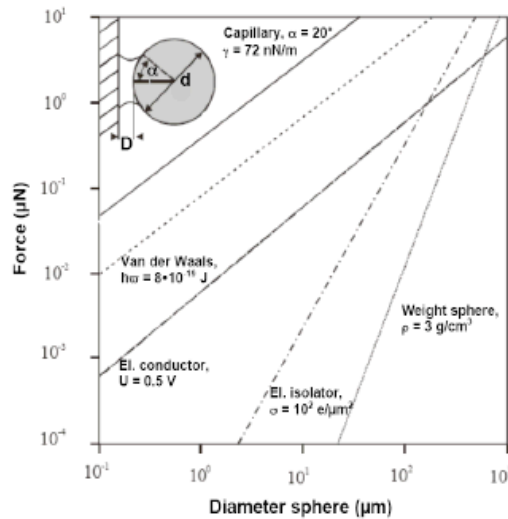
Fig. 5: Dependency of forces on the particle size (from [18])

The forces acting between particles are also dependent on their surface roughness, where particles with rough surfaces flow better than smooth particles. The presence of roughness decreases the adhesive forces by increasing the distance between the particles, whereby

7

decreasing contact area. The roughness has to be small enough to reduce the adhesive forces between particles; otherwise if it is not small the influence of the adhesive forces between the roughness itself and the particle becomes dominant relative to adhesive forces between particles themselves [2, 16, 19], see Fig. 6.
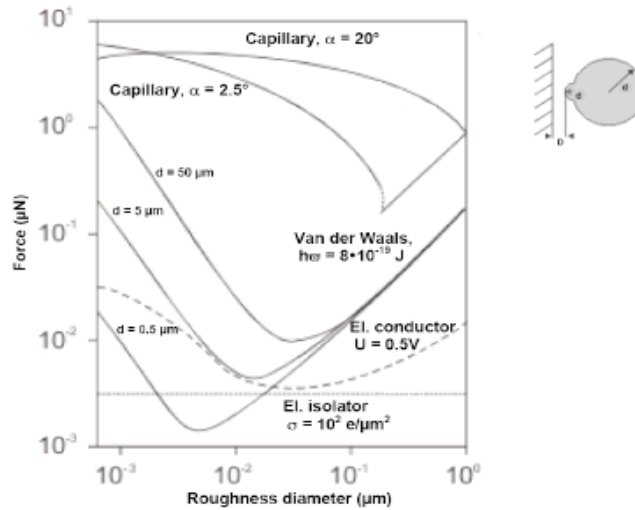
Fig. 6: Dependency of forces on surface roughness (from [18])

Compressive forces acting from outside on a bulk solid can increase the adhesive forces, as the particles are pressed and approach each other so that the contact areas increase thereby increasing cohesiveness. The dependence of the adhesive forces between the particles (especially for cohesive bulk solids) on external forces exerted on a bulk solid is characteristic of bulk solids, and they have to be taken into account to evaluate the bulk solid, this is referred to as stress history. In other words the stress history is the procedure by which a bulk solid sample has been consolidated to a definite state [1, 2, 20, 21].

1.1.4   Methods for flowability measurements

Schulze has given an overview of various methods used for the characterization of the flowability of bulk solids, he also introduced the following criteria to evaluate different methods [2, 22]:

1. Consolidation procedure followed by measurement of strength.

2. Consolidation of the bulk solids sample up to steady state flow.

3. Coincidence of the directions of major principle stresses at both consolidation and failure.

4. Reproducible stressing conditions of the bulk solid sample at consolidation (4a) and failure (4b).

5. Known average stresses and uniform stress distribution in the plane of interest at consolidation (5a) and failure (5b).

6. Possibility for varying the consolidation stresses (with regard to application).

7. Possibility for measuring time consolidation.

Criteria 6 and 7 are desirable capabilities but are not necessary if only flowability has to be determined. However, the criteria listed previously are fulfilled best by shear testers [2, 22]. Fig. 7 gives a survey of possible shear principles and names some testers used in soil mechanics and powder technology [21, 22, 23]. Shear testers are either direct or indirect testers. Regarding direct shear testers, their design defines the location of the shear zone and the major principal stress is not fixed during the test. Whereas in indirect shear testers the shear zone develops more or less depending on the applied state of stress and the directions of the principal stresses are fixed and remain constant during the test [21, 24].
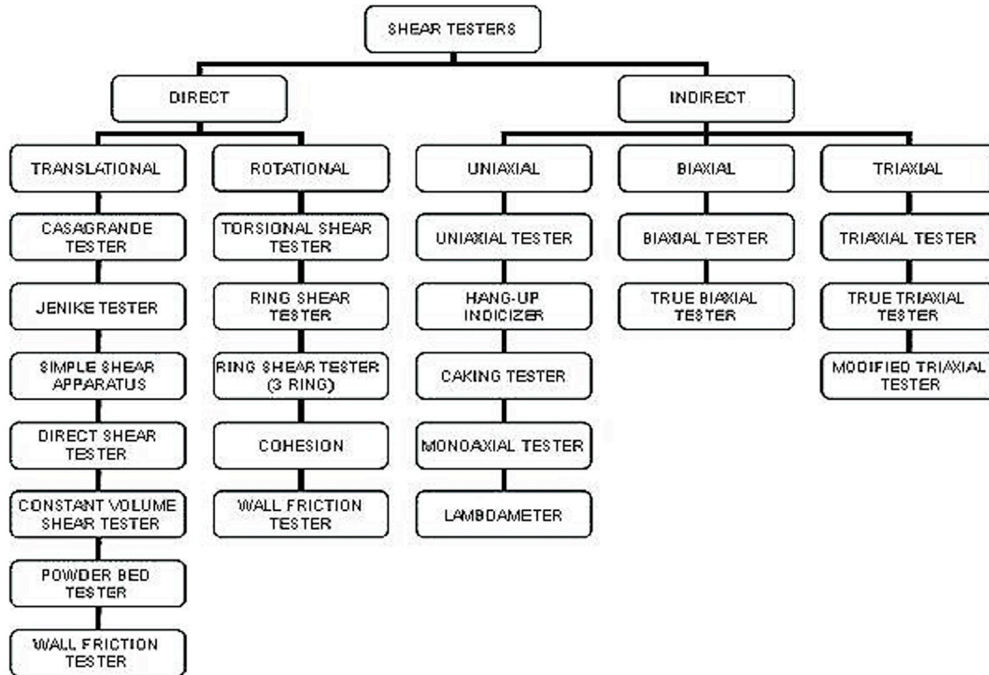
Fig. 7: Shear testers (from [22])

Some of the testers mentioned in the previous figure will be explained as follows:

1.1.4.1 Direct shear testers

1.1.4.1.1 Translational testers

The most popular tester in this category is the Jenike shear tester, which has served successfully as an engineering tool for silo design [14, 21]. Jenike was one of the pioneers in this field, when in the 1960s he published his fundamental work on silo and bulk solid technology and introduced his tester [1, 14, 25]. This tester is operated manually, where the sample is filled into the cell which consists of a bottom ring (mould ring), a ring of the same diameter (upper ring) lying above it, and a lid. The lid is loaded centrally with a normal force. The upper part of the cell is displaced horizontally against the fixed bottom ring by a motor driven stem which pushes against a bracket fixed to the lid. A manual twisting procedure is performed (pre-consolidation) before the sample is pre-sheared and then sheared to failure. The goal of a shear test is to measure the yield limit of a consolidated bulk solid, which is called yield locus in bulk solids technology. The yield locus consists of a number of points.

10

Each point is obtained as a result of consequent preshear and shear processes. For the Jenike tester a new specimen is required each time a point is measured on the yield locus. This tester fulfils the criteria proposed by Schulze, but its use is restricted because it is operator sensitive, time consuming, not suitable for all bulk solids due to its limited shear displacement (maximum 4 to 5 mm) and measurements at very small stresses are not possible (lower limit 3 to 4 KPa) [1, 2, 14, 21, 22, 26-29].

1.1.4.1.2 Rotational testers

Among these testers are the torsional shear testers (e.g. Peschl's tester) and the ring shear testers (e.g. Schulze's tester). Testers with rotational displacement have unlimited strain, where the shear procedure is induced by rotation around a vertical axis. Therefore, these testers can be applied for a variety of bulk solids compared to translational testers with their limited strain. The covers of these testers are roughened or are equipped with bars to ensure shearing within the bulk material. The base is rotating and the moment acting on the lid is measured. The testers with a circular cross section are called torsional shear testers while those with an annular one are called ring shear testers. The torsional shear testers have no shear in the centre exerted on the sample i.e.; deformation in the centre is zero (ring shear testers do not have this un-uniformity in deformation). Comparative studies between these testers and others showed that the torsional shear testers did not always show agreement, and if they differ they always underestimate the strength. Whereas the ring shear testers (with the proper test procedure and proper cell design) can achieve reproducible and close results to those obtained with Jenike shear testers. The advantages of these testers are their simplicity and possibility to be used in an automated mode as well as the size of the cell that can be small, thus small amounts of the sample are required. Also, they allow the measurement of a complete yield locus with only one sample as well as measurements at very low stresses are possible. Besides, they are neither operator dependent nor time consuming. They fulfil the

criteria proposed by Schulze with certain limitations with (5b) due to variation of deformation with radius in case of torsional shear testers and the ratio of the inner to outer shear cell diameter and appropriate test procedure for the ring shear testers [2, 21, 22, 23].

1.1.4.2 Indirect shear testers

1.1.4.2.1 Uniaxial testers

Examples for such testers are the uniaxial compression tester; monoaxial tester and Johanson hang up indicizer.

(1) Uniaxial compression tester:

In uniaxial testers a sample is filled into a cylinder (frictionless) and consolidated vertically by a normal consolidating stress. After removing the cylinder the sample is loaded again with an increasing normal stress up to the point of failure, leading to the unconfined yield strength. The uniaxial tester is regarded as a simple tester and the test can be performed quickly but the results cannot be very accurate. It underestimates the unconfined yield strength and overestimates the flowability, because consolidation by a vertical force only does not guarantee a homogeneous compaction (only obtained with steady state flow achievement). The uniaxial tester is suitable when cohesive bulk solids are tested which guarantees a stable sample after consolidation and removing the cylinder. For the same reason no tests are possible in the low stress region. Therefore, this tester complies with the criteria proposed by Schulze except (2) where it does not attain steady state flow and (5a) where this criterion is only fulfilled if cylinder's wall is frictionless. Despite the disadvantageous pointed out this tester is useful for time consolidation measurements of coarse particles where other shear testers cannot be used [2, 21, 22, 23].

(2) Monoaxial shear test

This test is similar to the uniaxial compression test. Like in uniaxial tests the sample is consolidated in vertical direction where the state of stress is well known and sufficiently

homogeneous. After vertical consolidation the sample is stressed horizontally with an increasing stress up to failure, whereby the equivalent state of stress in the sample is not homogeneous (free surface at the top) and not known. Another disadvantage of this procedure is the direction of stress application, being perpendicular to the one at consolidation. Compared to the uniaxial compression test (which underestimates strength), the measured strength is further underestimated due to the anisotropic effects caused by the difference in direction between consolidation and strength measurements. Therefore this test complies with Schulze's proposed criteria except (2) and (3), whereas for Criterion (5a & 5b) the walls must be frictionless [2, 21, 22, 23].

(3) Johansen indicizer

A cylindrical specimen is compressed in axial direction via a piston consisting of two concentric areas. Subsequently the lower piston is removed and the inner part of the upper piston pushes on the sample until failure occurs. From failure force the unconfined yield strength can be computed. The comparative tests clearly show that the unconfined yield strengths obtained gained with the hang-up indicizer, are likely to be lower in comparison with Jenike's shear tester and the Schulze ring shear tester. In such tests stresses are not homogeneous and are not known during consolidation and failure because the stress decreases downwards due to wall friction depending on the bulk solid's properties and the specimen's geometry. Also no steady state flow can be achieved during consolidation 8 due to uniaxial compression procedure). Therefore, this tester complies with Schulze's criteria except (2), (3), and (5). For fulfilling criterion (7) long term storage under consolidation stress is a prerequisite [2, 21, 22, 23, 30].

1.1.4.2.2 Biaxial testers

A biaxial tester is a tester in which both methods of consolidation, either steady state flow or uniaxial compression can be realized. The sample is constrained in lateral x- and y-direction

by four steel plates. Vertical deformations of the sample are restricted by rigid top and bottom plates. The sample can be loaded by the four lateral plates which are linked by guides so that the horizontal cross-section of the sample may take different rectangular shapes. To avoid friction between the plates and the sample the plates are covered with a thin rubber membrane. Since there are no shear stresses on the boundary surfaces of the sample, the normal stresses are principal stresses and the complete state of stress is known. With the biaxial shear tester the measurement of both stresses and strains is possible. Comparative tests performed with Jenike's shear tester and the biaxial shear tester were in agreement. Biaxial testers are excellent research tool as they are capable of determining many influences on the stress-strain behaviour of bulk solids such as; stress history and the influence of different consolidation procedures on the unconfined yield strength. This tester fulfils the criteria proposed by Schulze [2, 21, 22, 23].

1.1.4.2.3 Triaxial tester

Since in literature only few results are published about these testers, it will be described here briefly [22]. Triaxial testers belong to the indirect shear testers in which the principal stresses in three dimensions are measured or applied. Triaxial testers are standard testers in soil mechanics, two of them are known from this sector, namely; the normal triaxial tester and the true triaxial tester. However, the procedure of running a test is relatively simple [21, 22].

In the normal triaxial tester the sample of cylindrical shape is covered by a rubber membrane and is placed in the vertical direction between two movable stamps. In the horizontal direction it is stressed by water pressure. By moving the stamps in the vertical direction towards each other the stresses σ_1 will increase until failure is obtained. After failure further measurements are not possible. Thus overconsolidated samples can only be tested up to the point of maximum shear stress. Since the principal stresses are known Mohr stress circles can be drawn. In the true triaxial tester six walls being the boundary of the sample are arranged in

such a way that deformations in x, y and z directions are possible at the same time, independent and at different rates. Again the sample has to be placed in a rubber membrane, which has to be pre-stressed in order to handle the sample before it is placed in the tester. Thus, only tests under high stresses give reliable results [21, 22, 23].

Therefore, to guarantee the measurement of flow functions without further assumptions Jenike's tester, ring shear testers and biaxial shear testers can be used. All other procedures to get a dependence of the unconfined yield strength on the consolidation stress (without reaching steady state flow) lead to smaller unconfined yield strengths. Those relationships can only yield estimates of the flow function. These estimates must be used with caution in case used for silos design [21, 22]. The results obtained from testers where the state of stress is not exactly known cannot be recommended for silo design [22].

1.1.4.3 Conventional simple test methods

Several empirical simple methods are used for the assessment of bulk solid properties, e.g.:

• Angle of repose: is the slope of a more or less conical pile of loose bulk solid, i.e. the angle formed between the horizontal and the surface of the pile. The angle of repose is often mentioned in literature. Different results are obtained even with this simple test procedure according to the way by which the cone is formed, i.e. whether the angle prevails in a conical heap, a wedge-shaped heap or a rotating drum. However, this method is suitable and reproducible when handling free flowing bulk solids. The reproducibility gets worse with cohesive bulk solids. The measured angle can be influenced by the way of sample preparation, particle size and particle size distribution [1, 11, 31]. Regarding Schulze's criteria, criteria from (2) to (6) are not applicable. And the test does not comply with criteria No. (1) and (7) concerning quantitative statements for flowability and time consolidation [2].

• Funnel methods: A bulk solid is allowed to flow through a funnel with varying outlet diameters. A critical diameter can be obtained as a measure of flowability. Alternatively, as

described in the monograph "Flow behaviour" in the Ph. Eur. [32] the time required for a sample of bulk solid to flow out of a funnel is determined. It is assumed that the flowability is increased with a decreasing discharge time. Results obtained are considerably influenced by the material and the geometry of the funnel. Thus no quantities can be derived, which only depend on the bulk solid [2]. However, those empirical methods can be used in special applications, but only if a correlation has been found between the special application and many empirical tests [22]. Similar to the angle of repose this test does not comply with Schulze's criteria No. (1) and (7).

• Compressibility test: As described in the monograph "Apparent and tapped volume" in the Ph. Eur. [33] for such tests two quantities are calculated, the bulk density for the loosely poured powder in a cylinder and the tapped bulk density obtained after tapping the powder using a tap volumeter. Two different parameters can be derived; the Hausner ratio and Carr index. Both the Hausner ratio and the Carr index are sometimes criticized as not having a strong theoretical basis. Despite criticism and unreliability [34] they are still used, because the equipment required to perform the analysis is relatively cheap and the technique is easy to learn. Similar to the previous tests, this test does not comply with Schulze's criteria No. (1) and (7) [1, 2, 11].

Other testers and methods for flowability assessment are available and applied but are not mentioned here. Generally, test devices which allow the defined preparation of the sample of bulk solid must be preferred (e.g. steady state flow as a defined consolidation procedure). It is only possible in this way to determine the relevant flow properties (unconfined yield strength, internal friction angle, wall friction angle, bulk density, time consolidation) independent from the devices used [1. 11, 35].

1.2   Shear testers

Shear testers are the internationally recognized means to measure the flow properties of cohesive bulk solids. In this research work two automated Schulze ring shear testers were compared. The Schulze testers are direct shear testers with rotational displacement and unlimited strain. Rotational displacement and consequently unlimited strain, is an advantage when very elastic bulk solids or products like sludge or wet clay are sheared [26], in order to assure reaching the stationary flow which is necessary for measuring a yield locus. The Schulze ring shear testers used are fully automated and therefore measurements are neither time consuming nor difficult to operate.

1.2.1   Flow properties measured using the Schulze ring shear tester

With the RST-control 95 software connected to the ring shear, flow properties of bulk solids can be measured [36, 37]. The parameters which describe the flow properties can be determined from the yield locus [12]. Flow Properties measured are:

(1) Flow property test (yield locus)

Flow property test (flowability test) is performed by measuring a yield locus, followed by constructing Mohr circles. From the Mohr circle analysis both the consolidation stress σ_1 and unconfined yield strength, σ_c are obtained. The flowability factor "ffc" is calculated from the ratio, ffc = σ_1 / σ_c and used to characterize flowability numerically. In this research work the flow property test was the point of interest, since the flowability (ffc) is the most important quantity for quality control, comparative tests and product development.

(2) Time consolidation test

The strength of a bulk solid can increase when stored at rest. This effect is measured in a time consolidation test. This test is performed by consolidating (preshearing) a sample of bulk solid, storing it at a consolidation stress for a certain period of time, and then shearing the bulk solid sample.

(3) Wall friction test:

For many processes, the friction between a bulk solid and the adjacent wall of a bin, a silo, etc. is important. The ring shear tester could be equipped with a wall friction cell, a wall friction test, i.e. the measurement of a wall yield locus, can be performed.

(4) Compressibility test

In such a test the sample is loaded by a stepwise increasing (vertical) normal stress without shearing, i.e. the sample is subjected to uniaxial compression. From the weight and the measured height of the bulk solid sample the mean bulk density in the shear cell is calculated for each normal load.

(5) Attrition test

Attrition tests help to evaluate particle breakage and fines generation by abrasion. Attrition of particles cannot be directly measured with a ring shear tester, but it is possible to shear a bulk solid at a well defined normal stress for a certain shear displacement. For evaluation, one can determine the amount of fines using an appropriate sieve before and after the test. Alternatively particle size distribution measurements can be carried out before and after shearing [1, 2, 36, 37, 38].

1.2.2 Schulze ring shear tester (RST-01.Pc)

In 1992 the ring shear tester (type RST-01.01) [2, 26] was developed by Schulze, followed by a computer-controlled version in 1997 (type RST-01.pc). It is connected to a personal computer running control software (RST control 95). With this control software yield loci, wall yield loci, time consolidation, etc. can be measured and calculated automatically [1, 36, 37].
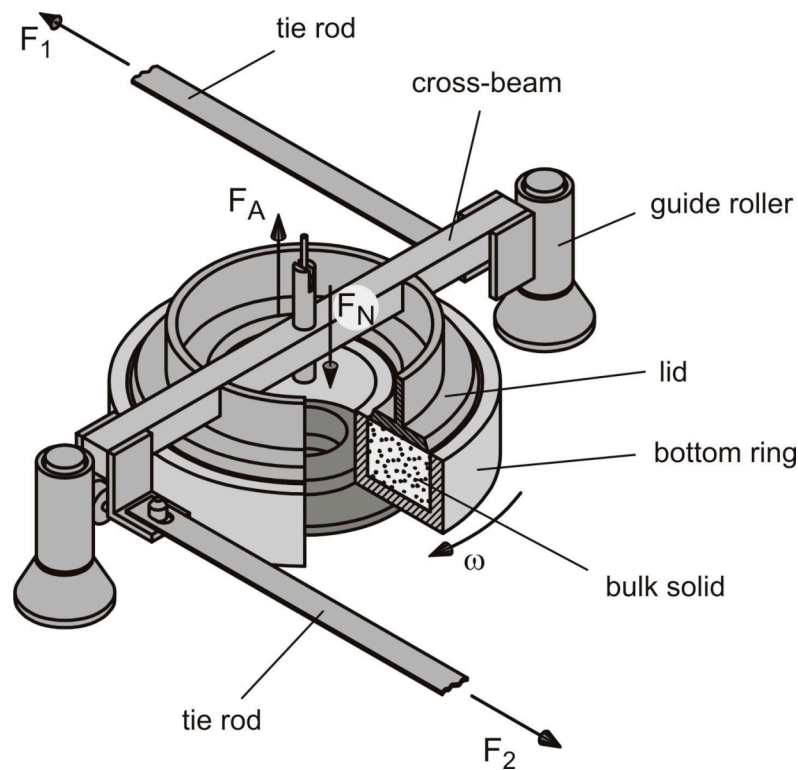
Fig. 8: Ring shear cell of Schulze (from [1])

The shear tester RST-01.pc of Schulze is shown in **Fehler! Verweisquelle konnte nicht gefunden werden.**. The sample is filled in an annular cell. An annular lid attached to a crossbeam lies on top of the sample. The lid has bars which are protruding into the bulk solid, to prevent slipping of the sample during shearing. A normal force F_N acts on the powder through a hanger attached to the crossbeam to apply the vertical stress σ on the specimen. An upward force F_A is applied on the crossbeam to counterbalance the weight of the lid and all other parts connected to it. The sample is sheared, when the cell is driven clockwise, with a standard shear speed of 1.5 mm/min (with reference to the mean radius of the shear cell). The lid is prevented from rotating by two tie rods connected at their rear ends to load cells. From the measured forces F_1 and F_2 through the rods, the shear stress τ acting in the bulk solid specimen is calculated [1, 26].

The goal of a shear test is to measure the yield limit of a well defined consolidated bulk solid. The yield limit is called yield locus in bulk solids technology. The protocol recommended in the ring shear tester's manual [38] and in the ASTM-Standard [39] is followed. First of all the shear cell is filled uniformly. In order to obtain a yield locus, the powder sample is sheared in

two steps. The first step called preshear in which the sample is consolidated. Where the sample is sheared under a normal stress σ_{pre} until a constant shear stress τ_{pre} (or τ_{sf}; shear stress at steady state flow conditions) is obtained. It is necessary to achieve steady state flow across the whole cross-section and in the same direction, whereby it guarantees a reproducible and a clearly defined consolidation where all influences of the stress history are eliminated [21, 22, 24]. Then the shear stress is reduced to zero and the second step known as shear is performed. The normal stress is reduced to $\sigma_{sh} < \sigma_{pre}$ and the sample is sheared until the shear stress has reached a maximum τ_{sh} (or τ_{if}; shear stress at incipient flow). The maximum is the point of incipient flow where the consolidated sample fails (begins to flow). In order to obtain a yield locus, several points of incipient flow at different levels of normal stress σ_{sh} have to be measured and drawn in a σ, τ-diagram (Fig. 9). The curve through the points of incipient flow in the σ,τ-diagram is called the yield locus [1, 26, 38]. Flow properties measured with a ring shear cell are: consolidation stress, unconfined yield strength, angle of internal friction, cohesiveness and bulk density. The most important quantity for quality control, comparative tests and product development is the flowability ffc.
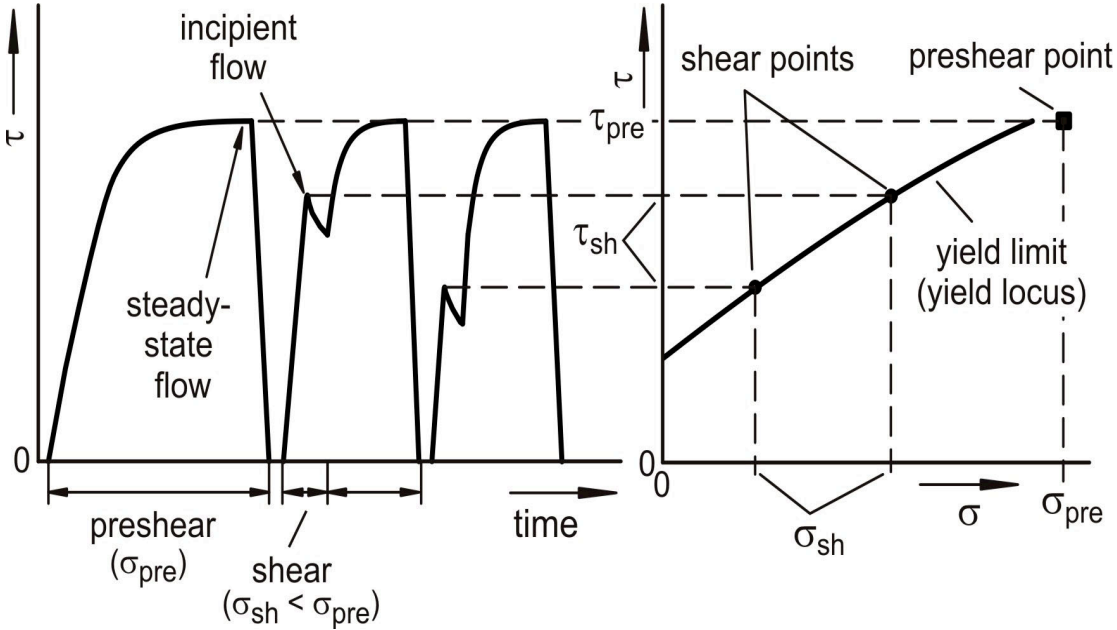
Fig. 9: Yield locus as constructed with a ring shear tester (from [1])

The parameters required to calculate ffc values can be determined by constructing Mohr circles (see Fig. 10). The constructed circle represents the stresses in the sample at the end of the consolidation procedure (stresses at steady state flow) and the relevant consolidation stress σ_1 is the major principal stress of the larger Mohr circle tangent to the yield locus. Whereby the unconfined yield strength is the major principle stress for the smallest Mohr circle passing through the origin (minor principal stress $\sigma_2 = 0$) and tangent to the yield locus as well [2, 11].
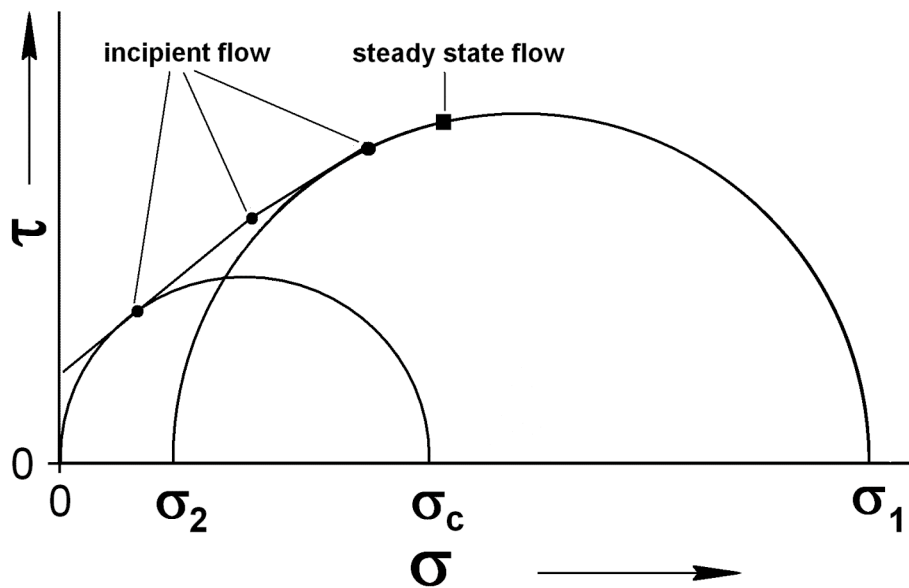
Fig. 10: Mohr stress circles ($\boldsymbol{\sigma_1}$ consolidation stress; $\boldsymbol{\sigma_c}$ unconfined yield strength)

The ratio ffc of consolidation stress σ_1 to unconfined yield strength, σ_c, as obtained by the Mohr's circles analysis is used to characterize flowability numerically, equation 4:

$$ffc = \sigma_1 / \sigma_c \qquad \text{Equation 4}$$

The flowability function is used to classify the flow behavior of bulk solids according to Jenike´s [25] powder classification as shown below.

ffc < 1 not flowing

1 < ffc < 2 very cohesive

2 < ffc < 4 cohesive

4 < ffc < 10 easy flowing

10 < ffc free flowing

1.2.3   Schulze ring shear tester (RST-XS)

A smaller computer-controlled ring shear tester (type RST-XS) has been available since 2002. This tester enables use of small sample volumes (9 ml, 30 ml, and 70 ml). In this study the 30 ml cell was used. The test procedure for this tester is the same as that for the large one. See table 1 in section 3.1 for the difference between the shear cells of both testers.

1.3   Glidants

Good flow properties are critical to the successful development of any pharmaceutical formulation. Therefore, flow properties of powders are often modified by the addition of materials in an attempt to improve their flow characteristics and their processability. These materials are called "glidants". Munzel was the first to employ the term glidant to designate agents added in small amounts and improve flowability [31]. Glidants are fine powders ranging from few nanometers up to 30µm in diameter incorporated into mixtures to improve their flow properties. There is some controversy about the exact mechanism, but two theories exist. The first is that small glidant particles coat the relatively larger host powders, increasing interparticle distance and decreasing interparticle forces [7, 40]. The second theory is that the glidant powders act in a manner analogous to ball-bearings, reducing friction of rough surfaces [12] and therefore changes the resistance to shearing and the flowability of the bulk powder [7, 41]. Glidants used in pharmacy include talc, colloidal silicon dioxide, calcium phosphates and to a certain extent various metallic stearates (salts of fatty acids)<. Since several groups have investigated the addition of glidants to a variety of powders and noted that silica-type glidants are the most efficient, they have been used in this work to improve flowability.

Silica types are characterized by their small particle size, where the submicron particles move easily between larger particles and forms a layer on their surface to aid flow. Aerosil[®] is a fine, white, fluffy and X-ray amorphous and ultra-pure powder consisting of primary particles in the nanometre range (10-40nm). Accordingly, the specific surface area as determined by

BET, range from approximately 50 to 400m^2/g. The primary particles are not isolated. They are rather present as aggregates and agglomerates, the sizes of which are undefined. During grinding and mixing processes, the agglomerates are reduced. Aerosil$^®$ also known as fumed silica is an exceptionally pure form of silicon dioxide manufactured by hydrolysis of silicon tetrachloride in an oxygen-hydrogen flame. The gaseous silicon tetrachloride reacts in a gas flame burner (1000°C) with just-formed water to produce silicon dioxide. Hydrochloric acid is the only by-product, and it is removed from the SiO_2 in the separation chamber. The HCl that remains adsorbed onto the colloidal silicon dioxide surface is removed in the de-acidification chamber by washing with water vapour ($SiCl_4 + 2 H_2 + O_2 \rightarrow SiO_2 + 4HCl$). The HCl is easily separated as it remains in the gas phase, while the fumed silica is solid. The freshly formed hydrophilic Aerosil$^®$ can react with organosilicon compounds to form hydrophobic Aerosil$^®$. The hydrophobic Aerosil$^®$ formed is denoted "R" for repellent. Through hydrophobic treatment, the density of silanol groups per nm² decreases from approx. 2 for hydrophilic Aerosil$^®$ to approx. 0.75 for the hydrophobic types. Aerosil$^®$ 200 is a hydrophilic highly dispersed colloidal silicon dioxide, where the number 200 stands for the specific surface area of 200m^2/g as measured by the BET method. This conventional colloidal silicon dioxide has low bulk and tapped densities and can produce dust if handled improperly. In order to improve the handling of colloidal silicon dioxide, special mechanical processes were developed and patented by the company (Evonik) for the homogeneous compaction of colloidal silicon dioxide [5]. As a result, densified products characterized by the suffix "V" like Aerosil$^®$ 200 V and Aerosil$^®$ R 972 V have been recently introduced: Aerosil$^®$ 200 V is hydrophilic and chemically identical to Aerosil$^®$ 200. It differs from conventional colloidal silicon dioxide only in its higher tapped density and its larger secondary agglomerates. The compacted product Aerosil$^®$ R 972 V is hydrophobic, as a result of dimethyl silyl groups chemically bound to the silica surface [5, 42, 43].

2 Aim of this work

The assessment of flowability of powdered materials in the pharmaceutical industry is a crucial step and a prerequisite for a cheap, not time consuming successful production. The main purpose of this work was to employ the ring shear tester as a convenient, reliable and rapid tool for the quantitative evaluation and assessment of the flowability of pharmaceutical substances and mixtures. And to apply it as a quantitative comparative test which can replace other inaccurate and operator influenced conventional methods, which give only poor quantitative statement concerning flowability but are often used for their simplicity. In order to achieve the aim of this work, the investigations were carried out in different studies. The ring shear tester was applied to measure the flowability (flow properties) of a poor flowing active pharmaceutical ingredient and evaluate its flowability enhancement and improvement on the addition of different types and percentages (0.1, 0.5, and 2%) of silicon dioxide. On the margin of this study a comparison between the ring shear tester and other conventional methods was carried out. Also a correlation between the flowability and capsules weight content variation was investigated. The tester was used to measure the flowability of a set of binary mixtures, each comprising a poor flowing powder (either a pharmaceutical excipient or an active ingredient) and a free flowing pharmaceutical excipient. It was also used to evaluate the flowability improvement of these mixtures with different percentages of the free flowing substance as well as estimating the volume fractions yielding the best flowability. The packing behaviour of these binary mixtures was studied as well, taking advantage of the ability of the ring shear tester to directly measure the samples densities under a given consolidation stress. In another study the ring shear tester was used as a tool for the assessment and evaluation of the flowability of powdered lipids, which according to literature have never been assessed using such testers before, and evaluating their flowability enhancement in the absence and presence of silicon dioxide. However, in this work two

automated Schulze ring shear testers were also compared. Finally to summarize the aim of this work, the ring shear tester was employed as a tool to assess the flowability of single components or binary mixtures of pharmaceutical excipients and active ingredients, and evaluating their flowability enhancement by either addition of glidants or by introducing a free flowing substance in different fractions. It was also interesting to apply the ring shear tester for the assessment of powdered lipids flowability in the presence and absence of silicon dioxide.

3   Results and Discussion

3.1   Comparison between two ring shear testers of different size

3.1.1   Aim of this study

In this work two automated Schulze ring shear testers were compared. The Schulze testers are direct shear testers with rotational displacement and unlimited strain. The Schulze shear tester RST-01.pc (larger tester) and the Schulze shear tester RST-XS (smaller tester) were compared. A 200 ml shear cell was used for the measurements carried out on the RST-01.pc tester while a 30 ml shear cell was used for the measurements on the RST-XS tester (see Table 1). A set of binary mixtures of different active ingredients and excipients were prepared and a total of 189 measurements were carried out on each tester. These substances were mixed in the turbula mixer for 15 minutes then stored over night in a conditioned room at 21ºC and 45% RH. The concentration was calculated on volume to volume bases. For each sample, yield loci were measured using both Schulze testers. The preshear normal stress was constant about 5000 Pa. Four shear normal stress levels were selected namely 1000, 2000, 3000 and 4000 Pa. Comparison has been done between the measured ffc values. The flowability function was used to classify the flow behaviour of bulk solids according to Jenike´s powder classification (see section 1.3.2).

Table 1 Shear cells used in this work

SHEAR CELL	RST-01.pc	RST-XS
External diameter	200 mm	64 mm
Internal diameter	100 mm	32 mm
Shear canal depth	10 mm	10 mm
Shear canal volume	200 ml	30 ml
Shear speed*	1.5 mm/min	0.75 mm/min

* At the mean radius of the shear cell

3.1.2 Results

Experiments were carried out with a number of active ingredients and excipients. For further details about substances used, their mean particle size, shape, generic name and manufacturer see table 3 in section 3.3.2 as well as tables 5 and 6 in sections 6.1.1 and 6.1.2 respectively.

3.1.2.1 ffc values of binary mixtures

It was of interest to investigate the behaviour of binary mixtures comprising a poor flowing and a free flowing component. Therefore, a set of binary mixtures of different active ingredients and excipients were prepared (eleven different concentrations were prepared from each binary mixture) and a total of 189 measurements were carried out on each tester.
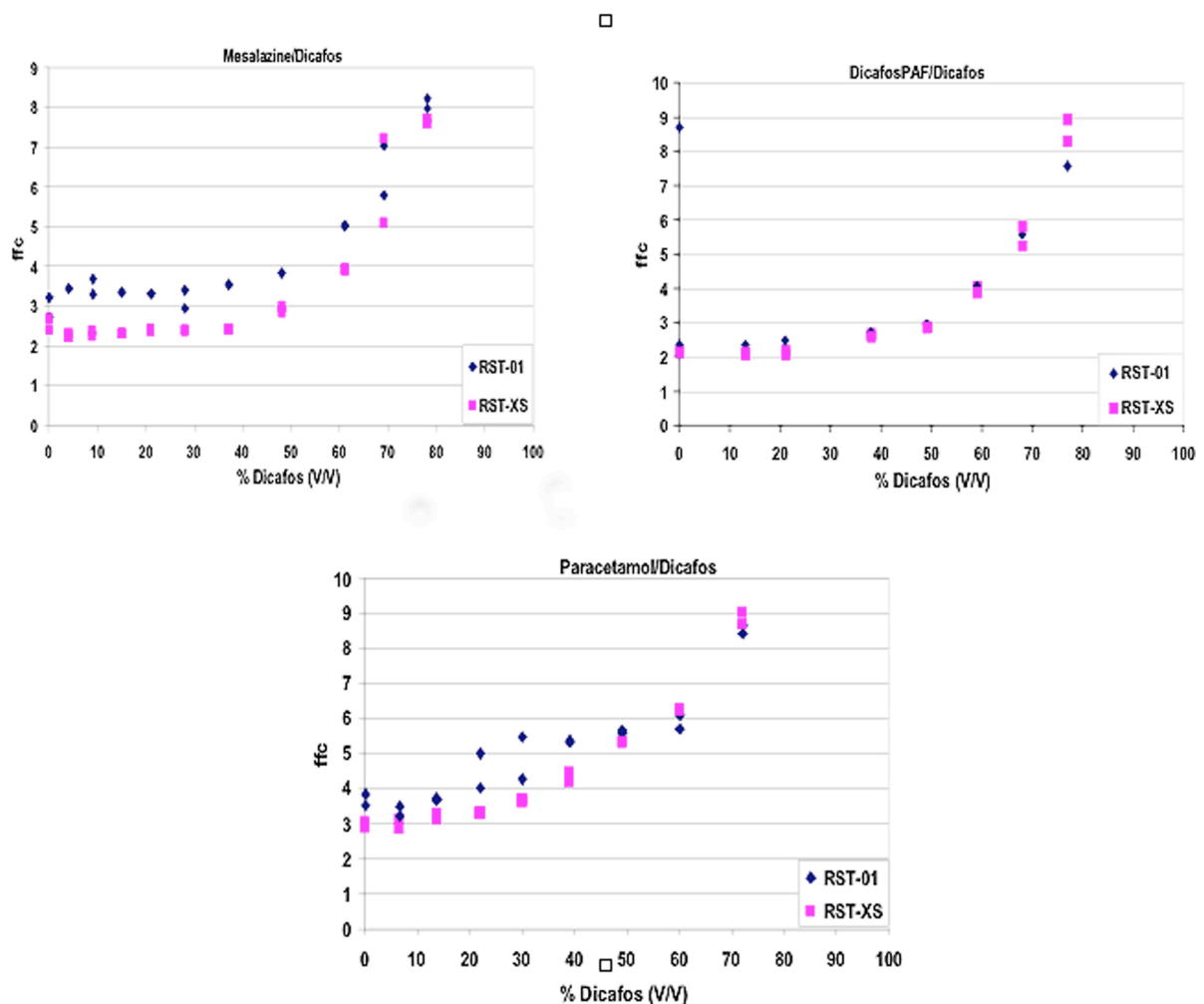
Fig. 11: ffc values of Dicafos mixtures with Mesalazine, Dicafos PAF & Paracetamol, n=2

As a conclusion, a non-linear relation between the ffc values and the volume fraction was observed, and the addition of small amounts of the poor flowing components Mesalazine, Paracetamol or Dicafos PAF decreased dramatically the ffc of the good flowing Dicafos, i.e. the poor flowing component dominated the flow behaviour of the mixtures, as will be discussed in details in section 3.4. It was also observed that the flow profiles (see figures 11, 12 and 13) of each mixture measured with both testers were not super-imposable, the smaller (RST-XS) tester showed slightly lower ffc values compared to the larger (RST-01.pc) tester.
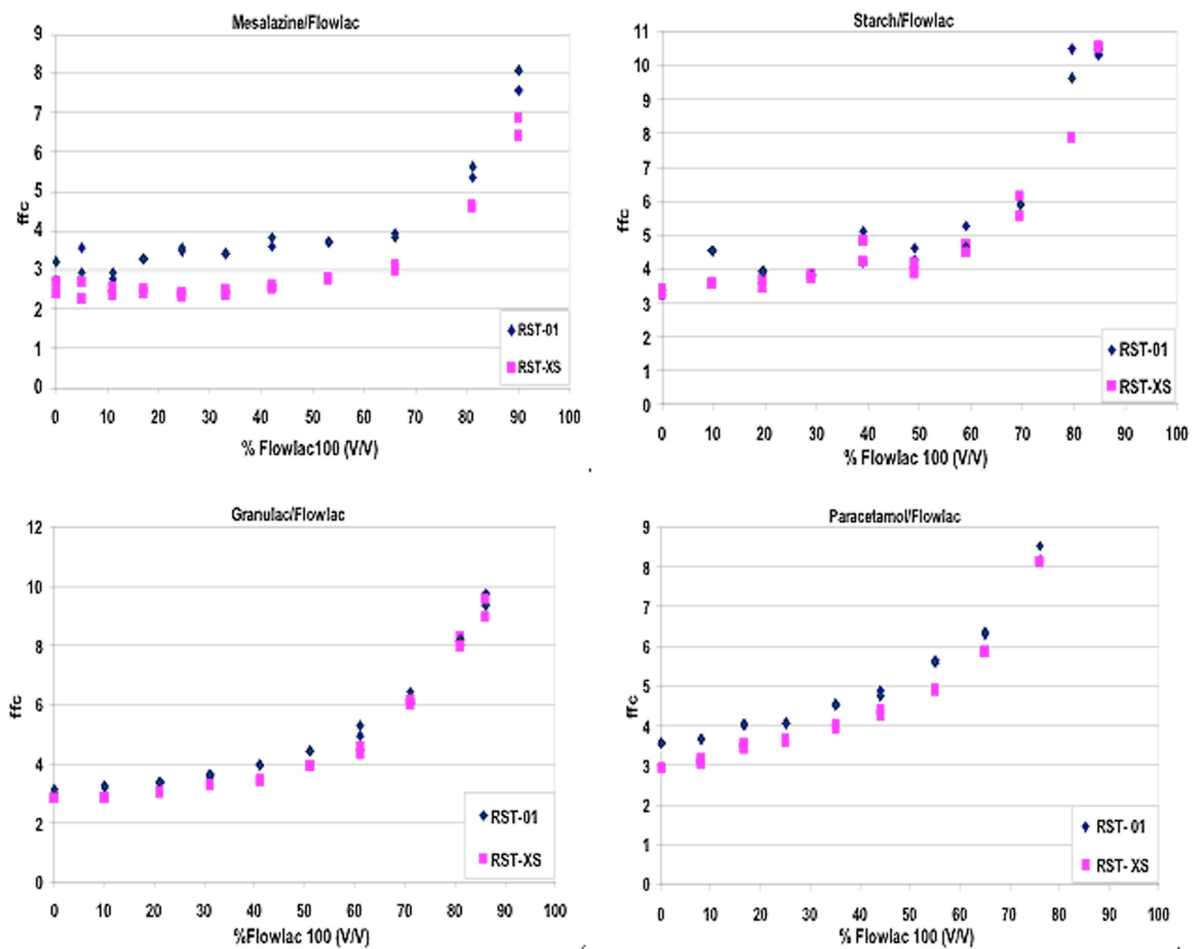
Fig. 12: ffc values of Flowlac 100 mixtures with Mesalazine, Starch, Granulac & Paracetamol, n=2
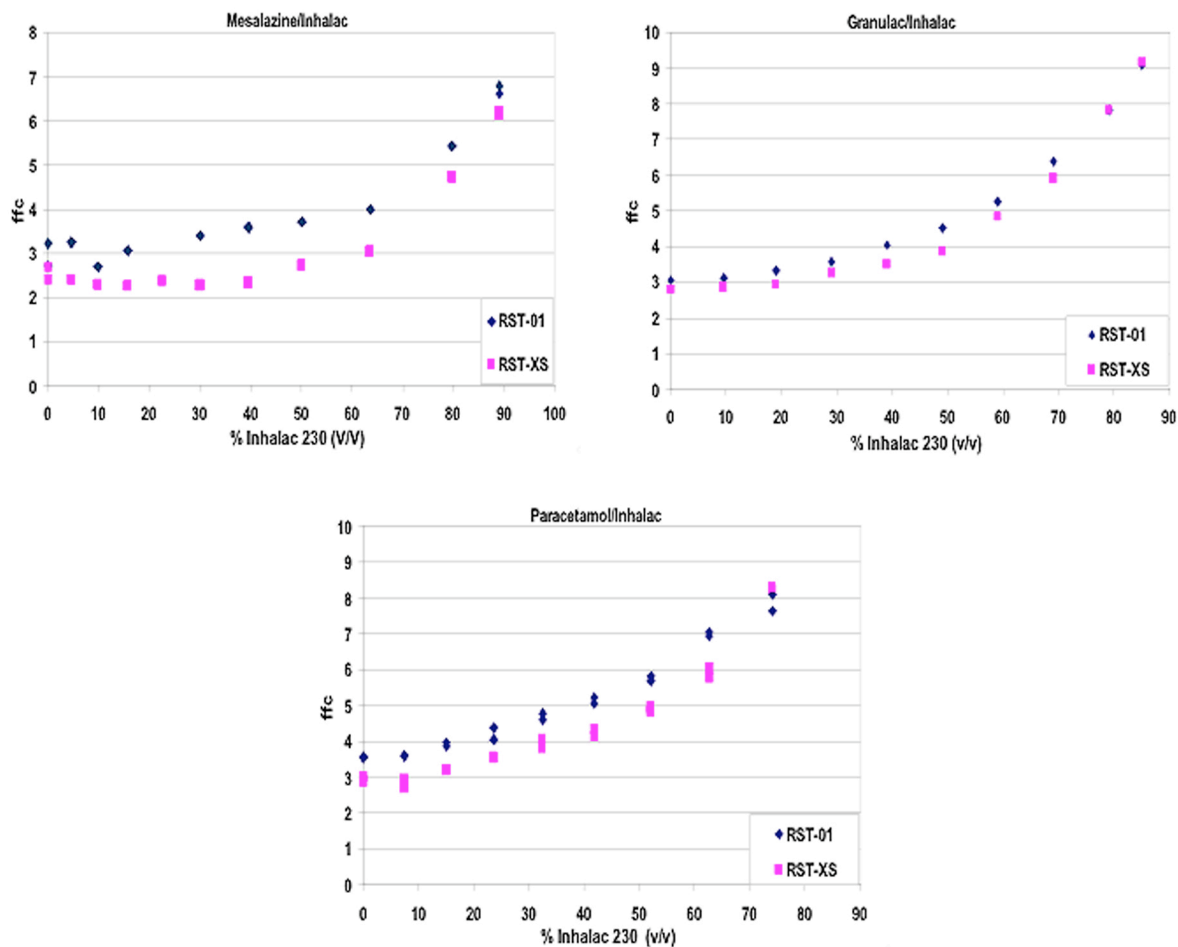
Fig. 13: ffc values of Inhalac 230 mixtures with Mesalazine, Granulac & Paracetamol, n=2.

It was observed that the degree of negative deviation of the flow profile measured with the small tester to that measured with the larger tester changes from one mixture to another and is most profound with mixtures comprising a needle shaped fine powder as the poor flowing component. However, some mixtures, especially those comprising the same molecule (chemical composition) but with two different flow behaviours, showed only a slight deviation, for example Dicafos PAF-Dicafos, Granulac-Flowlac and Granulac-Inhalac. Other mixtures such as Starch-Flowlac showed fluctuating results, and that is due to the slip stick effect which is a phenomenon caused as the surfaces alternate between sticking to each other and sliding over each other [2, 44] caused by the Starch.

3.1.2.2 Comparison of the large and small Schulze testers

Figures 14, 15 and 16 show the ffc values measured with both testers for binary mixtures with the three different excipients Flowlac 100, Dicafos and Inhalac 230 respectively. The mean ffc values from both testers plotted versus each other showed a good correlation with a correlation coefficient (r) ranging from 0.974 to 0.998, see table 2.
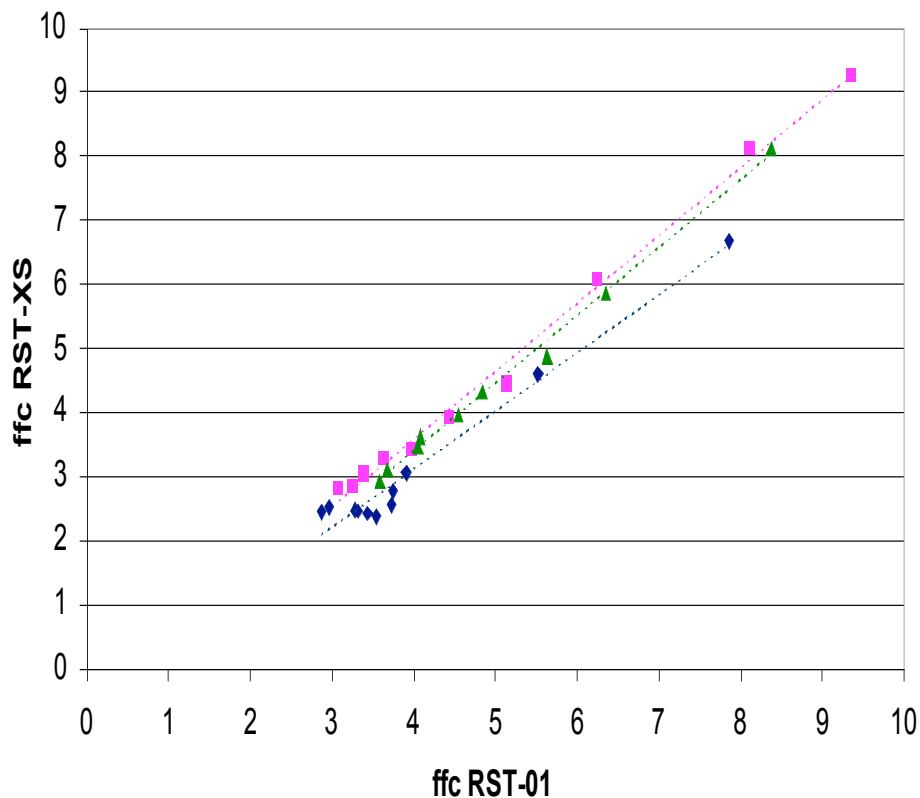
Fig. 14: Correlation between the ffc values from both large and small tester for binary mixtures of Flowlac 100, (♦) with Mesalazine, (■) Granulac 200 and (▲) with Paracetamol. Mean value of two measurements with regression lines; ffc values > 10 are not shown

Both testers led to low ffc values with cohesive mixtures and high ffc values with easy flowing mixtures. However, ffc values of free flowing samples which were more than 10 were not used in the comparison because these values were fluctuating; where the free flowing samples yield a very small Mohr circle with relatively small unconfined yield strength values (yield locus almost passes through the origin) see Fig. 10. So, the least deviation of the measurement values of the individual points of incipient flow would lead to larger changes of

30

the unconfined yield strength determined from the extrapolated yield locus towards the left in the area of very small stresses. These changes in the denominator (confined yield strength) lead consequently to large changes of the ratio σ_1 / σ_c [45]. Besides, values above 10 still referred to a free flowing mixture.
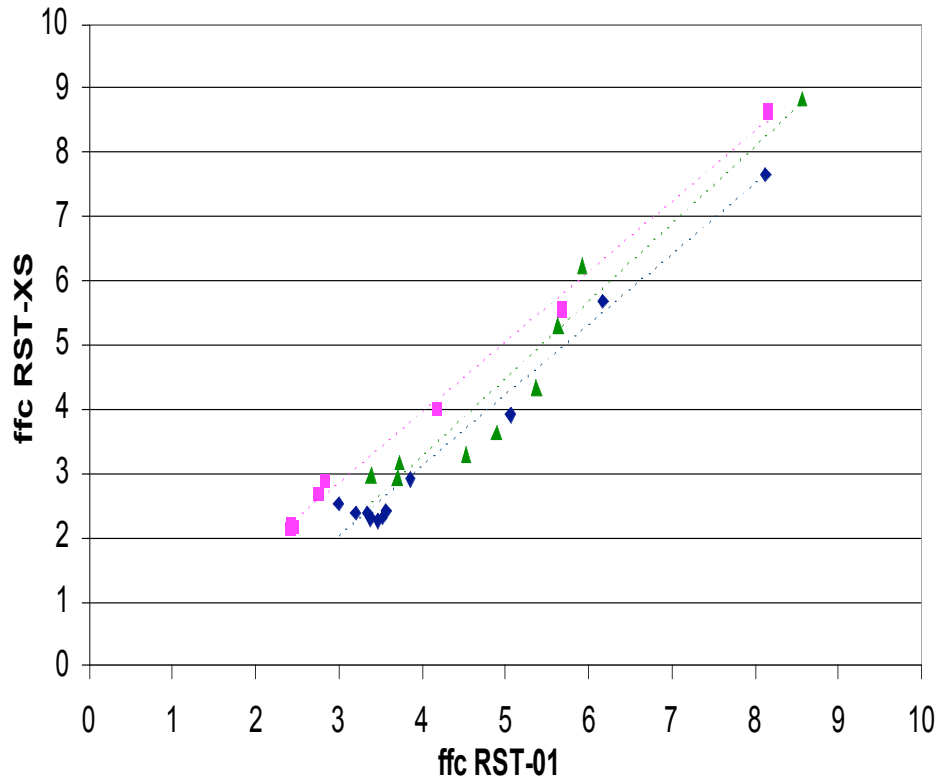
Fig. 15: Correlation between the ffc values from both large and small tester for binary mixtures of Dicafos, (♦) with Mesalazine, (■) Dicafos PAF and (▲) with Paracetamol. Mean value of two measurements with regression lines; ffc values > 10 are not shown

However, in order to compare both testers with one another the individual values from all measurements from both testers were plotted directly in Fig. 17. The easy flowing mixtures showed a broader ffc scatter while the cohesive powders showed a narrower scatter on both testers. Comparing the ffc values of both testers showed that the results were well correlated with a correlation coefficient r = 0.97. However, the smaller (RST-XS) tester showed slightly lower ffc values compared to the larger (RST-01.pc) tester.
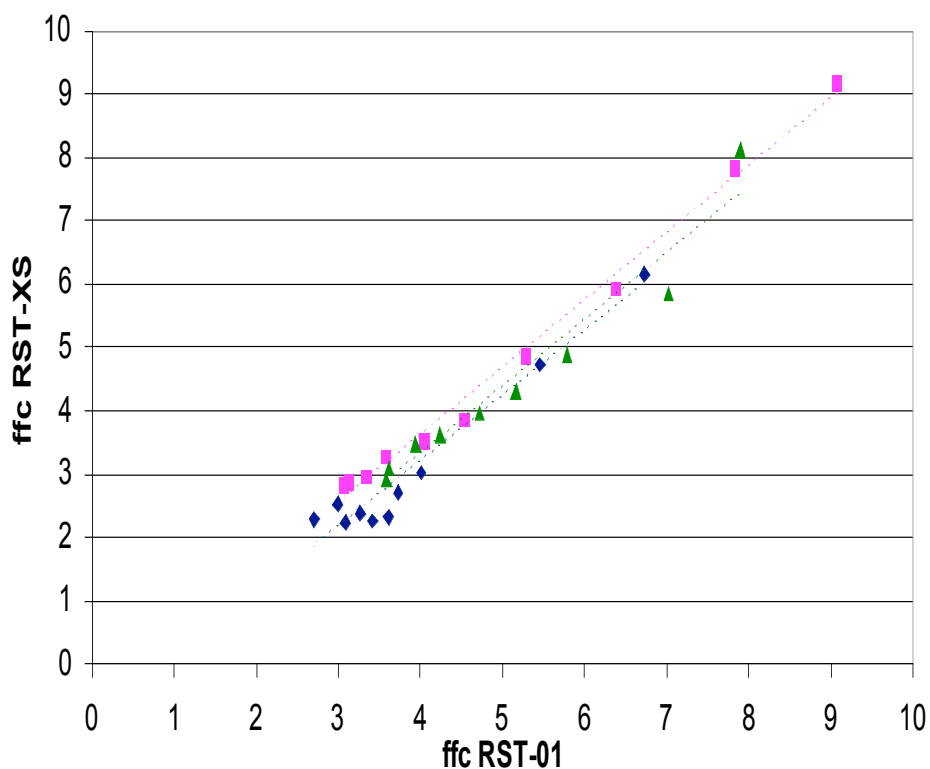
Fig. 16: Correlation between the ffc values from both large and small tester for binary mixtures of Inhalac 230, (♦) with Mesalazine, (■) Granulac 200 and (▲) with Paracetamol. Mean value of two measurements with regression lines; ffc values > 10 are not shown

Table 2: Slope, intercept and correlation coefficient r as represented with the linear regression equation for all binary mixtures

Component 1	Component 2	Slope	Intercept	r
Flowlac 100	Mesalazine	0.91	-0.5	0.986
Flowlac 100	Granulac	1.06	-0.64	0.997
Flowlac 100	Paracetamol	1.06	-0.81	0.998
Dicafos	Mesalazine	1.10	-1.3	0.989
Dicafos	Dicafos PAF	1.10	-0.50	0.998
Dicafos	Paracetamol	1.2	-1.6	0.969
Inhalac 230	Mesalazine	1.03	-0.93	0.976
Inhalac 230	Granulac	1.07	-0.65	0.996
Inhalac 230	Paracetamol	1.05	-0.86	0.974
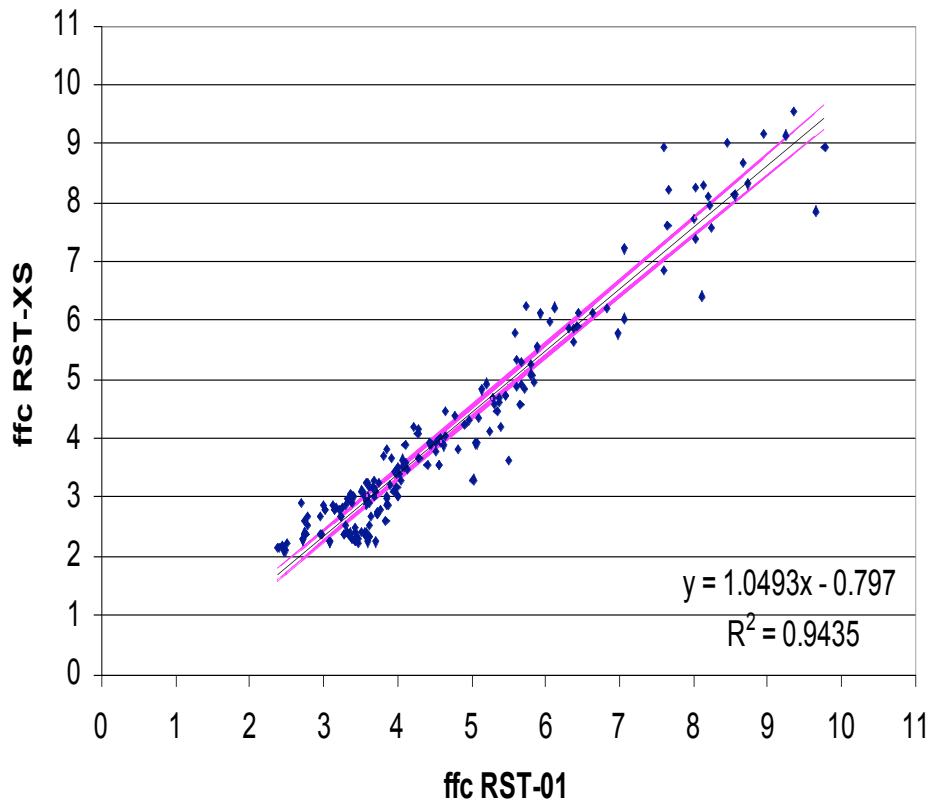
Fig. 17: Correlation between the ffc values from both large and small testers, regression line and 95% confidence interval of predicted mean (Y)

The 95% confidence intervals CI for the predicted mean (Y) was calculated (see Fig. 17). The confidence intervals for both slope and intercept were calculated as well, and it was observed that the CI for the slope does not enclose "1" (1.0493 ± 0.037) [1.012 to 1.086] and that for the intercept does not enclose "0" (-0.797 ± 0.180) [-0.98 to -0.62]. In other words the linear equation showed more or less a slope close to 1 and a negative intercept about 0.8 which indicates that the values determined using the small tester are always lower than those values determined with the larger one. Furthermore, the differences between the calculated Y values and the Y values calculated through substitution in the equation showed a maximum difference equal to 1.78 among all cases.

3.1.3 Discussion

As mentioned by Schulze [38] comparative tests with a standard shear cell showed that the smaller cell sometimes measured larger shear stresses compared to those measured with the standard cell (larger cell) and led to yield loci shifted towards larger shear stresses, which results in larger values of unconfined yield strength, and consequently lower ffc values (equation.4). In this work the small tester's cell with a cross sectional area about 25 cm^2 gave lower ffc values compared to the large tester with a 230 cm^2 cell, as estimated with the linear regression equation with a negative intercept equal approximately 0.8 which indicates that the values determined using the small tester are lower than those values determined with the larger one.

It was observed throughout all measurements that the smaller tester gave higher consolidation stresses as well as higher unconfined yield strength values compared to the larger tester. Consequently that led to lower ffc values. Generally, lower consolidation stresses in a range from 8895 to 9576 Pa were measured with the large tester compared to the smaller tester which measured a range from 9155 to 11217 Pa. However, the differences between the consolidation stress as measured with both testers was most obvious with the Mesalazine binary mixtures, where the smaller tester measured always a consolidation stress about 1500 to 2000 Pa more compared to that measured with a larger cell, consequently higher unconfined yield strength values were obtained. Differences above 500 Pa and less than 1000 Pa were observed with Paracetamol binary mixtures while differences less than 500 Pa were calculated with Granulac and Dicafos binary mixtures. These differences between the consolidation stresses measured on both testers might be due to the difference in the methods measuring the normal stress applied on the sample. Where, to achieve the normal stress required, a suitable normal load (given in Kg) is applied and divided by the area of the lid. However, regarding the large tester RST-01.pc a counterweight force (to counterbalance the

weight of the lid and all other parts connected to it) is known and taken into account experimentally when adjusting the normal load. On the other hand, the small tester RST-XS is not provided with a counterweight. Thus, here the normal stress is the result of the normal load exerted by the normal load system and the weights of the lid of the shear cell and the parts connected to it. This is taken into account arithmetically by the software RST-control 95 when adjusting the normal load [38].

Another argument could be also the ratio of cell size to particle size. Since the shear cells have significantly different size dimensions (with diameters 200 mm and 64 mm for the large and the small cells respectively) [46]. Schwedes and Schulze [23] investigated the influence of the ratio of shear cell diameter to particle size on the shear stress at steady state flow. It was found that the shear stress τ decreases with increasing D/x ratio (D: shear cell diameter and x: particle size) and levels out for high D/x ratios [22]. In this work the ratio of cell size to particle size varies widely, where $D/x_{50} = 1250$ for large tester to 400 for the small tester with the coarsest particle size ($x_{50} = 160~\mu$m) and a D/x_{50} about 40000 for large tester to about 12000 for the small tester with the finest particle size ($x_{50} = 5~\mu$m). As observed from the ratios, according to Schwedes and Schulze investigations it would be expected that the smaller tester will yield higher shear stresses compared to the larger tester consequently leading to slightly lower ffc values. However, that would not be the case comparing the very high D/x ratios observed in this work with those involved in Schwedes and Schulze investigations (maximum D/x ratio 300) [23].

Regardless the differences in composition, particle size (the finest about 5μm for Dicafos PAF and the coarsest about 160 μm for Dicafos) and shape (spherical, angular, needle like and irregular), comparing the ffc values of both testers showed that the results were well correlated with a correlation coefficient, r = 0.97. However, the smaller (RST-XS) tester showed slightly lower ffc values compared to the larger (RST-01.pc) tester according to the linear equation y= 1.0493x-0.797. For comparative tests this effect does not play a role as long as the same ring shear tester with the same shear cell size is used throughout the measurements. However, an advantage of the smaller cell is that a smaller amount of bulk solid is required for the measurements, because the internal volume of the small shear cell is only about 30 cm^3.

3.2 Investigating the influence of different Aerosil types and concentrations on powder flow using different methods

3.2.1 Introduction and objective

Good flow properties are critical to the successful development of any pharmaceutical tablet or capsule formulations to ensure quality and meet content uniformity specifications. Therefore, assessment of flow behavior is to be made in early stages in the development process so that an optimum formulation can be established, avoiding expensive and time-consuming studies of poor alternatives [7].

The flow properties of powders are often intentionally modified by the addition of flow additives, lubricants or glidants in order to improve their processability. The glidants promote powder flow by reducing inter-particulate friction and cohesion and therefore change the resistance to shearing and the flowability of the bulk powder [41].

The use of hard gelatine capsules as solid oral dosage forms is increasingly popular [47]. It has several advantages over using tablets such as taste masking or reducing levels of fillers used [48]. The relationship between capsule weight variation and powder flowability has been of interest for many research works, and contradictory observations were obtained [49]. Whereas some research groups suggested that good powder flowability might not be critical to achieve uniform weight content on a tamping type machine [49, 50], others reported an increase in weight variation with poorly flowing powders [49, 50, 51]. However, others suggested that an optimum flowability is required to achieve low weight variations [49, 51, 52, 53, 54].

The aim of this study is divided into two parts; the first part is concerned with investigating how the flowability of Paracetamol is influenced by different amounts and types of silicon dioxide (Aerosil®). A ring shear cell was used to measure shear properties, including their yield loci when pre-consolidated and their shear strength, measuring the so called flowability function (ffc). Besides other classical methods as the angle of repose, Hausner ratio and flow

rate were also used. The second part of this study investigates the variation in weight content of capsules filled with different Paracetamol / Aerosil® mixtures and relates it with their flowability (ffc values).

In this study silicon dioxide (fumed silica) was used as a glidant. The following types were used; Aerosil® 200, a hydrophilic and standard fumed silica, Aerosil® 200 V a hydrophilic and densified fumed silica, Aerosil® R 972 a hydrophobic standard and Aerosil® R 972 V, a hydrophobic, densified fumed silica were used as received from Evonik (Düsseldorf, Germany). Paracetamol was used as the poor flowing active ingredient as received from Ataby (Istanbul, Turkey). Empty hard gelatin shells size # 0 Capsule, from Capsugel. Further details about used substances are listed in section 4.1.1.

3.2.2   Results

Based on preliminary investigations, the Aerosil® concentration was set to 0.1, 0.5 and 2% w/w. The mixtures flowability was estimated using the Schulze ring shear tester RST-01.pc, angle of repose, Hausner ratio and flow rate as well. Besides, evaluation of the samples on a macroscopic level was carried out using the scanning electron microscopy. All experiments were carried out under similar conditions, 21°C and 45% relative humidity.

3.2.2.1 Flowability

The flowability was determined using a ring shear tester RST-01.pc with the cell type MV10. During the measurements the normal load of preshear was adjusted at 5000 Pa. Shearing proceeds at lower normal loads 1000, 2000, 3000, 4000 Pa consequently. The mean ffc value of 3 measurements was used. The ring shear tester's results (ffc) were depicted in Fig.18. The flowability of Paracetamol (ffc = 3.4) was generally improved on the addition of any of the Aerosil® types used.
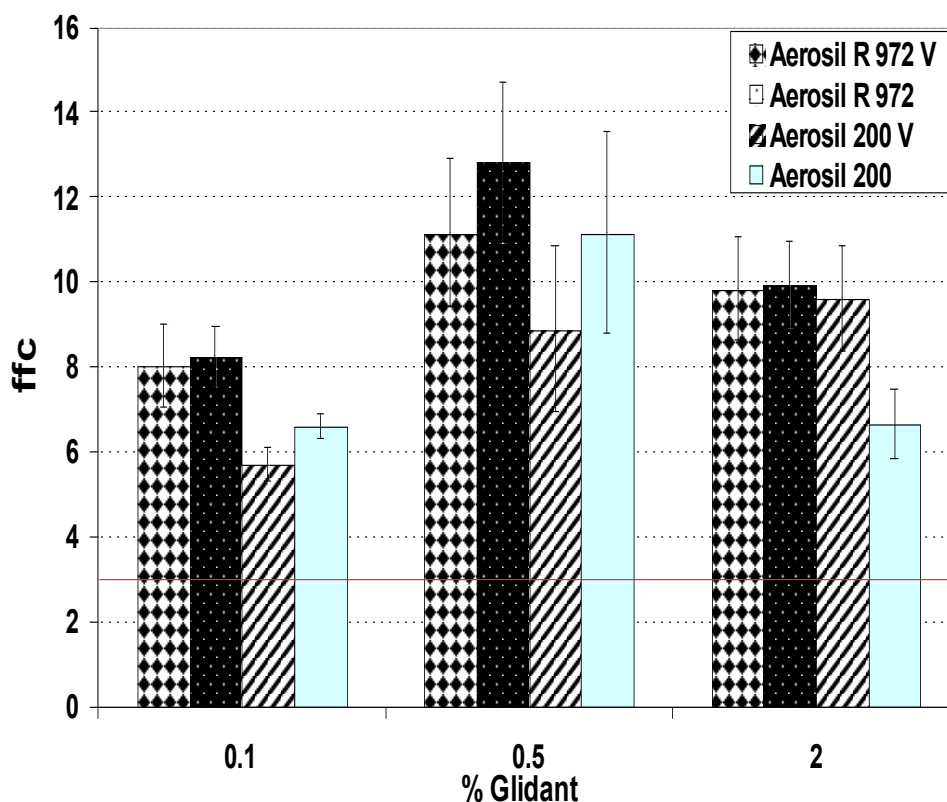
Fig.18: The ffc versus the percentage of glidant in the mixture, n=3 mean ± S.D. Paracetamol ffc = 3.4 ± 0.13

The ffc increased gradually as the percentage of glidant increased, until it reached a maximum with the mixtures containing 0.5% of either Aerosil[®] types, after which the ffc either remained constant or decreased. It was observed with the densified Aerosil[®] types (Aerosil[®] R 972 V and Aerosil[®] 200 V) that the ffc increased gradually as the percentage of glidant increased reaching a maximum with 0.5% and showed almost a constant behaviour with 2% glidant. On the other hand, the standard Aerosil[®] types (Aerosil[®] R 972 and Aerosil[®] 200) behaved also similarly concerning the maximum ffc value with 0.5% Aerosil[®] but showed a decrease in ffc with 2% Aerosil. It was also observed that the hydrophobic Aerosil types showed slightly higher ffc values compared to the hydrophilic types.

3.2.2.2 Conventional methods

As it was mentioned before that the first part of this work was concerned with measuring the flowability of both Paracetamol alone and together with four different glidants using a ring shear tester and correlating the results with those of angle of repose, Hausner ratio and flow rate.

3.2.2.2.1   Angle of repose

In Fig.19 the relation between the angle of repose and the percentage of Aerosil was shown. It was obvious that the angle of repose decreased as the percentage of Aerosil increased until it reached a minimum with 0.5%, after which it slightly increased or remained constant with 2% Aerosil. The hydrophobic Aerosil[®] types used had slightly lower angles of repose compared to the hydrophilic Aerosil[®] types. Correlating the angle of repose to the ffc, it was found that the angle of repose is inversely proportional to the ffc as shown in Fig.20, i.e. the angle of repose decreased as the ffc increased. Paracetamol showed an angle of repose = 58 degrees.
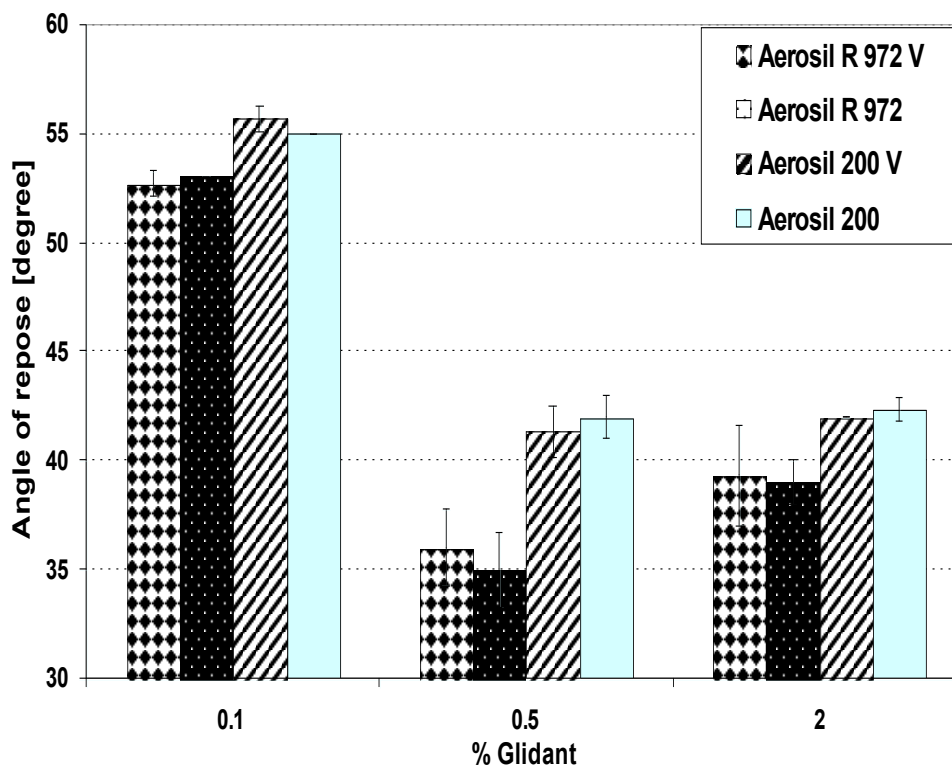
Fig.19: Angle of repose versus percentage of glidant in the mixture, n=3 mean ± S.D. Paracetamol = 58°

39
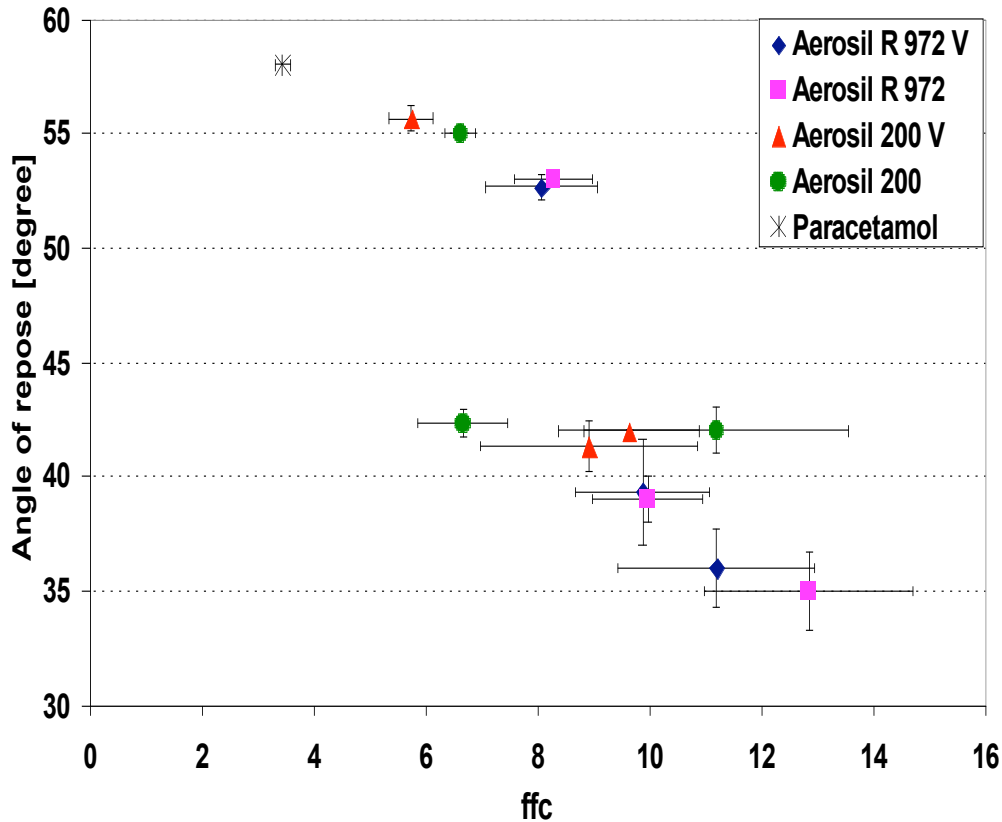
Fig.20: Angle of repose versus ffc, n=3 mean ± S.D.

3.2.2.2.2 Hausner ratio

It was observed that the Hausner ratio decreased with increasing the percentage of all Aerosil types (see Fig.21). Despite that decrease, no significant improvement in the flow behaviour was noticed. Plotting the Hausner ratio values versus those of ffc in Fig.22 showed no significant correlation. Where, the Hausner ratio results were within the range of the very bad flowing powders for Paracetamol (Hausner ratio = 1.58) and the range for both passable and bad flowing powders for the other mixtures containing different types and percentages of Aerosil (ratio between 1.22 and 1.54). These results complied with the ffc value of Paracetamol (ffc = 3.4) corresponding to cohesive powder flow, but did not comply with the ffc values of the other mixtures ranging between 4 and 13 and corresponding to easy and free flow behaviours. In this study the Hausner ratio was not a promising method for evaluating the flowability of Paracetamol in the presence of glidants, and its results were not in agreement with the ffc values.
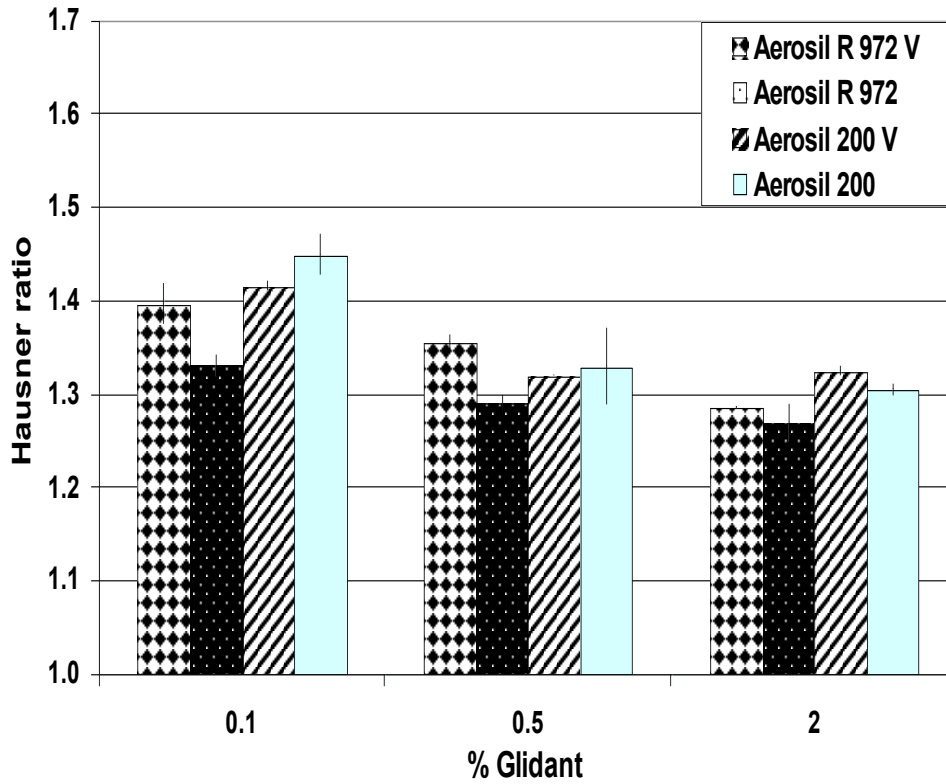
Fig.21: Hausner ratio versus % glidant, n=2, error bars indicating span (maximum / minimum values). Paracetamol = 1.58 ± 0.004
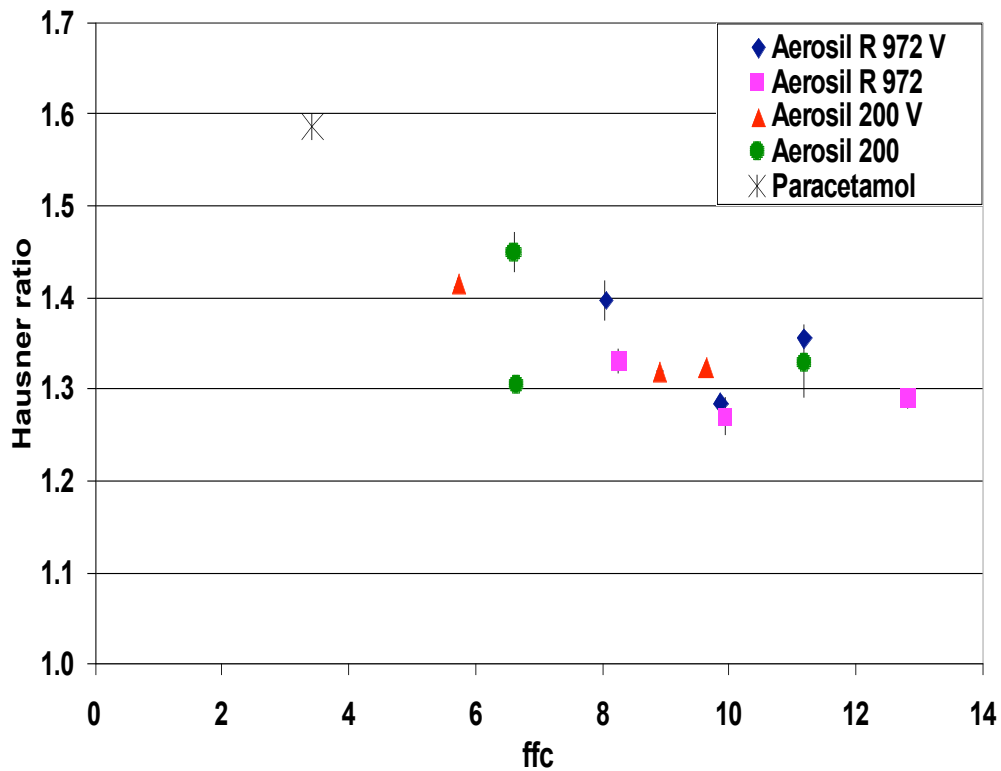
Fig.22: Hausner ratio versus ffc, n=2, error bars indicating span (maximum / minimum values)

3.2.2.2.3 Flow rate

Finally the flow rate results could not be shown because both the Paracetamol alone and its mixtures with 0.1% of any of the four glidants used in this study did not flow through the funnel. However, with the other two concentrations no general trend could be noticed.

3.2.2.3 Capsule filling

The second part of this work was concerned with studying the variation in weight of content of hard gelatin capsules, manually filled with Paracetamol alone and Paracetamol / Aerosil mixtures as well. The effect of the different Aerosil types and their different concentrations on the weight of content was investigated.

Three different formulations were prepared using each glidant. Each of which is prepared with different Aerosil® percentages 0.1, 0.5 and 2%, i.e. a total of 12 formulations. From each formulation three batches were produced (n=3), where each batch consisted of 30 capsules. Similarly, Paracetamol alone was filled in capsules as well. The mean weight content and the standard deviation of each batch were calculated. As shown in Fig. 23 capsules containing Aerosil® showed higher fill weights compared to capsules filled with Paracetamol alone. In other words the weight content was directly proportional to the ffc values. It was also observed that the hydrophobic Aerosil® types had slightly higher fill weights compared with hydrophilic Aerosil® types. The Uniformity in capsule filling was represented in terms of relative standard deviations (the mean value of three batches was used). It was observed that the capsules containing different types and percentages of Aerosil® possessed lower RSD values compared to capsules filled with Paracetamol alone. The easy (4 < ffc < 10) or free flowing (10 < ffc) samples had RSD percentages between 2 and 4%, while poor flowing samples (cohesive) had RSD values between 6 and 9%.
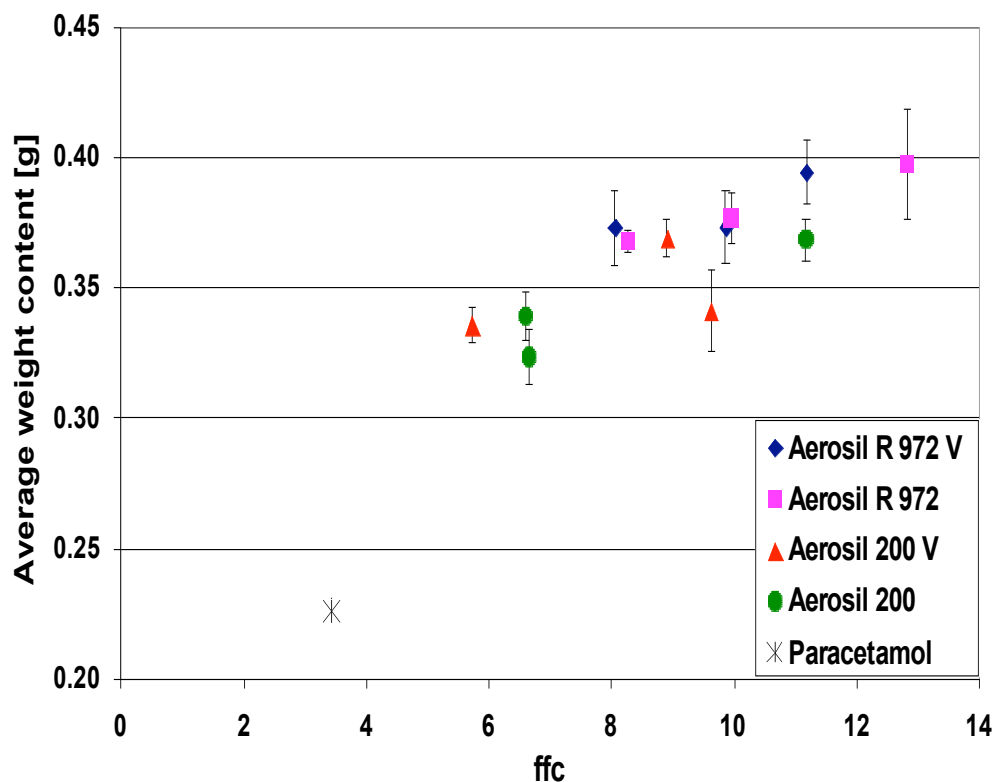
Fig. 23: Average weight content versus ffc values, n = 3 mean value ± S.D.

Fig.24 plots the mean relative standard deviation versus the flowability function. It showed that almost all formulations with Aerosil[®], those having higher ffc values, resulted in lower RSD% with less scattering values (with one exception, where a batch with Aerosil R 972V showed a higher RSD% and was marked as an outlier) compared to the formulation with Paracetamol alone which showed higher scattering values According to the classification of flowability function by Jenike. The Paracetamol is a cohesive powder because it has an ffc value of 3.4, while the other formulations are easy flowing powders having ffc values between 4 and 10 or free flowing having ffc values higher than 10. In other words uniformity in weight content can only be guaranteed by the introduction of glidants in the formulation which decreases the interparticle forces within a cohesive powder and improves its flowability, therefore facilitating the manual capsule filling process. However, comparing the RSD values of all capsules no significant difference could be observed between either the mixtures containing 0.1, 0.5 or 2% or the different types of Aerosil[®].
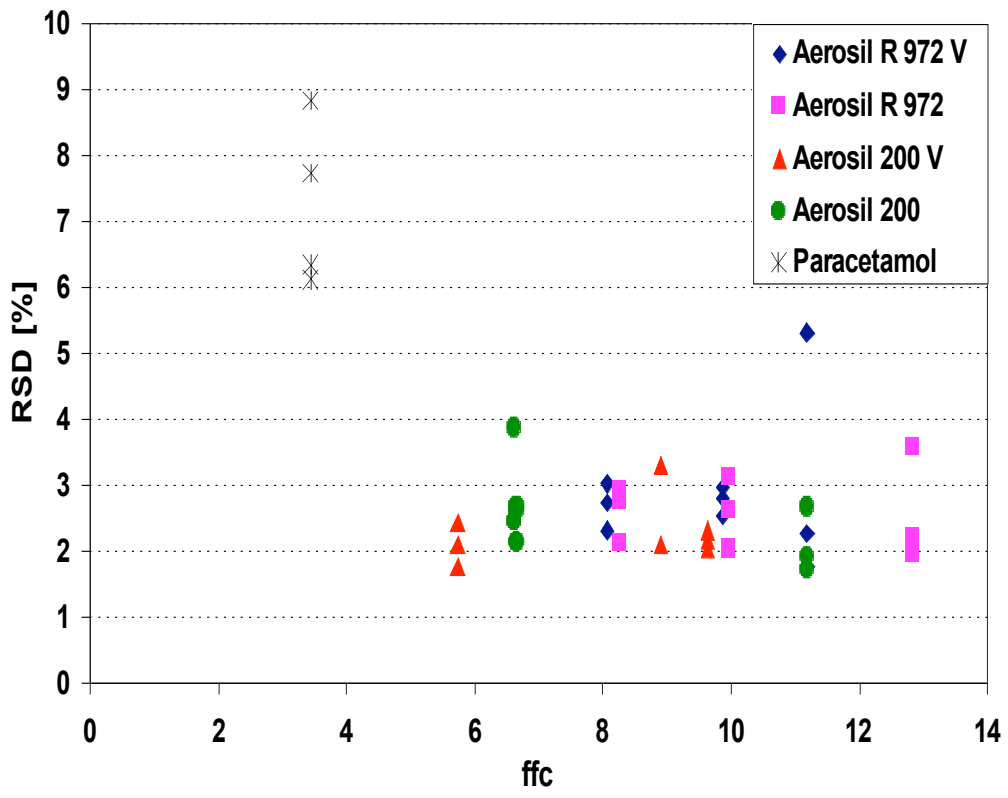
Fig.24: Relative standard deviation versus ffc for all batches.

3.2.2.4 SEM

Observing the SEM micrographs of the standard Aerosil® types (see Fig.24), it can be seen that with 0.1% Aerosil® 200 the amount of Aerosil® particles attached to the Paracetamol surface were hardly observed but still sufficient to increase the ffc of Paracetamol almost two folds. However, with 0.5% higher degree of coverage with small Aerosil® agglomerates could be observed on the surface leading to the maximum ffc values obtained. After that we can see a much more intense coverage of the Paracetamol particles with the 2% Aerosil® and bigger agglomerates could be observed. On the other hand, with the standard hydrophobic types more homogenous surface coverage was observed. Comparable to the hydrophilic type, a low surface coverage could be also observed with 0.1%, though it is considered higher in case of hydrophobic types. However, this amount was sufficient to improve Paracetamol flowability about 2.5 folds. At a concentration of 0.5% a homogenous dense surface coverage was observed with small Aerosil® particles or agglomerates. Similarly the 2% concentration showed a dense surface coverage but large Aerosil® particles or agglomerates could be observed.

Regarding the densified types (see Fig.24), the hydrophilic type showed inhomogeneous surface coverage which was hardly detectable with 0.1% and was highest with 2%, where large Aerosil® agglomerates could be detected. The hydrophobic Aerosil showed a similar behaviour to its standard analogue. Generally, it was observed that the surface coverage was denser and much more uniform and homogenous with the hydrophobic types compared to the hydrophilic ones.
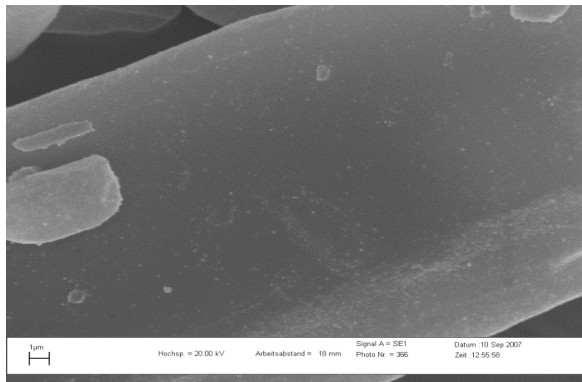
0.1% Aerosil 200

0.1% Aerosil R 972
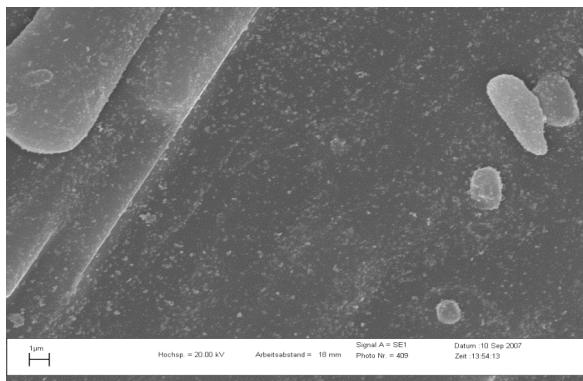
0.5% Aerosil 200
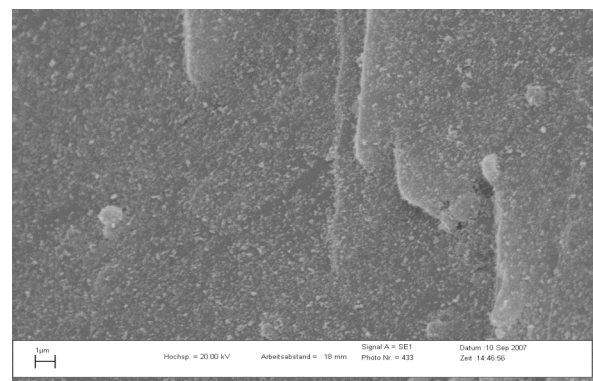
0.5% Aerosil R 972
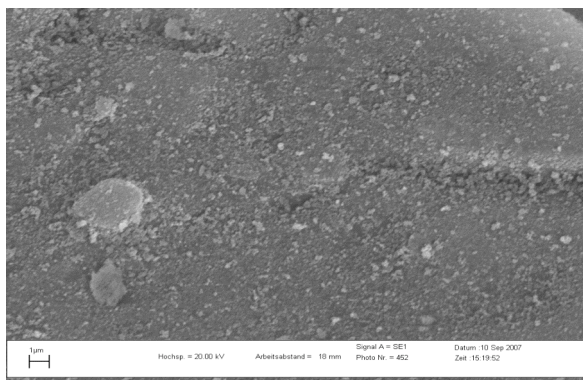
2.0% Aerosil 200
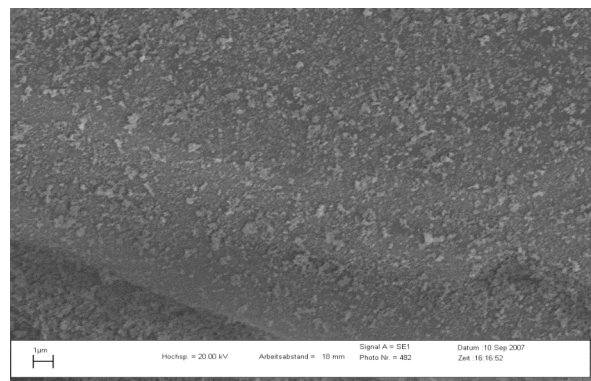
2.0% Aerosil R 972

Fig.24: SEM micrographs of Paracetamol with different percentages of standard hydrophilic (left) and hydrophobic (right) Aerosil
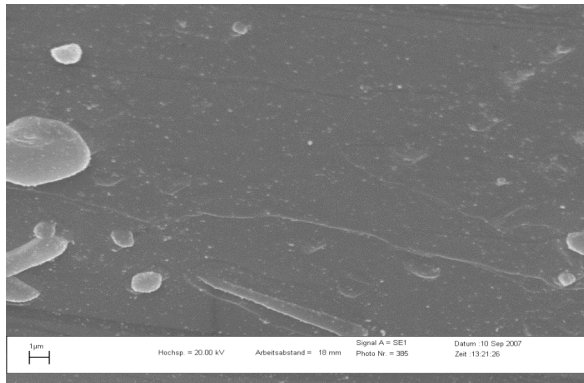
0.1% Aerosil 200 V
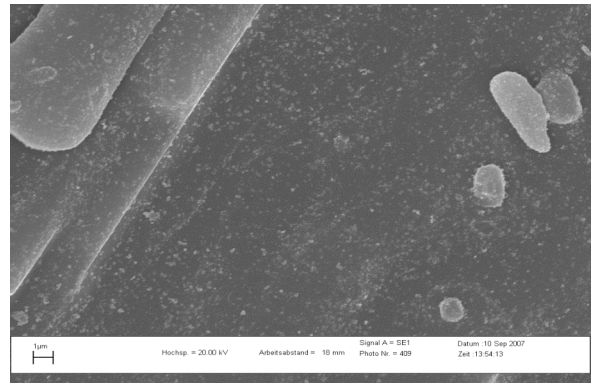
0.1% Aerosil R 972 V
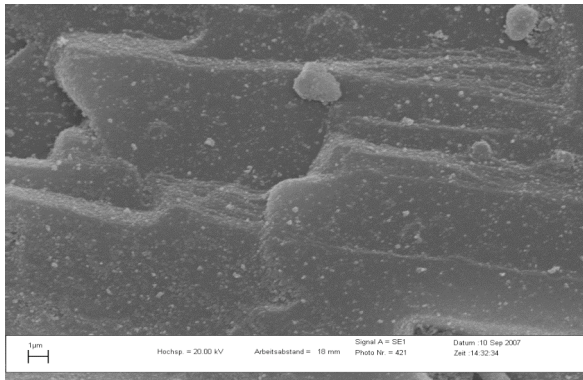
0.5% Aerosil 200 V
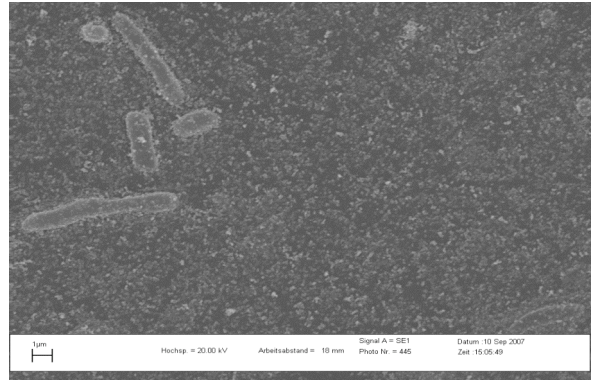
0.5% Aerosil R 972 V
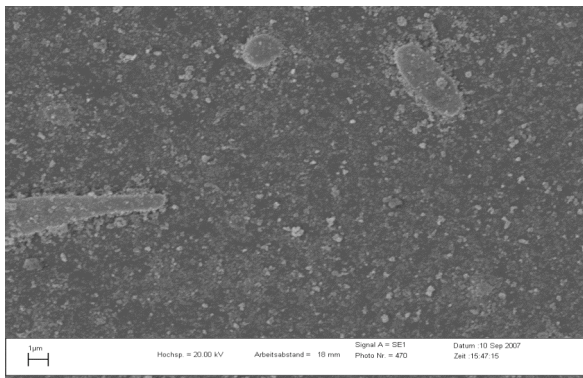
2.0% Aerosil 200 V
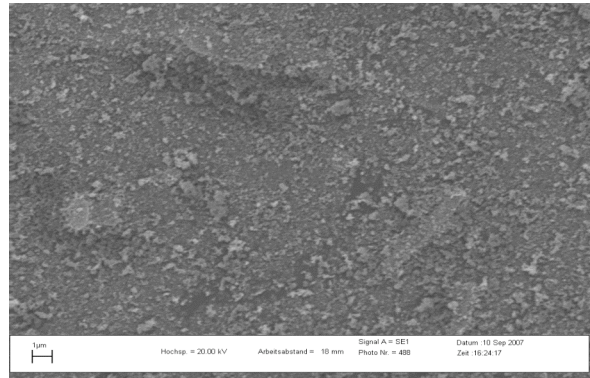
2.0% Aerosil R 972 V

Fig.24: SEM micrographs of Paracetamol with different percentages of densified hydrophilic (left) and hydrophobic (right) Aerosil

3.2.3 Discussion

In the first part of this study the influence of different types of Aerosil® on the flowability of Paracetamol was investigated by means of a ring shear tester, angle of repose, Hausner ratio and flow rate. It was observed that the ffc values increased with the increase of Aerosil® percentage, and then it either decreased or remained constant by further increase in percentage. The cohesive forces acting between particles are also dependent on the contact area between particles, i.e. the higher the contact area, the higher the cohesive forces. However, in dry powder the van der Waals forces are the prevailing inter-particular forces. According to Rumpf [19] roughness reduces the interparticle forces, and the smaller the particles adsorbed on the surface, the stronger the reduction of the van der Waals forces and the better the flow improvement. Here Aerosil® acts as surface roughness between Paracetamol particles. Therefore, decreasing the contact area and increasing the distance between interacting particles, in turn, decreasing van der Waals forces and enhancing the powder flowability.

It has been stated in literature that there are two main factors responsible for Aerosil® effect: the first is the degree of coverage of the Aerosil® particles or agglomerates on the particle's surface, and the second is the size of the Aerosil® agglomerates adhering to particle's surface, where smaller agglomerates are preferable for flow enhancement [5, 16, 40, 55, 56]. Therefore by applying these two factors on our findings, it is obvious that the ffc values increased by increasing the percentage of Aerosil®, because by increasing the amount of Aerosil® there are more agglomerates available to adhere to the particles surface, causing a higher degree of coverage and consequently decreasing the resistance to shearing and obtaining higher ffc values. The observed decrease or constant values of ffc at a certain percentage of Aerosil® may be explained according to Meyer [16, 40] who stated that with increasing glidant concentration a higher amount of Aerosil® is available, and its breakage

during the mixing process becomes incomplete. Consequently, the size of the attached agglomerates increases. The big agglomerates create a larger contact area when two particles touch. As agglomerates size increase a contact between the agglomerates themselves is established increasing the intermolecular forces between them, i.e. Van der Waals forces [16, 40]. Also Dünisch proved that even though further adsorption of nanomaterial reduces direct forces between carrier particles, but interparticular forces between nanomaterial particles themselves increase [57]. Similarly, Aerosil® agglomerates attached to the Paracetamol surface are larger in size at higher concentrations, so that agglomerate-agglomerate contact points are established. These contact points increase as the glidants concentration increases consequently inducing van der Waal forces.

Concerning the conventional methods tested the angle of repose decreased as we increased the percentage of Aerosil®, where the angle of repose was inversely proportional to the ffc values. The Hausner ratio did not agree with the ffc values. The flow rate also could not be measured for all samples, and the ones measured did not reveal any general trend.

An explanation to the slightly higher ffc obtained using hydrophobic Aerosil® types compared to hydrophilic types, depends on the different chemical structures of both types. The hydrophilic type contains silanol groups on its surface which are bound together through hydrogen bonds which are difficult to break up. The hydrophobic type is as a result of dimethyl silyl groups chemically bound to the silica surface, so they lack the hydrogen bonds and the alkyl groups are bound through van der Waal forces instead which are easily broken allowing a higher degree of coverage [5, 55].

The second part of this work was concerned with studying the variation in weight content of hard gelatine capsules, manually filled with paracetamol as well as Paracetamol / Aerosil® mixtures. The effect of the different Aerosil® types and their different concentrations on the weight content was investigated. It was observed that the capsules containing Aerosil® showed lower RSD values and higher fill weights compared to capsules filled with

paracetamol alone. However comparing the RSD values for all capsules, no significant difference could be observed between the mixtures containing 0.1, 0.5 or 2% Aerosil®, or between different types of Aerosil, i.e.; no specific trend was observed.

The improved flowability of the paracetamol / Aerosil® mixtures is due to Aerosil®, which as a glidant enhances the Paracetamol flow in the capsules shells by reducing the inter-particulate forces between the Paracetamol particles and increasing the roller friction compared to the sliding friction. Therefore, during tapping, the paracetamol particles move closer to each other reducing the space between them and consequently obtaining higher densities and fill weights [5].

3.3 Flow behaviour of binary mixtures with different concentrations:

3.3.1   Introduction and objective

In pharmaceutics the substances are not used individually as single components, but they are rather used as multi-component mixtures and formulations. The flowability assessment of these mixtures is a crucial and essential requirement and a prerequisite for a successful production. In addition to flow properties information about packing properties of powders is important as well especially in the production of solid dosage forms, where volumetric filling of a capsule or a die is desired [58, 59]. This information is also valuable in the production of powdered products in order to be packed in suitable containers, consequently reducing the space they may occupy during transportation and storage [60].

Several studies have been carried out and different models have been proposed to predict the packing properties of powders. The packing density is governed by the size ratio of coarse particles to fine particles and the volume fraction of both of them [58]. Among all proposed models none of them is able to predict maximum in volume reduction by application of vibration, small pressure or simple tapping [58]. The Kawakita model mainly relates the degree of volume reduction to the applied pressure, but it can also be employed to study the volume reduction of powder due to tapping [58, 59]. Using this model no direct packing density could be measured but only the maximum volume reduction due to packing as expressed by the Kawakita constant (a). Besides, inaccurate tapped density values could be measured according to the tapped density volumeter used, where after an initial densification of the powder a redispersion of the particles may occur [58]. One of the properties measured with the ring shear tester is the bulk density under certain consolidation, so it was interesting to apply this device to obtain directly packing densities of powders. The advantage of this procedure over comparing the loose density to its tapped density is that here the bulk density is a result of a well defined stress [2].

The aim of this work was to study the flow behaviour and the packing density of binary mixtures, combining a fine poor flowing powder with a coarser free flowing powder. Three different free flowing excipients were used for this purpose, namely Dicafos, Flowlac 100 and Inhalac 230. The poor flowing substances are mentioned in table 3. The flow properties for these binary mixtures were measured using the ring shear tester, RST-01-pc.

3.3.2 Results

A number of excipients and active ingredients were used in this study, see the following table.

Table 3: Active ingredients and excipients used in these experiments

Substance	Generic Name	True Density g/cm^3*	Bulk Density g/cm^3**	Mean Particle Size µm***	% Porosity****	ffc	Particle Shape
Flowlac 100	Lactose	1.53	0.67	130	56	20	Spherical
Inhalac 230	Lactose	1.52	0.70	112	51	17	Angular
Granulac 200	Lactose	1.54	0.70	30	49	3	Irregular
Di-Cafos	Dicalcium phosphate	2.31	0.82	160	64	21	Irregular
Dicafos PAF	Dicalcium phosphate	2.89	1.15	5	60	2.5	Irregular
Starch	Starch	1.52	0.60	12	58	3	Spherical
Mesalazine	Mesalazine	1.53	0.35	11	79	3	Needle
Paracetamol	Acetaminophen	1.27	0.50	34	58	3.5	Rod like
Praziquantel	Praziquantel	1.22	0.30	3	78	2	Needle

*measured using a helium pycnometer AccuPyc 1330 (Micromeritics GmbH, Mönchengladbach)
**measured with the ring shear tester Rst-01.Pc (at normal load = 5KPa)
***measured using a laser diffraction spectrometer (Helos/KF-Magic, Sympatec GmbH, Clausthal-Zellerfeld, Germany) using the dry-dispersing system (Rodos, Sympatec GmbH, Clausthal-Zellerfeld, Germany)
****Porosity calculated from bulk density and true density (see section 6.3.2)

3.3.2.1 Dicafos mixtures

3.3.2.1.1   ffc results

In Fig. 25 the flow behaviour of Dicafos mixtures was plotted as (log ffc) values versus the ascending concentration of the free flowing powder. The log values were used in order to obtain a linear function and interpret the results easily.
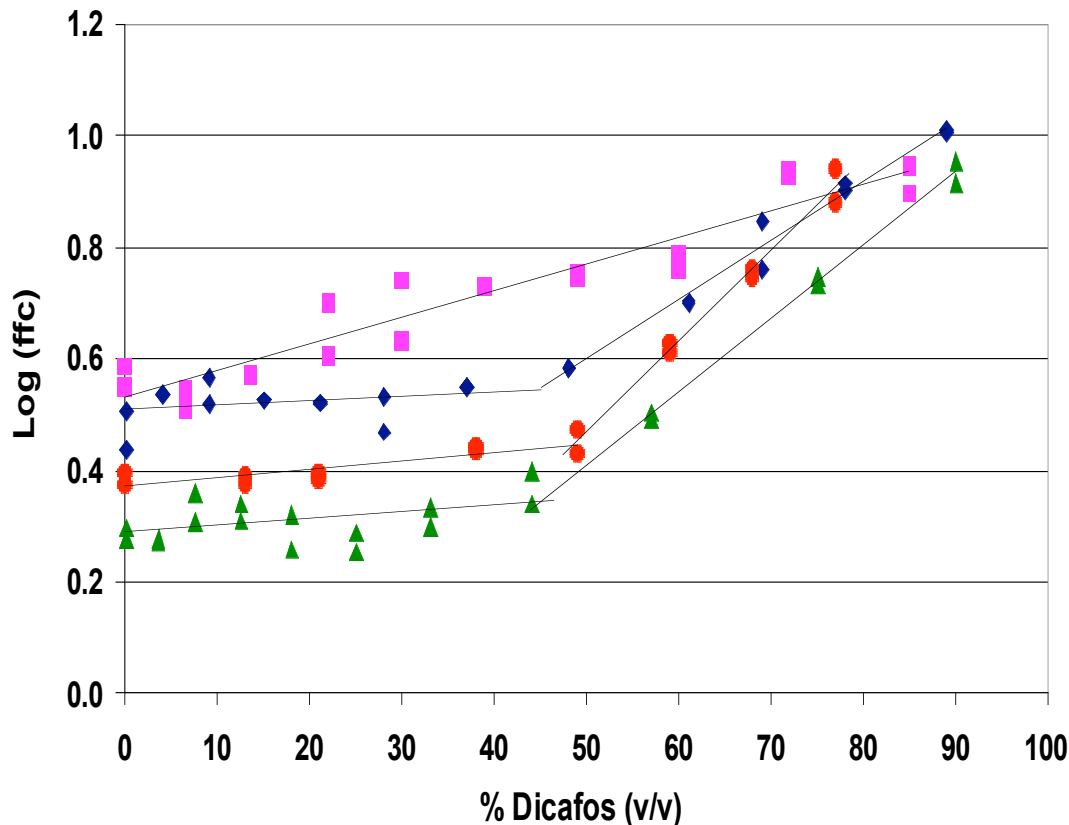
Fig. 25: Log **(**ffc) versus % Dicafos (V/V) with Paracetamol (■), Mesalazine (♦), Dicafos PAF (●) and Praziquantel(▲), n=2.

The flow behaviour of Mesalazine-Dicafos mixtures (fine needle shaped poor flowing and coarse irregular free flowing powders) was represented by two curve sections. The first section of the curve was almost steady and parallel to the x-axis indicating cohesive flow and no improvement of flowability, while the second section of the curve was steep indicating easy flow and flowability improvement. The two sections intersected at approx. 45% V/V Dicafos, after which the flow behaviour of these mixtures changed from cohesive flow to easy

53

flow behaviour. In other words, the flow behaviour of these mixtures was not sufficiently influenced with Dicafos concentrations less than 45%.

Similarly, the flow behaviour of the Praziquantel-Dicafos mixtures (fine needle shaped poor flowing and coarse irregular free flowing powders) was represented by two curve sections. The first section indicated cohesive flow behaviour, while the second section indicated improvement in flowability. The two sections intersected at approx. 45% V/V Dicafos. Similar to Mesalazine-Dicafos mixtures the flow behaviour of these mixtures was not sufficiently influenced or improved with Dicafos concentrations less than 45%. The flow behaviour of Dicafos PAF-Dicafos mixtures (fine irregular poor flowing and coarse irregular free flowing powders) was represented as well by two curve sections. Intersection point was around 48% V/V Dicafos, after which the flow behaviour of these mixtures was improved. Differently than the previous mixtures the flow behaviour of the Paracetamol-Dicafos mixtures (fine rod shaped poor flowing and coarse irregular free flowing powders) was represented only by one curve. The log ffc values increased proportionally with the increase in the percentage of Dicafos in the mixtures. The linear relation indicates flowability enhancement with very low concentrations of Dicafos (approx. 20% V/V) compared to the previous mixtures.

In the previous Fig. 25 we may conclude that the particle size rather than the particle shape influences to a great extent the flow behaviour of the binary mixtures. It was observed that the flowability of the mixtures increased as the particle size of the poor flowing component increased regardless its shape, where Mesalazine, Praziquantel and Paracetamol have almost the same shape but showed different flow behaviours. Flowability of Dicafos mixtures according to the poor flowing constituent could be arranged as follows; Paracetamol > Mesalazine > Dicafos PAF > Praziquantel-Dicafos mixtures noticing that the mean particles size are 34, 11, 5 and 3μm respectively. It was also observed that Paracetamol-Dicafos mixtures revealed a flow improvement from the beginning where only a concentration about

20% (V/V) Dicafos was enough to obtain an easy flow behaviour (4 < ffc < 10), respectively (0.6 < log (ffc) < 1). On the other hand, the Mesalazine, Dicafos PAF and Praziquantel-Dicafos mixtures showed almost the same flow profile, where all the mixtures showed almost steady ffc values at the beginning then after a kink in the curve (considering the two curves to be one and the intersection point to be the kink) they showed improvement in the flow behaviour. The kink (intersection point) is considered as the critical concentration of the free flowing constituent after which flowability is improved. It was generally observed that, it made no difference whether a fine needle or irregular shaped component was blended with the coarse irregularly shaped Dicafos, as long as the particle size was small enough to fit within the pores of Dicafos. However, the flowability increased as the size of the fine component increased.

3.3.2.1.2 Density results

As observed in Fig. 26 the density-concentration figures showed two different profiles according to the shape of the fine poor flowing component in the mixtures. The needle or rod shaped particles namely; Mesalazine, Praziquantel and Paracetamol showed a proportional increase in density with increasing the percentage of Dicafos and showed no maximum packing density. On the other hand the irregular particles (Dicafos PAF) showed an increase in the density with increasing the Dicafos percentage and reached a maximum packing density at 21% V/V. After reaching a maximum the density decreased with the further increase of Dicafos percentage.
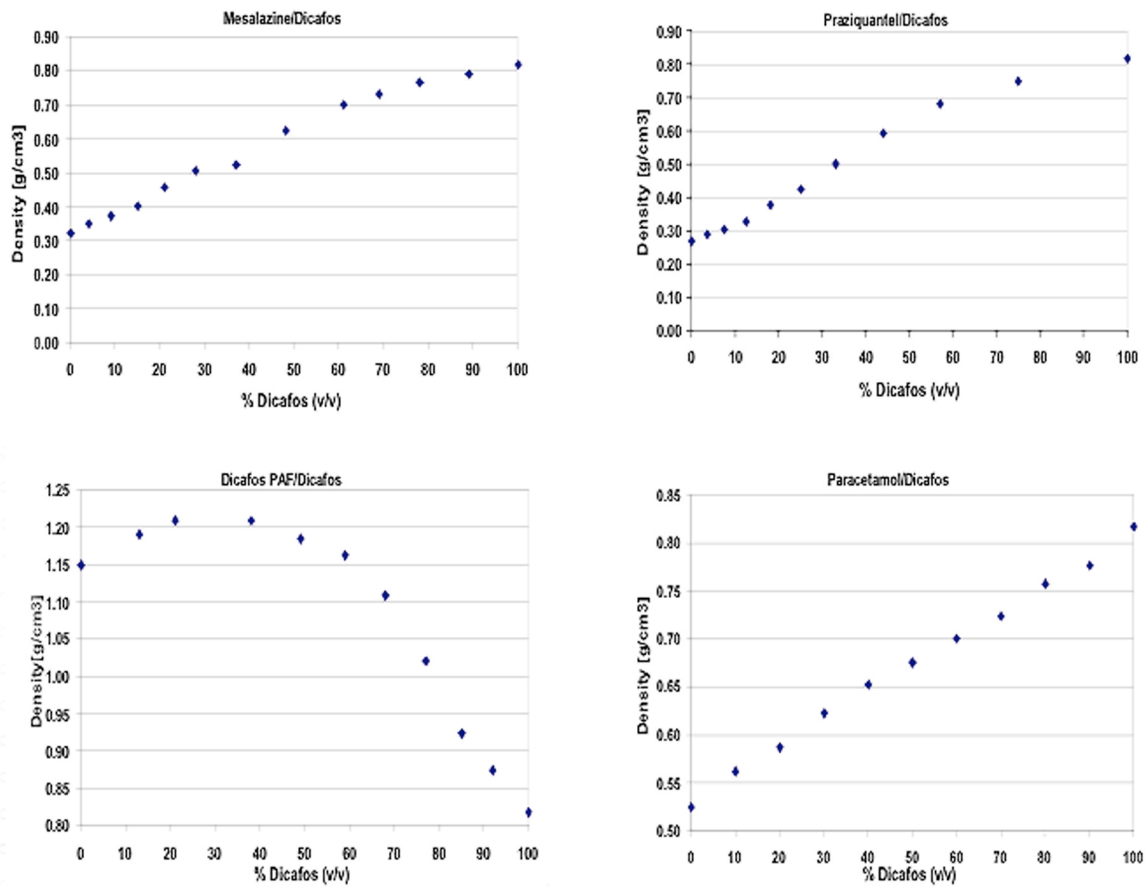
Fig. 26: Density versus percentage of Dicafos (V/V) for all four Dicafos mixtures (notice different scale of y-axis)

3.3.2.2 Flowlac mixtures

3.3.2.2.1 ffc results

In Fig. 27, the flow profile of Mesalazine-Flowlac mixtures (fine needle shaped poor flowing and coarse spherical free flowing powders) was also represented by two curve sections. The curve sections intersected at approximately 70% V/V Flowlac, above which an observable flow improvement was noticed. Regarding, Starch-Flowlac mixtures (fine spherical poor flowing and coarse spherical free flowing powders) already showed easy flow behaviour from the beginning. However, the first curve section was steady indicating no further improvement, while the second curve section was steep referring to further flow improvement. Flow improvement was obtained after the intersection point at 58% V/V Flowlac. The flow profile

of Granulac-Flowlac mixtures was represented by two curve sections intersecting at approximately 50% V/V Flowlac. Similar to what has been observed with Paracetamol-Dicafos mixtures, Paracetamol-Flowlac mixtures (fine rod poor flowing and coarse spherical free flowing powders) were represented only by one curve, referring to the low concentration of Flowlac (approx. 17%) required to improve the flow behaviour of such mixtures.
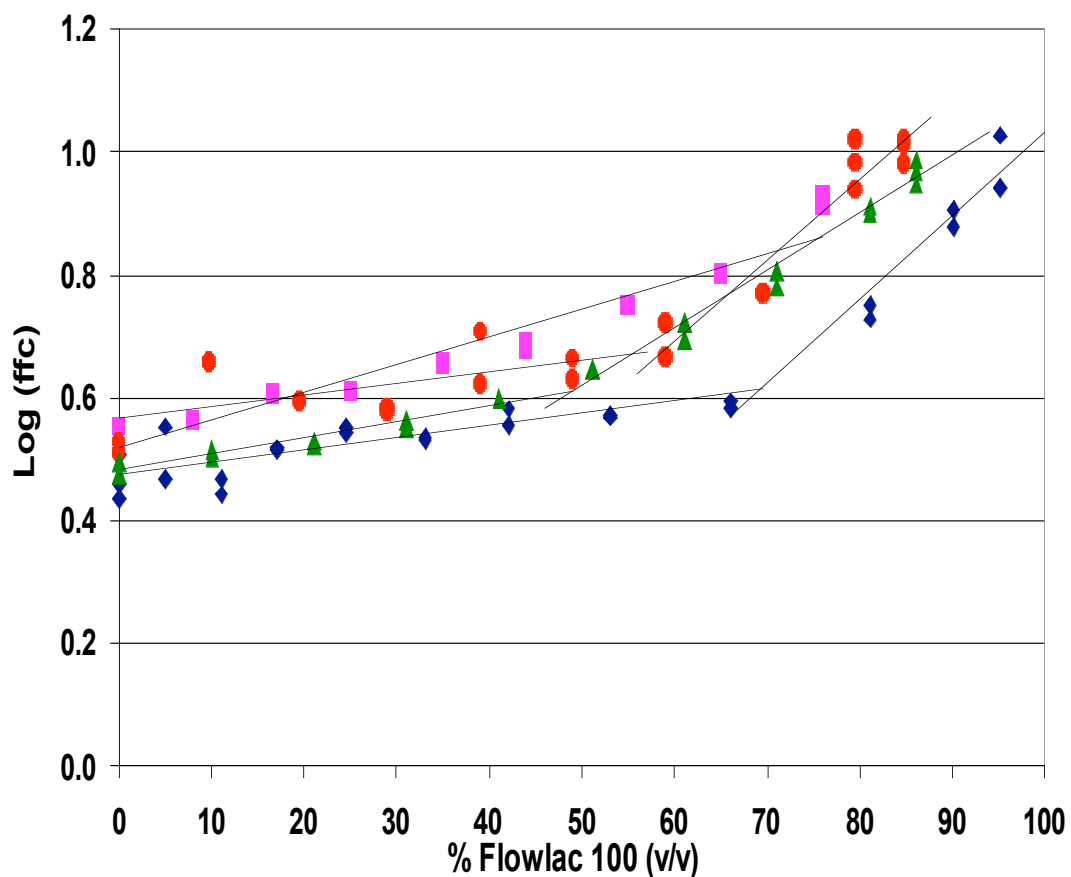
Fig. 27: Log **(**ffc) versus % Flowlac 100 (V/V) with Paracetamol (■), Mesalazine (♦), Starch (●) and Granulac (▲), n=2.

On the contrary to the previous observation with Dicafos mixtures - regarding the role the particle size plays on its flowability regardless the shape - Flowlac mixtures showed that particle's shape as well plays an important role on their flow behaviour. Fig. 27 showed that the poorest flowing mixtures are those of Mesalazine-Flowlac, where the 11µm needle shaped Mesalazine dominated the flow behaviour of the binary mixtures and flow improvement is achieved only at a concentration of 70% V/V Flowlac. However, mixtures containing the

12μm spherical shaped Starch as the poor flowing component of the mixture had easy flow behaviour from the beginning (probably due to the spherical shaped particles of both components, where spherical particles cause less friction and shear and hence assist in flow [6]) compared to mixtures with Mesalazine which has almost the same size but differs in shape. Starch mixtures required 58% V/V Flowlac to reach higher ffc values.

On the other hand, Paracetamol with its 34μm rod shaped particles yielded good flowing mixtures from the beginning. These mixtures achieved improved flowability on the addition of only 17% V/V of Flowlac, compared to the mixtures containing also the 30μm but irregular shaped Granulac which required 48% V/V of Flowlac to obtain an easy flowing binary mixture. Therefore, flowability of Flowlac mixtures according to the poor flowing constituent could be arranged as follows; Paracetamol > Starch > Granulac > Mesalazine-Flowlac mixtures. Regarding these observations it could be figured that both particle size and shape of both components influence the flow behaviour of the binary mixture. It was generally observed that spherical fine particles have better flow compared to needle shaped fine particles (of the same size) and irregular fine particles (larger in size) when blended with the coarse spherical Flowlac.

3.3.2.2.2 Density results

As observed in Fig. 28 the needle or rod shaped particles namely; Mesalazine and Paracetamol showed a proportional increase in density with increasing the percentage of Flowlac and showed no maximum packing density. On the other hand the spherical and irregular shaped particles (Starch and Granulac) showed an increase in the density with increasing the Flowlac percentage and reached a maximum packing density at 59% V/V and 41% V/V respectively. After reaching a maximum the density decreased with the further increase of percentage of Flowlac.
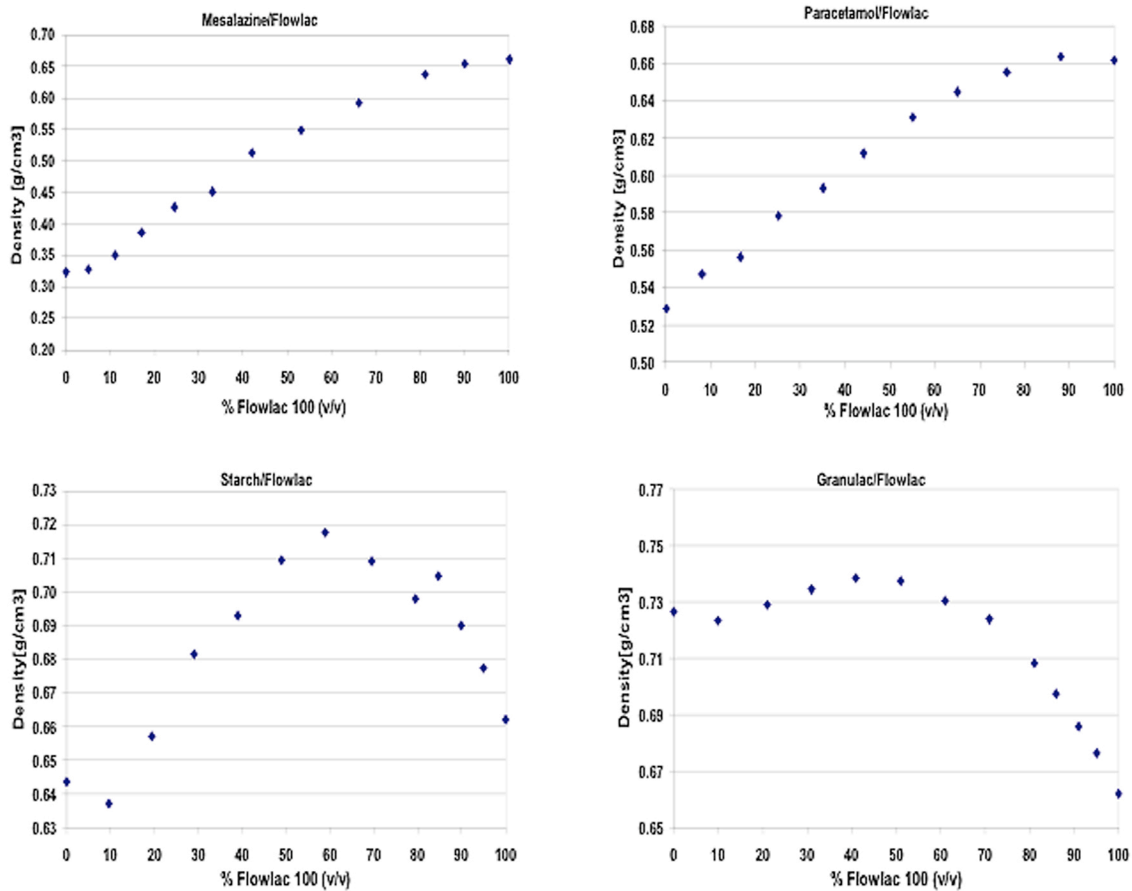
Fig. 28: Density versus percentage of Flowlac (V/V) for all four Flowlac mixtures

3.3.2.3 Inhalac mixtures

3.3.2.3.1   ffc results

Mesalazine-Inhalac flow profile (fine needle shaped poor flowing and coarse angular free flowing powders) is represented by two curve sections, which intersect at 65% V/V Inhalac. The log ffc values of the first curve section were more or less similar up to a concentration of 65% V/V Inhalac, above which the log ffc values increased proportionally to the further addition of Inhalac and achieved the easy flow range. Also Granulac-Inhalac flow profile (fine irregular shaped poor flowing and coarse angular free flowing powders) was represented by two curve sections, which intersected at 48% V/V Inhalac. Above this concentration the log ffc values increased proportionally to the further addition of Inhalac and achieved the easy

flow range. Paracetamol Inhalac flow profile (fine rod shaped poor flowing and coarse angular free flowing powders) was represented only with one curve. Flow improvement was observed with concentrations about 15% V/V Inhalac.
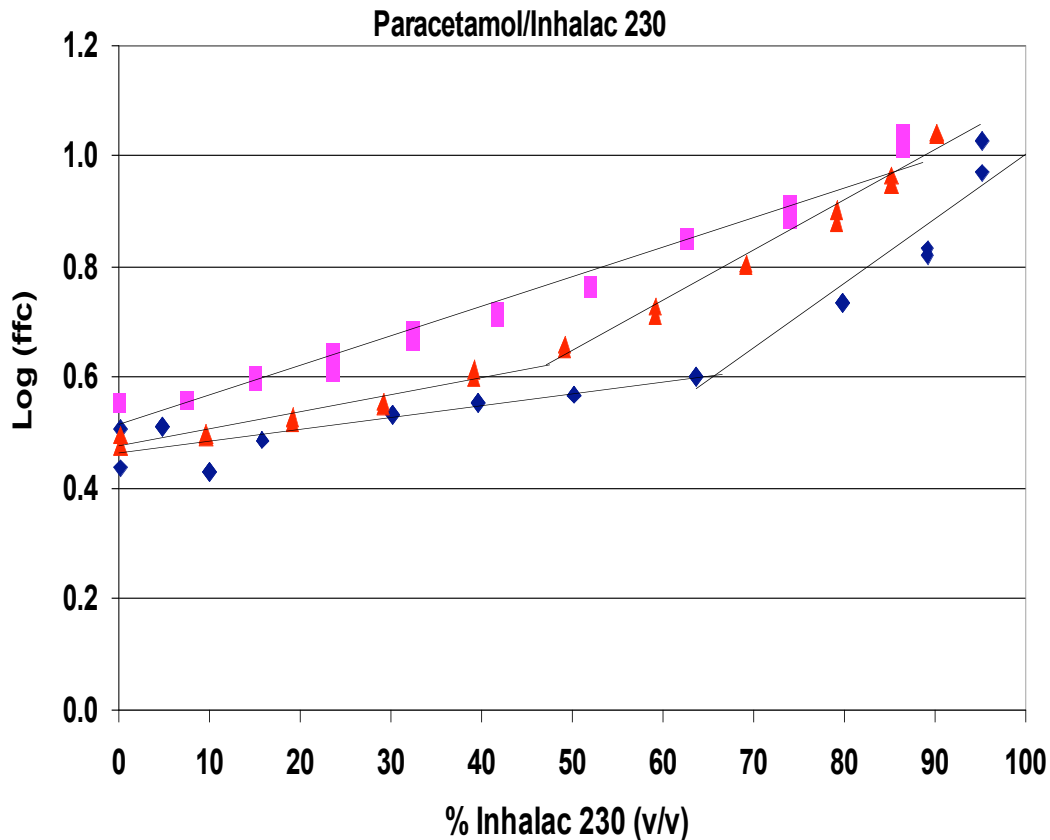
Fig. 29: Log **(**ffc) versus % Inhalac 230 (V/V) with Paracetamol (■), Mesalazine (♦) and Granulac (▲), n=2.

Therefore, as observed in Fig. 29 the flowability of Inhalac mixtures according to the poor flowing constituent could be arranged as follows; Paracetamol > Granulac > Mesalazine-Inhalac mixtures, noticing that their particle size are 34, 30 and 11μm respectively.

3.3.2.3.2 Density results

Fig. 30 depicted the behaviour of the needle or rod shaped particles namely; Mesalazine and Paracetamol and showed a proportional increase in density with increasing the percentage of Inhalac and showed no maximum packing density. On the other hand the irregular particles (Granulac) showed an increase in the density with increasing the Inhalac percentage and

reached a maximum packing density at 49% V/V. After reaching a maximum the density decreased with the further increase of percentage of Inhalac.
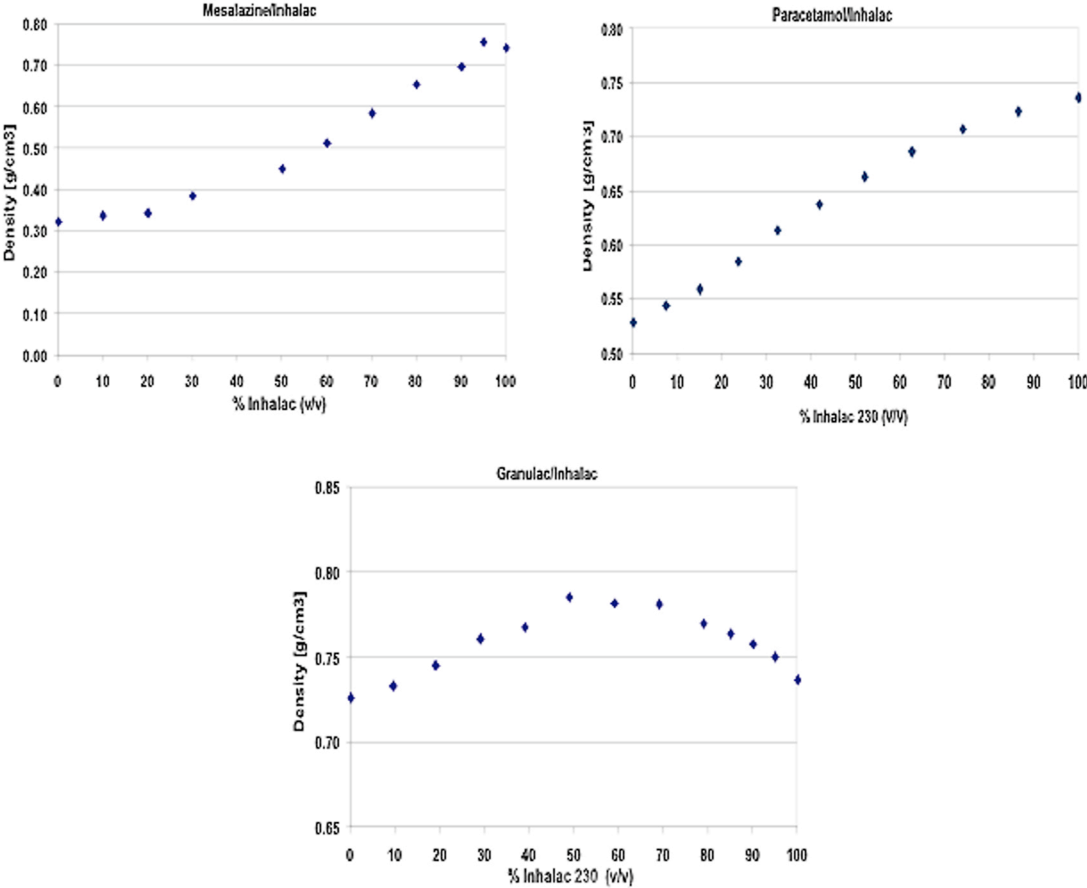
Fig. 30: Density versus percentage of Inhalac (V/V) for all three Inhalac mixtures

3.3.2.4 SEM

In Fig. 31 the scanning electron micrographs show the shapes of the different substances used in this study. It has to be mentioned that different magnifications were used. In the following micrographs the coarser particles have a 100µm scale while the fine particles have a 20µm scale except Granulac which has a 10µm scale.
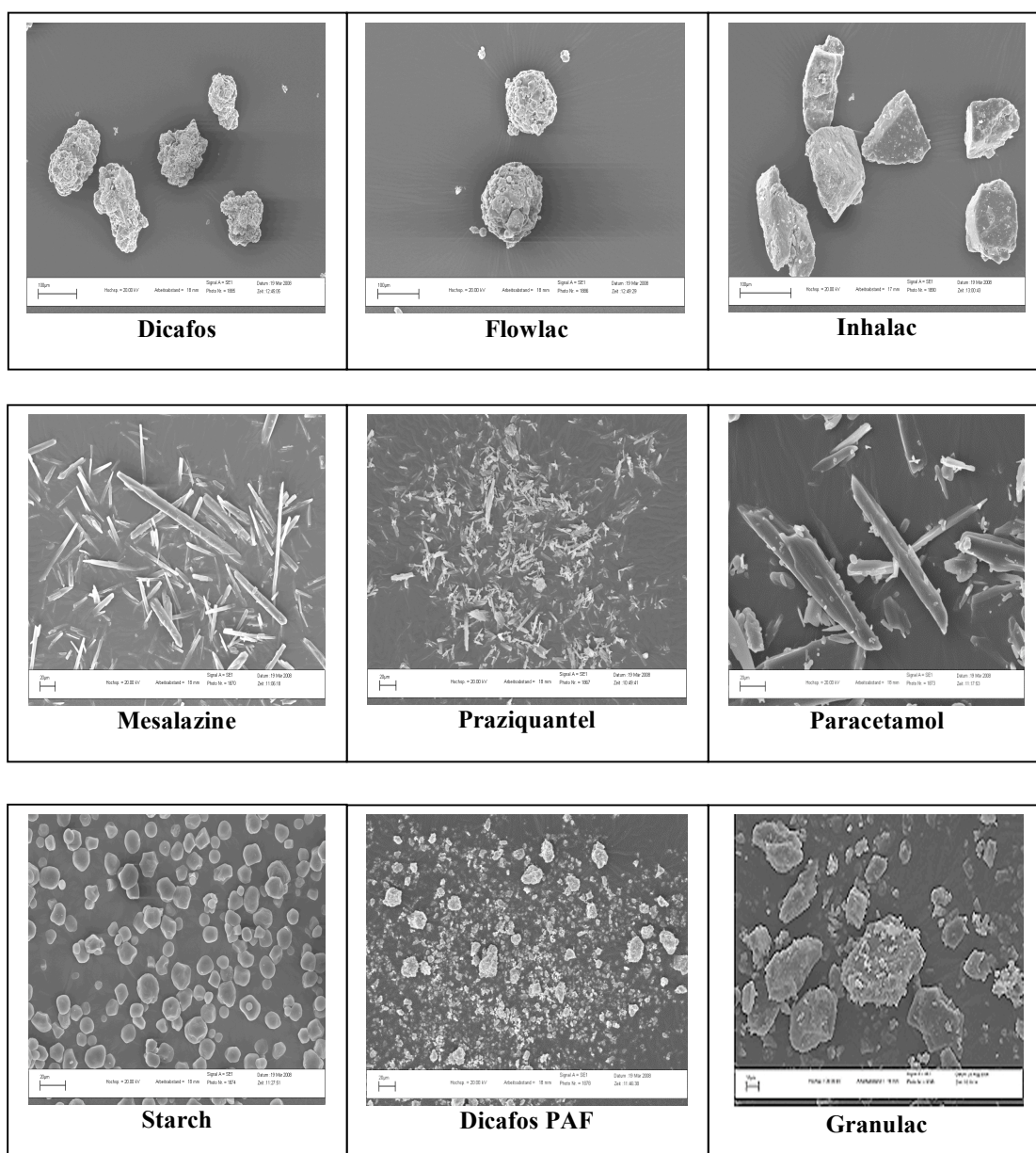
Fig. 31: Shape of materials used in this study

3.3.3 Discussion

On one hand it was observed that the flowability is influenced by the shape and size of both binary mixture components. This finding is in agreement with Podczeck and Miah [61], who stated that particle size and in particular particle shape influence the friction and flow properties of powders. Also Lahdenpää et al, studied three different grades of microcrystalline cellulose and found out that particle size and shape affected the powder flowability [62]. In 2006 Abhay [6] studied different shape factors and found that particle size is the most reliable indicator of powder flowability, and other parameters such as particle elongation and irregularity were also found to have an influence as well. Emery [12] also stated the dependence of flowability on both particle size and shape. However, on the other hand it was observed from this study that whether achieving a maximum packing density or not is mainly influenced by the shape of the fine component in the binary mixtures.

Regarding the flow behaviour of the mixtures it was found that the flow profiles for all mixtures examined were represented with two curve sections indicating the slight improvement in flowability at low concentrations of the free flowing component until reaching a critical concentration (point of intersection), after which significant flowability improvement was noticed with the further increase in the concentration of the free flowing component. Generally, it was observed that the flowability increased as the particle size of the fine poor flowing component in the mixture increased, this fact agrees with studies carried out before [6, 9, 12, 62, 63]. Only mixtures with Paracetamol as the fine poor flowing component were represented with one curve indicating the flow improvement on the addition of very small concentrations of the free flowing component, i.e. between 15 and 20 % V/V free flowing component. According to Emery's [12] findings, who determined that particle shape had a greater impact on flowability than did particle size for powders under 30μm, it must be referred to Paracetamol's relatively larger particle size (above 30μm) and its relatively higher

ffc value (3.5) compared to the other fine poor flowing substances applied in this study. However, in these mixtures the flow behaviour of the free flowing components dominates the flow behaviour of the binary mixture. While the mixtures with two curve sections indicate in most cases that the fine poor flowing component (all below 30µm) dominates the flow behaviour of such mixture, and the intersection point differs from a mixture to another according to the particle sizes and shapes involved in the mixtures.

Regarding the packing behaviour of the mixtures two profiles were noticed according to the shape of the fine poor flowing component in the mixture. The first profile yielded a maximum packing density with mixtures comprising fine (poor flowing) spherical or irregular shaped components (Granulac, Starch and Dicafos PAF) where such mixtures showed an increase in the density with increasing the concentration of the free flowing component and reached a maximum packing density, after which the density decreased with the further increase of percentage of free flowing component. That could be elucidated according to the bimodal packing of the Furnas model where the fine particles distribute and rearrange themselves between the pores of the larger packed particles [58, 64]. Consequently porosity is reduced and the density reaches a maximum. The decrease in density after reaching a maximum is due to the lack of the fine particles which could further fill in the pores [64]. The percentage of the free flowing powder at which a maximum packing density is obtained, differs from one mixture to another according to the particle size and shape of the components in the mixture. Dicafos-Dicafos PAF mixtures showed a maximum at 20% V/V Dicafos, where the high porosity of Dicafos consumed almost 80% of Dicafos PAF to fill in the voids. Comparing Flowlac-Granulac mixtures with Flowlac-Starch mixtures, the former showed a maximum at 45% V/V Flowlac, while the later showed a higher maximum at 60% V/V Flowlac. This result was expected because of the spherical shape of both components, where the pore space between Flowlac particles is large and Starch incorporation lead to additional pores and resisted closer packing at lower concentrations [58, 65]. However, according to literature

packing of mono-sized spherical particles, of which one fraction is coarse and the other is fine, should result in a maximum packing between 70% and 80% w/w of the coarser component (corresponds to approx. 70 to 80% V/V in this case) [58], but this maximum would be shifted towards higher concentrations of the finer component with a wider particle size distribution [65]. Finally, the Inhalac-Granulac mixtures showed maximum packing at 50% which is higher than the maximum reached by Flowlac-Granulac mixtures (45% V/V). It is suggested that irregular particles contradict dense packing [58]. Therefore it would be expected that incorporating such particles with spherically shaped components would improve their packing behaviour compared to incorporating them with angular particles having more contact points. From the previous findings it could be concluded that both particle size and shape influence the packing behaviour of powders, and both parameters seem to interact [58, 60, 66]. That is also with agreement with Podczeck and Sharma who stated that particle shape of both components in a binary mixture influences the maximum volume reduction due to packing, as well as their particle sizes with the exception of angular particles [58]. The second profile observed did not yield a maximum packing density with mixtures comprising fine (poor flowing) needle or rod shaped components (Mesalazine, Paracetamol and Praziquantel). However, the densities in that profile are additive and can be calculated from the densities and volume fractions of the components. Such particles seem to entangle and interlock together, so obstructing flowability [6] probably by building up a network through out the mixtures. Consequently, such fine particles could not arrange them selves within the pores of the coarser particles so that the porosity is reduced.

For all three good flowing excipients examined the mixtures comprising a fine poor flowing needle shaped component showed the least ffc values. The poor flow behaviour of needle shaped particles is in agreement with previous literature [6, 12, 61, 64, 67]. The fine needle shaped component seemed to dominate the flow behaviour of the mixture probably due to their high cohesiveness besides their interlocking behaviour. The previous explanation could

be applied here as well, where due to building up a network through out the mixtures, the coarser particles are entrapped within this network until they reach a certain volume fraction after which they are isolated, i.e. overcome and break this network. At this volume fraction the mixture shows improved flow behaviour. It was also observed that in mixtures comprising fine particles of the same size but of different shapes, the one with the spherically shaped fine particles revealed better flowability e.g.; Mesalazine (11µm) and Starch (12µm), that agrees with literature which states that flowability increase as the roundness as a shape factor increase [6, 12], or that pharmaceutical blends containing small spherical particles exhibit increased bulk and tapped density and hence improved flowability [12, 68].

Correlating the critical concentrations obtained (concentrations at intersection points) to the mixtures examined; no general rules about the influence of the particle size and shape on the flow behaviour of the mixtures could be predicted or proposed. Generally it was observed that the critical concentrations obtained with Dicafos mixtures are lower (ranging from 45 to 48% V/V) than the concentrations obtained with Flowlac and Inhalac mixtures (ranging from 48 to 70% V/V). Inhalac showed slightly lower concentrations compared to Flowlac mixtures. However from these experiments it could be concluded that the irregular shaped Dicafos showed flowability improvement at lower concentrations followed by the angular shaped Inhalac and finally the spherical shaped Flowlac. This ranking could not be related directly with the porosity or particle size of the excipients but it could be correlated to the bulk density of these substances as measured with the ring shear tester at normal load equal to 5KPa. The bulk densities of Dicafos, Inhalac and Flowlac are 0.82, 0.7 and 0.67g/cm^3 respectively. It has been already proved in a previous study that higher particle density can improve powder flow behaviour [69]. In other words, the amount of good flowing component required to improve flowability decreases as its density increases.

Therefore, it can be concluded that, the flowability is influenced by the shape and size of both binary mixture components. On the other hand whether a maximum packing density achieved

66

or not is influenced mainly by the shape of the fine poor flowing component of the binary mixtures. Generally, it has been observed that flowability of binary mixtures is improved as the particle size of the fine poor flowing component increases. However, the mixtures comprising the fine needle shaped poor flowing component had the worst flowability, while mixtures comprising the fine spherically shaped poor flowing component revealed better flow compared to mixtures comprising differently shaped, similarly sized fine particles.

3.4 The flow behaviour of different fats in absence and presence of Aerosil

3.4.1 Introduction and aim of work

3.4.1.1   Lipids

Lipids are a large and diverse group of naturally occurring organic compounds characterised by their solubility in non-polar organic solvents (e.g. ether, chloroform, acetone & benzene) and general insolubility in water. Lipids can be classified in many ways, due to their different composition, nature and origin. According to Bloor's classification in 1920, lipids can be divided in: simple lipids, compound lipids and derived lipids. The structure of simple lipids is chain-like molecules consisting of glycerol and the fatty acids. Compound lipids are such as phospholipids, sphingolipids, glycolipids and sulfolipids. Derived lipids include steroids, fat-soluble vitamins, and prostaglandins [70].

Lipid is a collective term and includes fats and oils. They are water-insoluble substances of plant or animal origin that consist predominantly of triglycerides. Those that are solid or semisolid at room temperature are normally called fats, while those that are liquid under the same conditions are called oils. Natural fats have a higher percentage of saturated fatty acids than do oils [70]. Natural and semi-derived fats and oils are usually mixed together and are mixtures of mono-, di-and triglycerides of fatty acids of different chain lengths. The central component of triglycerides is glycerol, where all three hydroxyl groups are esterified with fatty acids.

Lipid excipients have been of great interest in the pharmaceutical industry. Classical areas of their application include the use of oils and semisolid preparations for external use such as ointments, creams, pastes, oily eye drops or lipid based injections of lipophilic drugs or suppositories. The interest in lipid based oral drug delivery is relatively recent and is related to the growing need for novel drug delivery systems. Lipid excipients are used nowadays used for bioavailability enhancement and to improve the solubility of active ingredients.

They have been also used for the preparation of sustained release dosage forms. Furthermore, they have been applied as films or fat matrices for other reasons such as; taste masking of bitter tasting drugs [71], reduction of irritation of the gastro intestinal tract due to drugs with irritable properties. Low concentrations of lipid excipients are used as an adjuvant in the manufacture of tablets. They can act as glidants, lubricants and binders [72, 73].

3.4.1.2   Silicon dioxide (Aerosil®)

In this study the aim was to investigate the effect of densified hydrophilic and hydrophobic fumed silica types (Aerosil®) on the flow characteristics of a number of lipids. The ffc values of all lipids were measured in the absence and presence of 2% of both silica types; Aerosil® 200 V and Aerosil® R 972 V. Furthermore, two of the lipids investigated in this study were measured with further concentrations of both silica types up to 15%, see table 7 under materials in section 6.1.3.

3.4.2   Results

3.4.2.1   ffc versus % Aerosil

The ffc values of seven different lipids were measured under similar conditions, 21°C and 45% relative humidity, see table 4. As shown in figure.34 the mean ffc values of the pure lipid, and the lipid blends with 2% Aerosil R972 V (hydrophobic) as well as Aerosil 200 V (hydrophilic) were plotted. More details about the substances used and the method of their preparation are mentioned under the experimental part in sections 4.1 and 4.2 respectively.

Table 4: lipids used in this study

Substance	Generic name	Abbreviation	Composition (according to specification)	Mean Particle Size µm*	Specific Surface Area m^2/g±SD**	Shape
Precirol ATO 5®	Glyceryl palmitostearate	PRATO5	25–35% Triglyceride 40–60% Diglyceride 8–22% Monoglyceride	42	0.63 ±0.01	Spherical
Compritol 888 ATO®	Glyceryl dibehenat	COM888	21–35% Triglyceride 40–60% Diglyceride 13–21% Monoglyceride	47	0.32 ±0.01	Spherical
Imwitor 900 K®	Glyceryl monostearate	IMW900	5–15% Triglyceride 30–45% Diglyceride 40–55% Monoglyceride	285	0.14 ±0.01	Spherical
Dynasan 118®	Glyceryl tristearate	DYN118	>95% Triglyceride	27	4.6 ±0.07	Irregular
Dynasan 116®	Glyceryl tripalmitate	DYN116	>95% Triglyceride	580		Irregular
Dynasan 114®	Glyceryl trimyristate	DYN114	>95% Triglyceride	20	4.1 ±0.2	Flakes like agglomerates
Witocan 42/44®	Hydrogenated Coco glycerides	WIT42/44	>90% Triglyceride	112		Irregular & agglomerated particles

*Particle size was measured using a laser laser diffraction spectrometry (Helos/KF-Magic, Sympatec GmbH, Clausthal-Zellerfeld, Germany) using the dry-dispersing system (Rodos, Sympatec GmbH, Clausthal-Zellerfeld, Germany.
**Specific surface area m^2/g as measured with BET ± standard deviation (Dynasan 114 & Witocan 42/44 could not be measured)

Among the seven measured lipids four of which are cohesive, indicated with their low ffc values according to Jenike's classification (2 < ffc < 4 cohesive) namely; Dynasan 114, Dynasan 118, Witocan 42/44 and Precirol ATO 5. The first three lipids mentioned showed insufficient improvement on the addition of 2% of either glidants used in this study while

Precirol ATO 5 showed flow improvement. On the other hand, the other remaining three lipids had ffc values in the easy flowing category (4 < ffc < 10). These three lipids showed improvement in their flowability on the addition of 2% of either glidants. Generally, higher ffc values are obtained with blends containing Aerosil® R972 V.
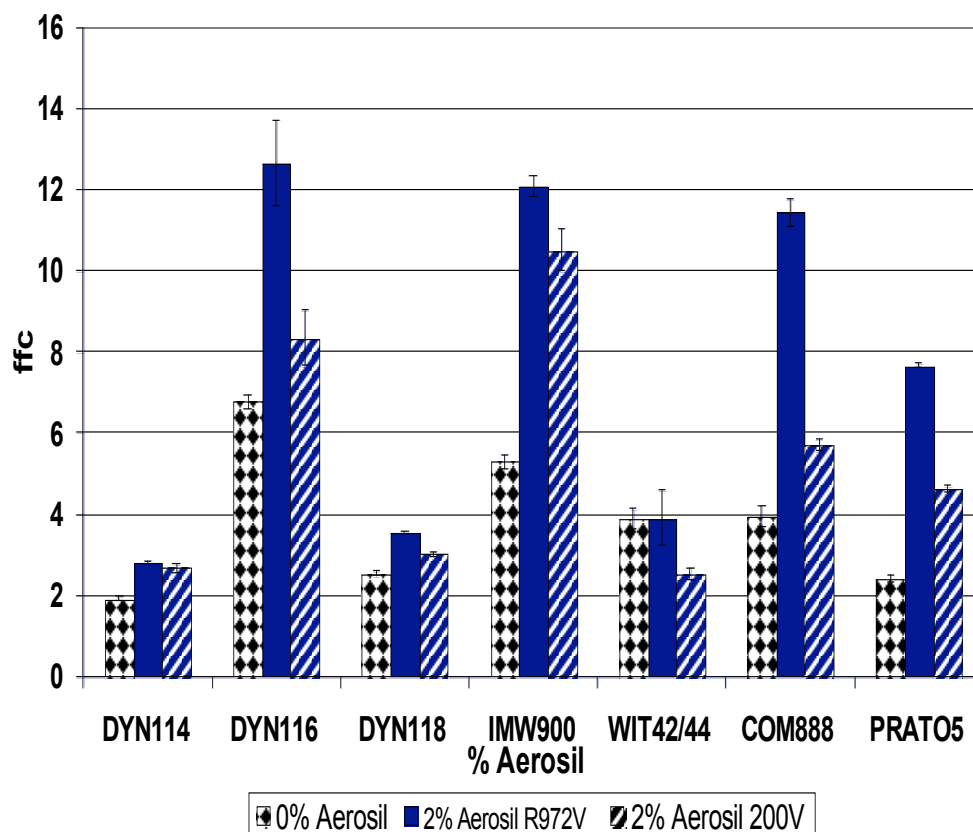
Fig. 32: ffc values with or without Aerosil R 972 V and Aerosil 200 V. n=3, mean value ± S.D.

It was interesting to investigate the influence of further percentages of Aerosil. Therefore, Dynasan 118 and Imwitor 900 K were chosen as models for this investigation, see Fig 33. Dynasan 118 is a poor flowing powder (ffc = 2.5) due to its 27μm mean particle size and rough irregular shaped particles. While Imwitor 900 K indicates the good flowing powder (ffc = 5) with a 285μm mean particle size and almost smooth spherical shaped particles. Two sets of Imwitor 900 K / Aerosil R 972 V and Imwitor 900 K / Aerosil 200 V mixtures were prepared, comprising 0.1, 0.5,1, 2 and 7% of either glidants. Similarly, two sets of Dynasan 118 were prepared, comprising 0.1, 0.5, 1, 2, 3, 5, 7, 8.5, 10 and 15% of either glidants.
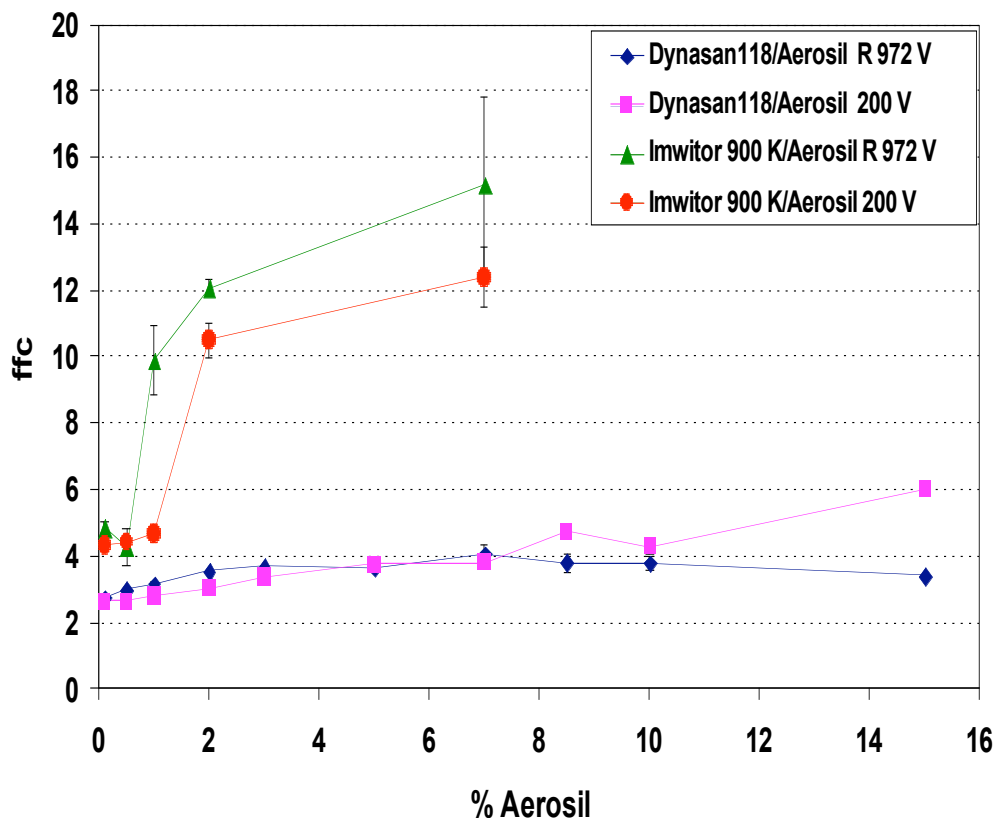
Fig 33: ffc values of Dynasan 118 and Imwitor 900K versus percentages of Aerosil R 972V and Aerosil 200V, n=3, mean ± S.D. (for some samples the standard deviation was smaller than the size of the symbol)

As mentioned in section 3.3 Aerosil is used as a flowability enhancer and yielded maximum ffc values with concentrations between 0.5 & 1% further increase led to either a decreased or constant ffc values. In this study Imwitor showed an initial flow improvement with 1% Aerosil R 972 V and 2% Aerosil 200 V. Further increase in the glidants amount up to 7% Aerosil concentrations led to further flow improvement with ffc values above 10. On the contrary, Dynasan 118 showed no significant improvement in its flowability with glidant concentration up to a 7%, where only ffc values around 4 were recorded. Further increase in glidant concentration up to 15% showed surprisingly flow improvement only with the hydrophilic glidant referred to with an ffc value equal approximately 6.

Generally, Fig 33 shows that Imwitor 900 K / Aerosil 200 V mixtures showed lower ffc values compared to Imwitor 900 K / Aerosil R 972 V mixtures. In case of Dynasan 118 mixtures with both glidants, the values were almost overlapping except at very high percentages, namely 15% of either Aerosil types.

3.4.2.2 SEM

Compritol and Precirol are spray dried [74, 75, 76] products with mean particle sizes 47 and 42μm respectively. They are characterized with their almost smooth spherical shapes, as observed from the SEM micrographs (Fig.33). Compritol has a smoother surface compared to Precirol which shows some roughness on its surface. Comparable to these products is Imwitor, which is also spherical in shape with a mean particle size 285μm and shows roughness on its surface. Regarding the three Dynasans used in this study they are all irregular in shape. The Dynasan 114 with its smallest particle size 20μm has the roughest surface among them, where it looks like agglomerated flakes. However, although Dynasan 118 and 116 have remarkably different particle sizes 27μm and 580μm respectively, their surfaces almost look the same. Finally Witocan with its 112μm has also an irregular shape in the form of almost spherical agglomerates. To avoid any discrepancies or misleading results it has to be mentioned that not all the SEM micrographs reflect the actual mean particle size of some of the lipids, for example; despite it has been mentioned that Dynasan 116 has a mean particle size about 580μm the particle in the micrograph considering Dynasan 116 is almost 5 times smaller than the actual particle size.
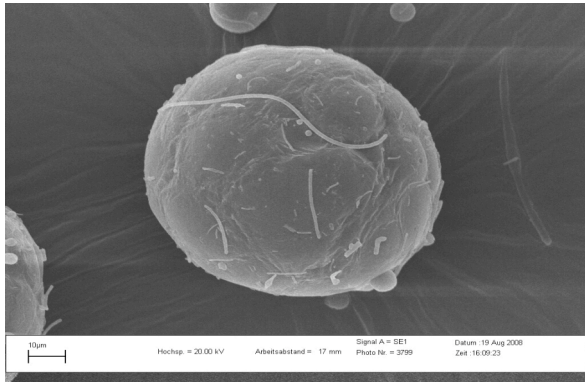
Compritol 888 ATO
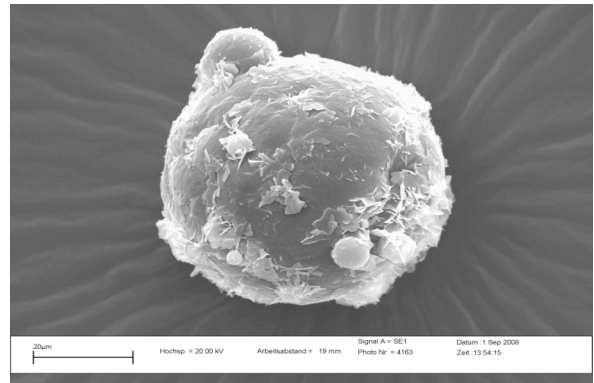
Precirol ATO 5
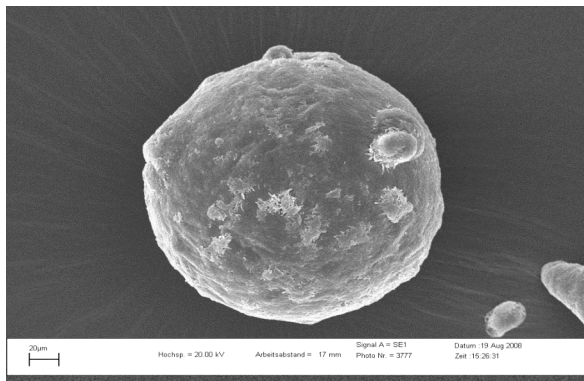
Imwitor 900 K
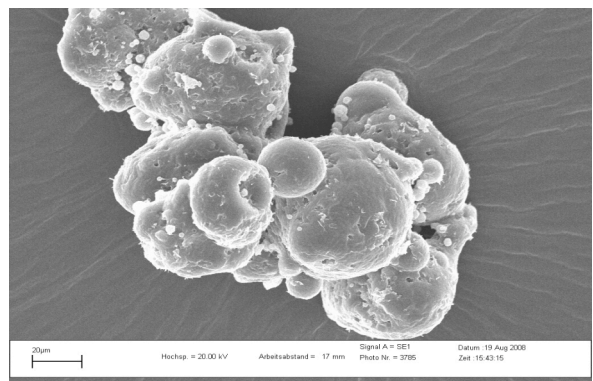
Witocan 42/44
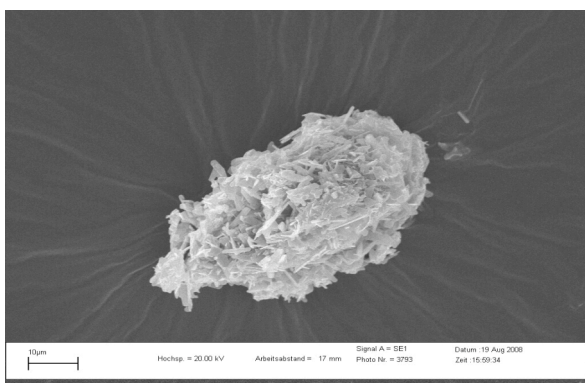
Dynasan 114
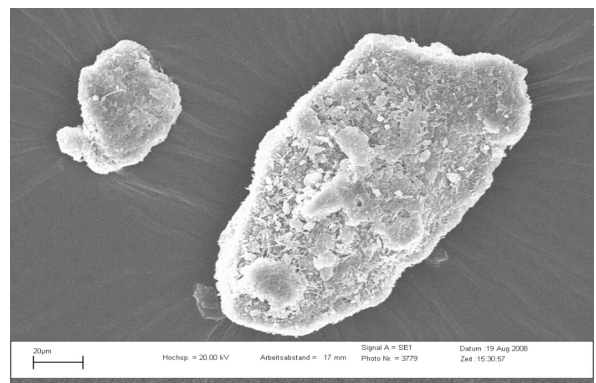
Dynasan 116
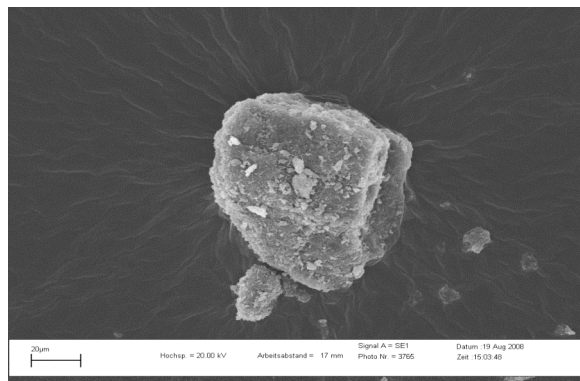
Dynasan 118

Fig.33: SEM micrographs of all lipids used in this study (different magnification)

3.4.2.3   BET

The specific surface area of the lipids was measured using the BET method, depending on the gas adsorption phenomenon. As shown in figure 37 it was observed that the ffc values of the lipids in the absence or presence of 2% of either Aerosil types decreased as their specific surface area increased. The decrease of the ffc values is more profound at lower specific surface areas. Probably that is related to the degree of coverage of the particles with Aerosil. The glidant plays its intended role only when it reaches an optimum coverage degree on the particles surface, where the least adhesive forces are established. Lower ffc values were measured with hydrophilic Aerosil. This could be elucidated by the difference in the chemical nature of both glidants, where one of which has more silanol moieties compared to the other i.e.; hydrophilic type. Therefore, hydrogen bonds are dominant between agglomerates rendering them stable and not easily broken. On the other hand, treatment of the silanol groups with organosilicon compounds to create the hydrophobic silica renders its agglomerates softer, due to lacking the strong hydrogen bonds responsible for the stability of the agglomerates formed. In other words the softer agglomerates of hydrophobic Aerosil are easily broken during the mixing process and are available for particles coverage. The specific surface area of Dynasan 116 and Witocan 42/44 could not be measured due to their large particle size and their very small surface areas.
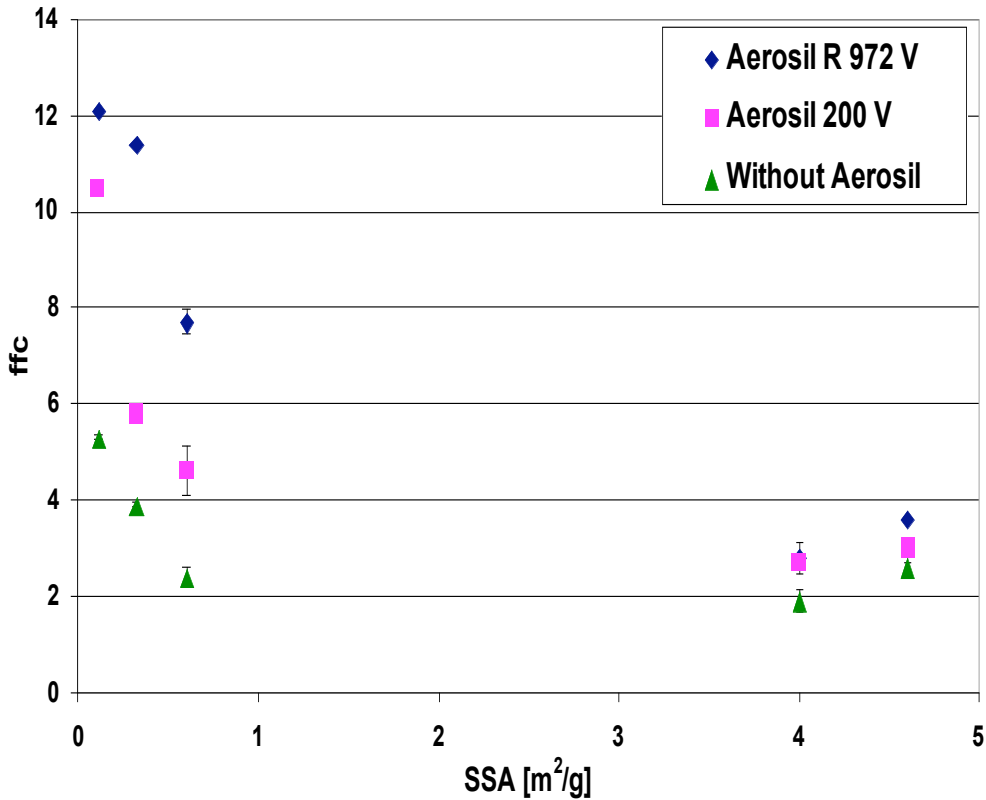
Fig 34: Relation between specific surface areas (SSA), [mean value ± S.D, n=3] as measured with BET method and the ffc values [mean value ± S.D., n=3] of 5 different lipids with 2% Aerosil 200 V and 2% Aerosil R 972 V

3.4.3   Discussion

Among the three Dynasans used, Dynasan 116 has the highest ffc value (ffc = 6.8) probably due to its large particle size (d_{50} = 580μm) and its flowability was further improved on the addition of 2% of either Aerosil types. However, the other Dynasans behaved differently where Dynasan 114 and Dynasan 118 have ffc values 1.9 and 2.6 respectively indicating very cohesive and cohesive flow behaviour according to Jenike's classification. Besides, their flowability is not enhanced on the addition of 2% of either Aerosil types, where it remains between 2 and 4 in both cases. To explain this behaviour it has to be mentioned that whether a given powder flows or not is primarily determined by the inter-particular forces and gravity. Whereas, gravity is usually relied upon to cause the powder to flow, the cohesion force prevents them from flowing. For most organic materials, at particle diameters smaller than 30μm, the cohesive forces exceed the particle weight. Therefore, small particles stick more

strongly together [5]. Also mentioned by [17] that the amplitude of the interaction forces becomes dominating compared to the weight of the particles when the size of the particles decreases. So the small particle size of Dynasan 114 (d_{50} = 20µm) and Dynasan 118 (d_{50} = 27µm) is responsible for their poor flow behaviour, on the contrary to the flow behaviour of Dynasan 116 with its larger particle size. Regarding the insignificant flow enhancement on the addition of 2% of either Aerosil types, probably the specific surface area, shape and surface roughness play the major role in this behaviour. That may be explained with the degree of coverage of the particles with the glidant [5, 55, 77] or density of coverage as referred to in other literature [40]. Observing figure 37 makes it obvious that the ffc decreases in the presence of 2% glidant as the specific surface area increases. In other words the 2% of glidant considered sufficient to obtain an optimum degree of coverage and improve flow behaviour of a powder with low specific surface area, is not sufficient to improve flowability of Dynasan 114 and Dynasan 118 with their high specific surface areas ranging from 4 to 4.7m^2/g. Besides, their large specific surface area Dynasan 114 and Dynasan 118 have irregular shapes and rough surfaces, especially Dynasan 114 with its agglomerated flakes like surface. The roughness in these particles surfaces may be the cause of the glidants entrapment in grooves and unevenness of the particles, making the amount of glidant available insufficient as a flowability enhancer. Furthermore, Dynasan 118 was taken as a model for a poor flowing lipid to investigate the optimum percentage of glidant required for improving its flow behaviour. Percentages up to 15% of both Aerosil types were used. Easy flowing powders were surprisingly achieved with the hydrophilic Aerosil. Considering that Dynasans are triglycerides of saturated fatty acids (see Table 4, section 3.4.2.1) and their hydrophobic nature, they lack the ability to form strong hydrogen bonds between their surface and the Aerosil agglomerates.

Witocan 42/44 is also a triglyceride with its 112µm irregular shape or agglomerated particles (agglomerated spheres) and has an ffc = 3.9. The addition of 2% Aerosil R 972 V did not

improve the flowability, that would be expected due to the irregular shape characterising this powder where the grooves and cavities would be a good trap for the hydrophobic Aerosil. Surprisingly, a decrease in the flowability (even less than the ffc value obtained with pure Witocan) occurred on the addition of 2% Aerosil 200 V. The possible explanation for such a decrease in ffc could be related to the melting point of Witocan (where it has the lowest melting point among the used lipids, see table 8 in section 6.1.4) and the fact that these experiments were carried out in summer time, mentioning that the mixing process was carried out in an unconditioned room.

Precirol ATO 5 which is a spray dried product with its 42μm spherical particles has an ffc value = 2.4. This product showed improved flowability on the addition of 2% of either Aerosil types, reaching a maximum ffc of approx. 8 on addition of Aerosil R972 V. This improvement could be referred to its small surface area ($0.6m^2/g$) and smooth surface and its nature as a partial glyceride comprising 40-60% diglycerides, consequently offering a high density of hydroxyl groups on its surface to attract the Aerosil by hydrogen bonds leading to a sufficient glidant degree of coverage. The other three lipids Dynasan116, Imwitor 900 K and Compritol 888 ATO have ffc values equal or higher than 4, i.e. they are easy flowing powders with 6.8, 5.3 and 3.9 ffc values respectively. Their flowability is improved on the addition of glidants reaching the free flowing ffc ranges ≥ 10 with Aerosil R 972 V. All three powders reached free flowing ffc ranges with hydrophobic types while only Imwitor 900 K reaches such ranges with the hydrophilic type as well, probably due to its large spherical particles as well as its nature as a partial triglyceride comprising 40-55% monoglycerides, offering higher density of hydroxyl group compared to the other two products to form hydrogen bonds with Aerosil agglomerates. However, Imwitor 900 K was used as an easy flowing lipid excipients model to investigate percentages of glidants required to further enhancing its flow behaviour. As shown in figure 35 the ffc values proceed to increase on the addition of 1% of the hydrophobic type and 2% of the hydrophilic type. Further increase of glidants percentage up

to 7% led to ffc values higher than 10, statistically the results at this concentration overlap with each other due to the fluctuation of the results with ffc values higher than 10. However, it was observed that hydrophobic glidants are better flow enhancers compared to hydrophilic glidants, in agreement with previous literature [5, 40, 57, 77, 78].

Generally, with most pharmaceutical excipients Aerosil concentrations between 0.2% and 1% are sufficient to establish flow improvement. A maximum flow improvement is achieved at 0.5% further increase in concentration up to 2% causes decrease in flowability (see section 3.2). On the other hand the lipids showed a different behaviour compared to other pharmaceutical substances. The easy flowing lipids required percentages of silicon dioxide higher than 0.5% to achieve the intended flow improvement for example; Imwitor 900 K which showed continuous flow improvement on addition of 1, 2 and 7% Aerosil. However, the poor flowing lipids showed two different behaviours as observed in this study. They either showed significant flow improvement with an Aerosil concentration equal 2% - believed to decrease flowability of other substances as seen in section 3.2 - (see Fig. 32) for example; Precirol ATO 5, or they showed no flow improvement even with very high concentrations of Aerosil, i.e. up to 15%, for example: Dynasan 118. Generally, glidants play their role first when reaching an optimum degree of coverage, above it or beneath it the glidant loses its flow enhancing and improving property. The specific surface area, particle size, shape and surface roughness play a great role on the flow enhancing property of the glidants. Comparing the influence of Aerosil on the flow behaviour of lipids in this study with those observed in section 3.2 (influence of Aerosil on flow behaviour of Paracetamol) it may be high-lighted that besides the specific surface area, shape, size and surface morphology of substances, the hydrophobic nature of lipids plays an important role on the flow enhancing property of the glidant. This role differs from one lipid to another according to its degree of hydrophobicity.

4   Summary

The assessment of flowability of powdered materials in the pharmaceutical industry is a crucial step and a prerequisite for a cheap, successful and non-time consuming production. In this work a ring shear tester was employed as a tool for the quantitative evaluation and assessment of the flowability of pharmaceutical substances and mixtures. The flowability (ffc) is represented as the ratio of the consolidation stress to the unconfined yield strength. The larger the ffc is, the better a bulk solid flows. A comparison between the large (RST-01.pc) and small (RST-XS) Schulze testers was carried out. Regardless the differences in composition, size and shape of the substances examined, comparing the ffc values of both testers showed that the results were well correlated with a correlation coefficient, r = 0.97. However, the smaller tester showed slightly lower ffc values compared to the larger tester. For comparative tests this effect did not play a role as long as the same ring shear tester with the same shear cell size was used throughout the measurements.

The influence of different types of Aerosil[®] on the flowability of Paracetamol was investigated by means of the ring shear tester. Other conventional easy applicable methods were also employed such as; angle of repose, Hausner ratio and flow rate. It was observed that the ffc values increased with the increase of Aerosil[®] percentage, and then they either decreased or remained constant with further increase in percentage. Aerosil percentage about 0.5% was enough to achieve a maximum flow improvement. The angle of repose decreased as we increased the percentage of Aerosil[®]. The angles of repose values were inversely proportional to the ffc values. The Hausner ratio did not show agreeable results to those of the ffc. The flow rate also could not be measured for all samples, and even the samples measured did not reveal any general trend. As a conclusion the ring shear tester can be applied as a quantitative comparative test to replace other inaccurate and operator influenced conventional methods. Besides, it was observed that the capsules containing different types and percentages of Aerosil possessed lower relative standard deviation values (RSD) compared to capsules

filled with Paracetamol alone. The capsules containing Aerosil® showed higher fill weights compared to capsules filled with paracetamol alone, where Aerosil® reduces the interparticulate forces between paracetamol particles which consequently move closer reducing the space between each other and obtaining higher densities and fill weights. However, plotting the RSD versus the ffc showed that all samples prepared with Aerosil®, which have higher ffc values, showed lower RSD values with lower scattering values compared to those prepared with Paracetamol alone.

Also the flow behaviour of binary mixtures was investigated. It was found that the flow profiles (the graphical presentation of the ffc values versus the percentage of the free flowing component in the mixture) for almost all mixtures examined were represented with two curve sections. The first section indicating the slight improvement in flowability at low concentrations of the free flowing component until reaching a concentration (the point of intersection between the two curve sections), after which a significant flowability improvement - represented with the second curve section - was noticed with the further addition of the free flowing component. In such mixtures the bulk properties of the fine poor flowing components dominated the flow behaviour of the binary mixtures. The intersection point differed from a mixture to another according to the particle sizes and shapes involved in the mixtures. On the other hand mixtures with Paracetamol as the fine poor flowing component were represented with only one curve indicating the flow improvement on the addition of very small concentrations of the free flowing component i.e.; about 20 % V/V free flowing component. However, in these mixtures the flow behaviour of the free flowing components dominated the flow behaviour of the binary mixture. Regarding the packing behaviour of the mixtures two profiles were noticed according to the shape of the fine poor flowing component in the mixture. Mixtures comprising fine spherical or irregular shaped components showed a profile with a maximum packing density, after which the density decreased with the further increase of percentage of free flowing component. Mixtures

comprising fine needle or rod shaped components yielded a profile without a maximum packing density. In the second profile the densities are additive and can be predicted from the densities and volume fractions of the binary mixture components. Generally it can be concluded that the flowability of the binary mixtures was influenced by the shape and size of both components and whether the binary mixture achieved a maximum packing density or did not was influenced mainly by the shape of the fine component in the binary mixtures. However, the concentration at which maximum packing occurred depended on both parameters of each component.

The flow behaviour of lipids in the presence and absence of Aerosil® was also examined. Most pharmaceutical substances investigated in this work established a maximum flow improvement with only 0.5% Aerosil, while lipids showed a different behaviour. The easy flowing lipids (ffc > 4) required percentages of Aerosil higher than 0.5% to achieve the intended flow improvement. However, the poor flowing lipids (ffc < 4) showed two different behaviours as observed in this study. They either showed significant flow improvement with 2% Aerosil (believed to decrease flowability of other substances as seen in paracetamol section), or did not show flow improvement even with very high concentrations of Aerosil i.e.; up to 15%. Comparing the influence of Aerosil on the flow behaviour of lipids with those observed in section 3.2 (influence of Aerosil on flow behaviour of Paracetamol), it may be high-lighted that besides the specific surface area, shape, size and surface morphology of substances, the hydrophobic nature of lipids plays an important role on the flow enhancing property of the glidant. This role differs from one lipid to another according to its degree of hydrophobicity.

5 Zusammenfassung der Arbeit

Die Bewertung der Fließfähigkeit von pulverförmigen Materialien in der pharmazeutischen Industrie ist ein wichtiger Schritt und eine Voraussetzung für eine kostengünstige, erfolgreiche und zeitsparende Produktion. In dieser Arbeit wurde ein Ringschergerät für die quantitative Beurteilung der Fließfähigkeit von pharmazeutischen Wirkstoffen und Mischungen eingesetzt. Die Fließfähigkeit (ffc) beschreibt das Verhältnis der Verfestigungsspannung zur Schüttgutfestigkeit. Je größer ffc ist, desto besser fließt ein Schüttgut. Ein Vergleich zwischen großem (RST-01.pc) und kleinem (RST-XS) Schulze-Ringschergerät wurde durchgeführt. Ungeachtet der Unterschiede in Zusammensetzung, Größe und Form der untersuchten Substanzen korrelierten die mit den beiden Ringschertestgeräten gewonnenen ffc-Werte (Korrelationskoeffizient r = 0,97). Im Vergleich mit dem größeren Tester führte der kleinere Tester zu etwas niedrigeren ffc-Werten. Für vergleichende Untersuchungen spielte dieser Effekt keine Rolle, solange das gleiche Ringschergerät mit der gleichen Scherzelle während der Messungen benutzt wurde.

Der Einfluss verschiedener Aerosil®-Typen auf die Fließfähigkeit von Paracetamol wurde mit dem Ringschergerät untersucht. Andere konventionelle, einfach anwendbare Methoden wurden ebenfalls durchgeführt, zum Beispiel Böschungswinkel, Hausner-Faktor und Fließgeschwindigkeit. Es wurde festgestellt, dass die ffc-Werte mit Zunahme der Aerosil®-Konzentration anstiegen und dann bei weiterer Erhöhung des Aerosil®-Anteils entweder wieder absanken oder konstant blieben. Ein Anteil von etwa 0,5% Aerosil® war ausreichend, um eine maximale Verbesserung der Fließfähigkeit zu erreichen. Der Böschungswinkel nahm mit zunehmendem Aerosil®-Anteil ab. Die Werte des Böschungswinkels waren umgekehrt proportional zu den ffc-Werten. Die Ergebnisse des Hausner-Faktors zeigten keine Übereinstimmung mit den ffc-Werten. Die Fließgeschwindigkeit durch einen Trichter konnte nicht für alle Proben gemessen werden, und auch die Proben, die gemessen werden konnten,

zeigten keinen einheitlichen Trend. Das Ringschergerät kann als eine quantitativ vergleichende Prüfmethode verwendet werden, um andere ungenaue und vom Anwender beeinflusste konventionelle Methoden zu ersetzen. Außerdem wurde beobachtet, dass die Masse von Kapseln, die Aerosil® unterschiedlichen Typs und Konzentration enthielten, niedrigere relative Standardabweichungen (RSD) im Vergleich zu Kapseln aufwiesen, die nur mit Paracetamol gefüllt waren. Die Aerosil® enthaltenden Kapseln zeigten höhere Füllgewichte als mit reinem Paracetamol gefüllte. Aerosil® reduziert die interpartikulären Kräfte zwischen den Paracetamol-Partikeln, die sich folglich näher aufeinander zu bewegen und raus höhere Dichten und Füllgewichte resultieren. Die Auftragung der RSD % gegen ffc zeigte, dass alle Proben, die Aerosil® enthielten und höhere ffc-Werte aufwiesen, niedrige RSD% mit einer geringeren Streuung im Vergleich zu Proben aus reinem Paracetamol ergaben.

Auch das Fließverhalten von binären Mischungen wurde untersucht. Es wurde festgestellt, dass die Fließprofile (grafische Darstellung der ffc-Werte gegen den Anteil an frei fließender Komponente in der Mischung) für fast alle untersuchten Mischungen durch eine Kurve mit zwei Kurvenabschnitten dargestellt werden konnten. Der erste Abschnitt zeigte eine leichte Verbesserung der Fließfähigkeit bei niedrigen Konzentrationen der frei fließenden Komponente bis zum Erreichen einer bestimmten Konzentration (der Schnittpunkt zwischen den beiden Kurvenabschnitten), nach der eine erhebliche Verbesserung der Fließfähigkeit - dargestellt durch den zweiten Kurvenabschnitt - mit weiterer Erhöhung der frei fließenden Komponente festgestellt wurde. In solchen Mischungen dominierten die Haufwerkseigenschaften der schlecht fließenden Komponenten das Fließverhalten der binären Mischungen. Die Lage des Schnittpunkts unterschied sich von einer Mischung zur anderen in Abhängigkeit von den Partikelgrößen und -formen der komponenten. Auf der anderen Seite zeigten Mischungen mit Paracetamol als feine schlecht fließende Komponente nur einen Kurvenabschnittt. Diese Mischungen zeigten bereits eine Fließverbesserung durch den Zusatz

geringer Mengen der frei fließenden Komponente (um 20% V/V). In diesen Mischungen dominierte das Fließverhalten der frei fließenden Komponenten das Fließverhalten der binären Mischung. In Bezug auf die Packungsdichte der Mischung wurden zwei Profile in Abhängigkeit von der Form der feinen schlecht fließenden Komponente in der Mischung erhalten. Mischungen aus feinen sphärischen oder unregelmäßig geformten Bestandteilen ergaben ein Profil mit einen Maximum der Packungsdichte, nach dem die Dichte mit weiterem Anstieg des Anteils der frei fließenden Komponente abnahm. Die Mischungen aus feinen nadel- oder stäbchenförmigen Komponenten zeigten kein Maximum in der Packungsdichte. In diesem Fall waren die Dichten additiv und konnten aus den Dichten und Volumenanteilen der binären Mischungskomponenten vorhergesagt werden. Generell kann festgestellt werden, dass die Fließfähigkeit der binären Mischungen durch die Form und Größe der beiden Komponenten der binären Mischung beeinflusst wurde. Ob die binären Mischungen eine maximale Packungsdichte erreichten oder nicht war vor allem durch die Form der feinen Komponente in den binären Mischungen bedingt. Die Konzentration, bei der maximale Packungsdichte auftrat, hing von beiden Parametern der einzelnen Komponenten ab.

Das Fließverhalten von Lipiden in An- und Abwesenheit von Aerosil® wurde ebenfalls untersucht. Die pharmazeutischen Substanzen, die in dieser Arbeit untersucht wurden, erreichten eine maximale Fließverbesserung mit nur 0,5% Aerosil®. Die Lipide zeigten ein anderes Verhalten. Die gut fließenden Lipide (ffc > 4) benötigten Prozentsätze von mehr als 0,5% Aerosil®, um eine vorgesehene Fließverbesserung zu erreichen. Die schlecht fließenden Lipide (ffc < 4) zeigten zwei verschiedene Verhaltensweisen. Sie zeigten entweder eine signifikante Fließverbesserung mit 2% Aerosil®, oder sie zeigten keine Verbesserung auch bei sehr hohen Konzentrationen (bis zu 15%) von Aerosil®. Vergleicht man den Einfluss von Aerosil® auf das Fließverhalten von Lipiden mit dem auf Paracetamol (Abschnitt 3.2), kann festgestellt werden, dass neben der spezifischen Oberfläche, Form, Größe und Morphologie

der Oberfläche von Stoffen die hydrophobe Natur der Lipide eine wichtige Rolle für die Verbesserung der Fließfähigkeit durch Fließregulierungsmittel spielt. Der Einfluss des Fließregulierungsmittel unterscheidet sich von einem Lipid zu einem anderen bedingt durch den Grad der Hydrophobie.
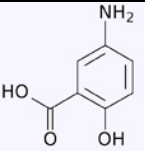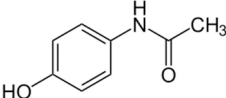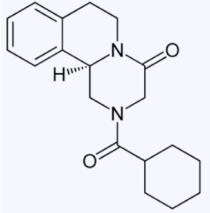
6 Experimental Part

6.1 Materials

6.1.1 Active ingredients

Three active ingredients were used through out this work, as mentioned before in Table 3 in section 3.3.2. Further information is mentioned in the following table.

Table 5: Further information about active ingredients used in this work

Substance	Generic Name	Manufacturer	Batch-No.	Structure
Mesalazine	Mesalazine	Ferring Copenhagen/Denmark	KD2026	
Paracetamol	Paracetamol	Atabay Istanbul/Turkey	2703151	
Praziquantel	Praziquantel	Bayer AG Leverkusen/Germany	KP04WXZ01	

6.1.2 Excipients

Six excipients were used through out this work, as mentioned before in Table 3 in section 3.3.2. Further information is mentioned in the following table.

Table 6: Further information about excipients used in this work

Substance	Generic Name	Manufacturer	Batch-No.	Comment
Flowlac 100	α-Lactose monohydrate	Meggle AG Wasserburg/Germany	L0605 A4921	Spray dried lactose
Inhalac 230	α-Lactose monohydrate	Meggle AG Wasserburg/Germany	0345	Sieved lactose
Granulac 200	α-Lactose monohydrate	Meggle AG Wasserburg/Germany	L0532 A4172	Milled lactose
Di-Cafos	Dicalcium phosphate dihydrate	Budenheim KG Budenheim/Germany	0036997	Fine granulated calcium phosphates
Dicafos PAF	Dicalcium phosphate anhydrous	Budenheim KG Budenheim/Germany	A59165B	Powdered calcium phosphates
Starch	Starch	Cargill Krefeld/Germany	1102159	Corn starch

6.1.3 Silicon dioxide (Aerosil®)

As glidants in this work 4 types of fumed silica (silicon dioxide) were used as received from Evonik (Düsseldorf, Germany).

Table 7: Glidants used in this study

Substance	Manufacturer	Batch-No.	Particle size nm	Specific surface area m²/g	Tapped density g/l	comment
Aerosil® 200	Evonik Düsseldorf, Germany	2110	12	200	50	Hydrophilic
Aerosil® 200 V	Evonik Düsseldorf, Germany	2124	12	200	120	Hydrophilic
Aerosil® R972	Evonik Düsseldorf, Germany	2727033	16	110	50	Hydrophobic
Aerosil® R972 V	Evonik Düsseldorf, Germany	3156020921	16	110	90	Hydrophobic

6.1.4 Lipids

In this study seven different powdered lipids were used, see Table 4 in section 3.4.2.1. Further details are mentioned in the following table.

Table 8: Further information about lipids used in this study

Substance	Manufacturer	Batch-No.	Fatty acids	Melting range (°C)
Precirol ATO 5®	Gattefossé,Weil am Rhein, Germany	26489	C16:40-60% C18:40–60%	53–57
Compritol 888 ATO®	Gattefossé,Weil am Rhein, Germany	26800	C16 < 3%, C18< 5% C20< 10% C22< 83% C24< 3% C26< 3%	69-74
Imwitor 900 K®	Sasol,Witten, Germany	603009	C18:60-80% C16+C18: min 90%	54-64
Dynasan 118®	Sasol,Witten, Germany	606734	C18 > 99%	70-74
Dynasan 116®	Sasol,Witten, Germany	906016	C16 > 99%	61-65
Dynasan 114®	Sasol,Witten, Germany	706162	C14 > 99%	55–58
Witocan 42/44®	Sasol,Witten, Germany	705025	C8/10 < 5%, C12~35%, C14~14%, C16~19%, C18~27%	42–44

6.2   Methods

6.2.1   Samples preparation

For all methods the blending process was carried out using a Turbula mixer (T10B, W. A. Bachofen AG, Basel, Switzerland) with a rotational speed of 42 rpm. Mixing was carried out in an unconditioned room. However, the measuring procedures and sample's storage took place in a conditioned room, 21°C and 45% relative humidity.

6.2.1.1   Paracetamol / Aerosil mixtures

Based on preliminary investigations, the Aerosil®concentration was set to 0.1, 0.5 and 2% w/w. The Aerosil® was screened through a 315μm sieve before combined with the Paracetamol. First of all half the amount of Paracetamol was weighed directly in the mixing container then the amount of Aerosil required was added before adding the remaining amount (other half) of Paracetamol weighed. The powders were mixed for 30 minutes in a turbula mixer using a 1L container, and a maximum filling degree of 75%. The samples were stored over night in a conditioned room 21º C and 45% RH and measured on the next day under the same conditions.

6.2.1.2   Binary mixtures

The binary mixtures were prepared by first weighing the free flowing powder directly in a 1L container and then the amount of the poor flowing substance was added. These substances were mixed in the turbula mixer for 15 minutes then stored over night in a conditioned room 21º C and 45% RH. Eleven different concentrations were prepared from each binary mixture. The concentration was calculated on volume to volume bases.

6.2.1.3   Lipids / Aerosil mixtures

Similar to Paracetamol/Aerosil mixtures, half the amount of lipid was weighed directly in the mixing container then the sieved amount of Aerosil required was added before adding the remaining amount (other half) of lipid weighed. The powders were mixed for 15 minutes in a

turbula mixer using a 1L container, and a maximum filling degree of 75%. The samples were stored over night in a conditioned room 21° C and 45% RH and measured on the next day under the same conditions.

6.2.2   Ring shear tester

The flowability was determined using fully automated Schulze ring shear testers. Two types where used in this work a RST-01.pc ($200cm^3$) and RST-XS ($30cm^3$) (Dr. Dietmar Schulze Schuettgutmesstechnik, Wolfenbuettel, Germany). More details about these testers were mentioned in section 1.2. The powder was packed gently in the annular trough and the excess material on the surface was removed and the surface was smoothed using a scraper without applying any stress to the sample. The weight was determined prior to the measurement. During the measurements the normal load of preshear was adjusted at 5000 Pa., it is the load under which the sample is consolidated and kept in a steady state i.e; constant bulk density and shear stress. Shearing proceeded at lower normal loads 1000, 2000, 3000, 4000 Pa consequently. The normal stresses and determined shear stresses, where incipient flow occurs were plotted in a σ, τ - diagram. By means of a Mohr's circles analysis a yield locus is obtained. The ratio of the consolidation stress σ_1 to the unconfined yield strength σ_c is called the flowability function (ffc). The analysis of the results is performed using the software RST-Control 95, Version 1.0 (Dr. Dietmar Schulze Schuettgutmesstechnik). For the measurements the automatic mode of operation was used with the recommended standard settings. The yield locus was represented as a curve consisting of straight sections (instead of a regression line). The prorating procedure was switched on, where prorating is the mathematical procedure by which shear stresses at shear are rated according to the ratio of the corresponding shear stress at preshear to the yield locus mean shear stress at preshear. Slip stick detector was off with some samples. This phenomenon is an alternating change between static and dynamic friction which may yield inaccurate results and increase time of measurement. Shear velocity mode was set to normal. Tolerance (accepted range of scatter of steady state flow) was increased to

400% in some samples. The RST-control 95 tolerates only small fluctuations for its default settings (100%), therefore during preshear it may not recognize the steady state flow, thus shearing will continue. So we increase the tolerance against fluctuations in order to operate in automatic mode. The ffc was used to classify the flow behavior of bulk solids according to Jenike´s powder classification. The mean of 2 measurements was used.

6.2.3 Poured and tapped densities

According to the Ph.Eur, approximately 50 g of powder was gently poured into a tarred 250ml graduated cylinder and the initial volume (V_0) was recorded to the nearest graduated unit and the poured density (g/ml) was calculated as the quotient m/V_0. The graduated cylinder was placed on a tap density tester (J. Engelsmann AG Tap Density Tester, Apparatebau Ludwigshafen a. Rh.) and the volume was recorded after 10, 500 and 1250 taps, to obtain V_{10}, V_{500} and V_{1250} respectively. Another 1250 taps were carried out when the difference between V_{500} and V_{1250} was greater than 2mL. The tapped density (g/ml) was expressed as the quotient of m/V_{1250} or m/V_{2500}. The Hausner ratio was calculated as follows;

$$H.R= \rho_T / \rho_b \qquad \text{Equation 5}$$

Where, ρ_b is the bulk density and ρ_T is the tapped density. Measurements were performed in duplicate and the mean value was taken.

6.2.4 Angle of repose

It was measured according to the DIN ISO 4324/ 1983 and ISO 4324/ 1977; proceeding according to Dr.Pfrengle. Approximately 100 g of powder is poured through a glass funnel. The powder settles as a conical heap on a 25 mm high and 100 mm diameter transparent plastic plate. For the poor flowing samples a stirrer was used. The angle between the slopped surface of the conical heap and the horizontal plane is recorded as the angle of repose.

Lower angle of repose values represent better flow. The angle was calculated according to the following equation;

$$\tan \theta = h/r \qquad\qquad \text{Equation 6}$$

Where, h is the height of the conical heap formed by the powder divided by the radius of the plastic plate (r). Measurements were performed in triplicate and the mean value was taken.

6.2.5 Flow rate

According to the Ph. Eur. 100 g of powder is gently poured into a closed stainless steel funnel. The funnel has three different orifice openings, namely, 10, 15 and 25 mm in diameter. In this work the samples passed freely only through the 25 mm orifice. The orifice is opened to allow the powder to flow. The time required for the powder to flow through the orifice is recorded. Measurements were performed in triplicate and the mean value was taken.

6.2.6 Capsule filling

According to DAC-Anlage G-method B using a manual filling machine, powder was spread over a tray with 30 holes containing the opened capsule bodies. Size 0 capsules (0.68ml) were used. The capsules were filled by spreading the powder over the bodies with a scraper. Tapping the powder manually into the capsule body was performed when required. Three batches, 30 capsules each, were prepared from each paracetamol/Aerosil mixture and the mean weight of content was used. Also the relative standard deviation (RSD) was calculated for each batch and the mean RSD of three batches was used. The RSD is the standard deviation of a batch divided by its mean multiplied by 100.

6.3 Characterisation of powders

6.3.1 Helium pycnometer density

A helium pynometer (AccuPyc 1330, Micromeritics, Norcross, Georgia, USA) was used for the determination of the particle density. Temperature within the pycnometer was kept

constant during all experiments at $25 \pm 0.1°C$. The $10cm^3$ sample chamber was used. The obtained helium density values are the mean values of three measurements.

6.3.2 Porosity

The powders porosity was calculated using the particle density (ρ_T) obtained by the helium pycnometer and the bulk density (ρ_b) as measured with the ring shear tester (normal load 5KPa) as follows:

% Porosity = $(1- \rho_b/\rho_T)*100$ Equation 7

6.3.3 Laser diffractometer

The particle size measurements were determined using laser light diffraction (Helos/KF-Magic, Sympatec GmbH, Clausthal-Zellerfeld, Germany) including a dry dispersing system (Rodos, Sympatec GmbH, Clausthal-Zellerfeld, Germany). The powder was applied on the Vibri feeder (Sympatec GmbH) transporting the powder to the dry dispersing system. The atomizing air was adjusted at 2.0 bar with a feeding rate of 80%. The results were analyzed by Windox 4.0 software (Sympatec GmbH). The value of the median (d_{50}) is the average of three measurements.

6.3.4 BET gas adsorption

The specific surface area of the pure materials (lipids) was determined using nitrogen gas adsorption based on the Brunauer, Emmett and Teller (BET) method. The measurements are carried out using the measuring device Tristar 3000 (Micromeritics GmbH Mönchengladbach, Germany). The samples were degassed for 20 hours at 25°C using the Vac Prep 061, Micromeritics GmbH, Mönchengladbach and their weights were recorded. After degassing the vessels are transferred to the Tristar 3000 device and the samples are cooled with liquid nitrogen. Nitrogen adsorption was carried out at eleven different relative pressures in the range from 0.05 to 0.30. The saturation pressure is measured in a separate vessel. The amount of

nitrogen adsorbed is recorded on establishment of equilibrium at different relative pressures. The analysis was performed using the software Win Tristar 3000 V6.00 (Micromeritics GmbH, Mönchengladbach). The specific surface area is calculated using the BET equation.

6.3.5 SEM

Each sample was mounted on a brass pin with double sided carbon adhesive tape prior being coated with a thin layer of gold using a sputter coater (Agar Manual Sputter Coater, Agar Scientific Ltd., Stansted, Essex, England). The samples were sputtered with gold for 180s under argon atmosphere. The samples morphologies were examined with a scanning electron microscope (LEO VP 1430, Carl Zeiss NTS GmbH, Oberkochen, Germany) under vacuum adjusting 20 kV operating voltage.

7 References

1] Schulze D. Flow properties of powders and bulk solids. 2006. www.dietmar-schulze.de.

2] Schulze D. Powders and bulk solids: Behaviour, characterization, storage and flow. Berlin: Springer; 2008. PP. 20-27, 35-43, 49-50, 57, 98, 165-173, 178-179,182, 190-192, 195, 198, 211-214.

3] Schulze D. Flow properties of powders and bulk solids and silo design for flow. www.dietmar-schulze.de.

4] Schulze D. Zur Fließfähigkeit von Schüttgütern-Definition und Meßverfahren. Chem.-Ing.-Tech. 1995; 67 (1): 60-68.

5] Jonat S. The mechanism of hydrophilic and hydrophobic colloidal silicon dioxide types as glidants [Dissertation], Tübingen-Universität - Tübingen; 2005.

6] Bodhmage A. Correlation between physical properties and flowability indicators for fine powders [Thesis], University of Saskatchewan; 2006.

7] Taylor MK, Ginsburg J, Hickey AJ, Gheyas F. Composite method to quantify powder flow as a screening method in early tablet or capsule formulation development. AAPS PharmSciTech. 2000; 1 (3) article 18.

8] Royal T. A. & Carson J. W. Fine powder flow phenomena in bins, hoppers and processing vessels. Bulk 2000: Bulk material handling towards the year 2000, (1991): 1-10.

9] Fitzpatrick, J. J., Barringer, S. A., and Iqbal, T. Flow property measurement of food powders and sensitivity of Jenike's hopper design methodology to the measured values. Journal of Food Engineering 2004; 61: 399-405.

10] Prescott J. K. & Barnum R. A. On Powder Flowability. Pharmaceutical Technology 2000; 24 (10): 60-84.

11] Schulze D. The behaviour of powders and bulk solids. www.dietmar-schulze.de

12] Emery E. Flow properties of selected pharmaceutical powders [Thesis], University of Saskatchewan; 2008.

13] Schulze D. Storage of powders and bulk solids in silos. www.dietmar-schulze.de.

14] Standard Shear Testing Technique for Particulate Solids using the Jenike Shear Cell, The Institution of Chemical Engineers, UK; 1989.

15] Schubert H. Grundlagen der Agglomerierens. Chemie-Ingenieur-Technik 1979; 51 (4); 266–277.

16] Meyer K. & Zimmermann I. Effect of glidants in binary powder mixtures. Powder Technology 2004; 139: 40– 54.

17] Fatah N. Study and comparison of micronic and nanometric powders: Analysis of physical flow and interparticle properties of powders. Powder Technology 2009; 190: 41-47.

18] Kabliz C. Dry coating- a characterization and optimization of an innovative coating technology [Dissertation], Heinrich-Heine-Universität-Düsseldorf; 2007.

19] Rumpf H. Die Wissenschaft des Agglomerierens. Chemie-Ingenieur-Technik 1974; 46 (1): 1-11.

20] Castellanos A, Valverde J. M., Quintanilla M. A. S. The Sevilla powder tester: A tool for characterizing the physical properties of fine cohesive powders at very small consolidations. KONA 2004; 22: 66-81.

21] Schwedes J. Testers for measuring flow properties of particulate solids. Powder Handling & Processing 2000; 12 (4): 337-354.

22] Schwedes J. Review on testers for measuring flow properties of bulk solids. Granular Matter 2003; 5 (1): 1-43.

23] Schwedes J, Schulze D. Measurement of flow properties of bulk solids, Powder Technology 1990; 61: 59-68.

24] Röck M., Morgeneyer M., Schwedes J., Kadau D., Brendel L. and Wolf D. E. Steady state flow of cohesive and non cohesive powders. Granular Matter 2008; 10 (4): 285-293.

25] Jenike A. W. Storage and flow of solids, Bull. 123, Engineering Experiment Station, University of Utah, 1964.

26] Schulze D. Development and application of a novel ring shear tester. Aufbereitungstechnik 1994; 35 (10): 524-535.

27] Feise H. J., Carson J. W. Review: The evolution of bulk solids technology since 1982. Chem. Eng. Technol. 2003; 26 (2): 121-131.

28] Carstensen J. T., Ertell C., Geoffroy J. Physico-chemical properties of particulate matter. Drug Development and industrial pharmacy 1993; 19 (12): 195-219.

29] Bean H. S., Beckett A. H., Carless J. E. Advances in Pharmaceutical Sciences, Vol. 3. Academic Press: London and New York, 1971; PP. 185-186.

30] Johanson J. R. The Johanson indicizer system versus the Jenike shear tester. Bulk Solids Handling 1992; 12 (2): 237-240.

31] Gold G., Duvall R. N., Palermo B. T., Slater J. G., Powder flow studies II. Effect of glidants on flow rate and angle of repose. Journal of Pharmaceutical Sciences 2006; 55 (11): 1291-1295.

32] The European Pharmacopoeia 5 (2005), Pharmaceutical Technical Procedures, 2.9.16 Flow Behaviour: 301-302.

33] The European Pharmacopoeia 5 (2005), Pharmaceutical Technical Procedures, 2.9.15 Apparent and Tapped Volume: 301.

34] Li Q., Rudolph V., Weigl B. & Earl A. Interparticle van der Waals force in powder flowability and compactibility. International Journal of Pharmaceutics 2004; 280: 77-93.

35] Ho R., Bagster D. F. & Crooks M. J. Flow studies on directly compressible tablet vehicles. Drug development and industrial Pharmacy 1977; 3 (5): 475-487.

36] Schulze, D.: RST-CONTROL 95 – Software for computer-controlled powder testing with the Ring Shear Tester RST-01.pc (2001) (English).

37] Schulze, D.: RSV 95 - Software for the evaluation of shear test data measured with the Ring Shear Tester RST-01.pc (1999/2001) (English).

38] Schulze D. Ring shear tester RST-01.pc, Operating Instructions (1999/2004) (English).

39] ASTM Standard D6773-02: Standard shear test method for bulk solids using the Schulze Ring Shear Tester, ASTM International.

40] Meyer K.; Nanomaterialien als Fließregulierungsmittel [Dissertation], Bayerische Julius-Maximilians-Universität-Würzburg; 2003.

41] Cooke J.; Freeman R., The flowability of powders and the effect of flow additives, World Congress on Particle Technology 5 (2006).

42] Properties of CAB-O-SIL® M-5P Fumed Silica, Cabot Corporation (2004).

43] Evonik (Degussa). Product, Safety and Technical Information. www.aerosil.com.

44] Schulze D. Time and velocity dependent properties of powders effecting slip-stick oscillations. Chem. Eng. Technol. 2003; 26 (10): 1047-1051.

45] Schulze D. Flowability and time consolidation measurements using a ring shear tester. Powder Handling & Processing 1996; 8: 221-226.

46] Schmitt R, Feise H. Influence of tester geometry, speed and procedure on the results from a ring shear tester. Part. Part. Syst. Charact. 2004; 21: 403-410.

47] Podczeck F., Lee-Amies G. The bulk volume changes of powders by granulation and compression with respect to capsule filling. International Journal of Pharmaceutics 1996; 142 (1): 97-102.

48] Podczeck F; Newton J M. Powder filling into hard gelatine capsules on a tamp filling machine. International Journal of Pharmaceutics 1999; 185 (2): 237-254.

49] Nair R., Vemuri M., Argawala P. & Kim S. Investigation of various factors affecting encapsulation on the in-cap automatic capsule filling machine. AAPS PharmSci. 2004; 5 (4) article 57.

50] Felton L., Garcia D., Farmer R. Weight and weight uniformity of hard gelatine capsules filled with microcrystalline cellulose and silicified microcrystalline cellulose. Drug Development & Industrial Pharmacy 2002; 28: 467-472.

51] Tan S.B. & Newton J. M. Powder flowability as an indication of capsule filling performance. International Journal of Pharmaceutics 1990; 61: 145-155.

52] Patel R. & Podczeck F. Investigation of the effect of type and source of microcrystalline cellulose on capsule filling. International Journal of Pharmaceutics 1996; 128: 123-127.

53] Kurihara K., Ichikawa I. Effect of powder flowability on capsule filling weight variation. Chemical & Pharmaceutical Bulletin 1978; 26: 1250-1256.

54] Heda P. K., Muteba K., & Augsburger L. L. Comparison of the Formulation Requirements of Dosator and Dosing Disc Automatic Capsule Filling Machines. AAPS PharmSci. 2002; 4 (3) article 17.

55] Jonat, S.; Hasenzahl, S.; Gray, A.; Schmidt, P. C. Mechanism of glidants: investigation of the effect of different colloidal silicon dioxide types on powder flow by atomic force & scanning electron microscopy. Journal of Pharmaceutical Sciences 2004; 93 (10): 2635-2644.

56] Applications of CAB-O-SIL® M-5P Fumed Silica in the Formulation and Design of Solid Dosage Forms, Cabot Corporation (1995).

57] Dünisch S. Untersuchung der Wirkungsweise von nanomaterialien, [Dissertation], Bayerische Julius-Maximilians universität – Würzburg.

58] Podczeck F., Sharma M. The influence of particle size and shape of components of binary powder mixtures on the maximum volume reduction due to packing. International Journal of Pharmaceutics 1996; 137: 41-47.

59] Freeman R.E., Cooke J.R, Schneider L.C.R. Volumetric dosing efficiency in relation to the bulk, flow and shear properties of powders. Partec 2007.

60] Itiola OA.,Odeku OA. Packing and cohesive properties of some locally extracted starches. Tropical Journal of Pharmaceutical Research 2005; 4 (1): 363-368.

61] Podczeck F., Miah Y. The influence of particle size and shape on the angle of internal friction and the flow factor of unlubricated and lubricated powders. International Journal of Pharmaceutics 1996; 144 (2): 187-194,

62] Lahdenpää, E., Niskanan, M., and Yliruusi, J. Study of some essential physical characteristics of three Avicel PH grades using a mixture design. European Journal of Pharmaceutics and Biopharmacetics 1996: 42 (3): 177-182.

63] Abdullah, E. C. and Geldart, D. The use of bulk density measurements as flowability indicators. Powder Technology 1999; 102: 151-165

64] Zheng J., Carlson W. B. & Reed J. S. The packing density of binary powder mixtures. Journal of the European Ceramic Society 1995; 15; 479-483.

65] Lam D. C. C., Nakagawa M. Packing of particles. III: Effect of particle size distribution shape on composite packing density of bimodal mixtures. Nippon seramikkusu kyokai gakujutsu ronbunshi 1994; 102 (2): 133-138

66] Shotton E, Obiorah BA The effect of particle shape and crystal habit on properties of sodium chloride. J Pharm Pharmacol. 1973; 25 (Suppl): 37P-43P.

67] Larhrib, H., Martin, G. P., Prime, D. and Marriott, C. Characterisation and deposition studies of engineered lactose crystals with potential for use as a carrier for aerosolised salbutamol sulfate from dry powder inhalers. European Journal of Pharmceutical Science 2003; 19 (4): 211-221.

68] Kaerger J. S, Edge S &. Price R. Influence of particle size and shape on flowability and compactibility of binary mixtures of paracetamol and microcrystalline cellulose. European Journal of Pharmaceutical Sciences 2004; 22 (2-3): 173-179

69] Hou H., Calvin S. C. Quantifying effects of particulate properties on powder flow properties using a ring shear tester. Journal of Pharmaceutical Sciences 2008; 97 (9): 4030-4039.

70] Alvarez A., Rodriguez M. Lipids in pharmaceutical and cosmetic preparations Grasas y Aceites 2000; 51: 74-96.

71] Krause J.; Novel paediatric formulations for the drug sodium benzoate [Dissertation], Heinrich-Heine-Universität - Düsseldorf ; 2008.

72] Reitz C., Kleinebudde P. Solid lipid extrusion of sustained release dosage forms. European Journal of Pharmaceutics and Biopharmaceutics 2007; 67: 440–448.

73] Reitz C.; Extrudierte Fettmatrizes mit retardierter Wirkstofffreigabe [Dissertation], Heinrich-Heine-Universität - Düsseldorf ; 2008.

74] Pharmazeutisch-kosmetische Anwendung nanostrukturierter Lipidcarrier (NLC); Lichtschutz und Pflege, www.diss.fu-berlin.de.- Freie Universität Berlin (2008).

75] Gattefosse GmbH. www.gattefosse.com; Pharmaceutical / products / oral (2007).

76] Michalk A. Geschmaksmaskierung durch Festfett-Extrusion [Dissertation], Heinrich-Heine-Universität - Düsseldorf ; 2007.

77] Jonat S., Hasenzahl S., Drechsler M., Albers P., Wagner K.G., Schmidt P.C. Investigation of compacted hydrophilic and hydrophobic colloidal silicon dioxides as glidants for pharmaceutical excipients, Powder Technology 2004; 141: 31-43.

78] Eber M.; Wirksamkeit and Leistungsfähigkeit von nanoskaligen Fließregulierungsmitteln [Dissertation], Bayerische Julius-Maximilians-Universität – Würzburg; 2004.

SELBSTSTÄNDIGKEITSERKLÄRUNG

Die hier vorgelegte Dissertation habe ich eigenhändig ohne unerlaubte Hilfe angefertigt.

Die Dissertation wurde in der vorgelegten Form bei keiner anderen Institution eingereicht.

Ich habe bisher keine erfolglosen Promotionsversuche unternommen.

Düsseldorf, den

(Hind Jaeda)